Source Apportionment Study for Skopje urban area –identification of main sources of ambient air pollution

Шведска
Sverige

TACKLING AIR POLLUTION
IN THE CITY OF SKOPJE

UNDP

AMBICON.UGD

May 2022

Document title:	Source Apportionment Study for Skopje urban area – identification of main sources of ambient air pollution	
Name of the organization:	University Goce Delcev, Shtip, AMBICON Lab – Faculty of Natural and Technical Sciences	
Country	Republic of North Macedonia	
Project title:	Tackling Air Pollution in the City of Skopje	
Project Number:	00109164	
Submitted To:	UNDP, Skopje	
Date of submission	10.05.2022	
Project team	Team leader	Prof. Dejan Mirakovski – UGD FTNS
	Chemical speciation and modeling group	Ass. Prof. Afrodita Zendelska – UGD FTNS Prof. Blazo Boev – UGD FTNS Prof. Tena Sijakova-Ivanova– UGD FTNS Ass. Prof. Ivan Boev– UGD FTNS
	QA/QC group	Ass. Prof. Marija Hadzi-Nikolova– UGD FTNS Prof. Nikolinka Doneva– UGD FTNS
	Supporting group (documents drafting)	Prof. Milka Zdravkovska, MD – UGD FMS Doc. Biljana Eftimova, MD – UGD FMS Prof. Sonja Lepitkova – UGD FTNS Ass. Prof. Gorgi Dimov– UGD FTNS Ass. Prof. Blagica Doneva – UGD FTNS
	Technical group	Boban Samardziski, M.Sc. – FTNS, AMBICON Igor Pavlov – FTNS, AMBICON Elena Naunova – FTNS, AMBICON Goce Bogatinov– UGD IT SG Jordan Tikvesanski – UGD IT SG
	Students' internship group	Ana Mihailovska Elena Doneva Simona Angelovska Jovana Petrovska

Disclaimer

This study was prepared by the Ambicon UGD Lab, part of Faculty of Natural and Technical Sciences, University Goce Delcev in Stip, as part of the project "Tackling Air Pollution in the City of Skopje" implemented by the United Nations Development Programme (UNDP) in partnership with the Ministry of Environment and Physical Planning and the City of Skopje. The project is financially supported by Sweden.

The views expressed in this document are those of the authors and do not necessarily reflect the views of Sweden, UNDP or the other project partners."

Table of Contents

Executive summary 9
1. Introduction 19
2. Background information's 21
2.1. Skopje urban area 21
2.1.1. Topography 21
2.1.2. Climate 23
2.1.3. Transportation and energy infrastructure 26
3. Major emission sources 27
3.1. Emission inventory 27
3.1.1. Heat and energy production 27
3.1.2. Industry 28
3.1.3. Traffic emissions 28
3.1.4. Domestic heating 29
3.1.5. Waste management 29
3.1.6. Construction 29
3.1.7. Agriculture 30
3.2. Total emissions 30
3.3. Source profiles 31
4. Particulate matter sampling and analysis 38
4.1. Sampling and determination of mass concentration of ambient particulate matter (PM2.5) 44
4.1.1. Sampling procedure 44
4.1.2. Filters handling and weighing 45
4.2. Chemical speciation 46
4.2.1. Elemental analysis using energy dispersive X-ray fluorescence spectrometry 46
4.2.2. Analysis of water-soluble ions 48
4.2.3. Elemental Carbon analysis 49
4.3. Observations and results 50
4.3.1. Statistical evaluation 50
4.3.2. Results and discussion 61
5. Positive Matrix Factorisation 66
5.1. Input data and PMF model setting 68
5.2. Factor attribution to sources 72
5.3. Sources Contribution 78
6. Conclusions and recommendations 82
Supplementary material 83
References 83

List of figures

Figure 1. Skopje topography (ESRI digital elevation map) 22
Figure 2. Monthly averaged temperatures in Skopje (2017-2021) 23
Figure 3. Monthly precipitation in Skopje urban area (2017-2021) 24
Figure 4. Monthly averaged sunshine hours for Skopje urban area (2017-2021) 24
Figure 5. Monthly averaged percentage of cloud covers for Skopje urban area (2017-2021) 25
Figure 6. The wind rose in 2015, reflecting the average wind speed and direction in Skopje. 25
Figure 7. Particulate matter emission contribution by sources in Skopje 31
Figure 8. Cement industry chemical profile 32
Figure 9. Still production industry chemical profile 32
Figure 10. Biomass burning in closed fireplace chemical profile 33
Figure 11. Open burning of crop residues chemical profile 33
Figure 12. Construction activities chemical profile 34
Figure 13. Exhaust diesel and gasoline chemical profile 34
Figure 14. Urban traffic chemical profile 35
Figure 15. Road dust chemical profile 35
Figure 16. Soil dust chemical profile 36
Figure 17. Residual oil chemical profile 37
Figure 18. Fuel oil chemical profile 37
Figure 19. Monitoring sites map 38
Figure 20. Sequential sampling system PNS 18T-DM 6.1 44
Figure 21. Weighing room- AMBICON UGD Lab 45
Figure 22. NEX CG by Rigaku 47
Figure 23. Spectroquant® Prove 600, Merck 48
Figure 24. Magee Scientific, SootScan™ Model OT21 Optical Transmissometer 49
Figure 25. PM 2.5 Mass concentrations – permanent monitoring sites 61
Figure 26. PM 2.5 Mass concentrations –indicative (short term) monitoring sites 61
Figure 27. PM 2.5 seasonal variations in Skopje urban area 62
Figure 28. Major components and elemental groups in Skopje urban area 62
Figure 29. Annual concentration of lead (Pb) in particulate matter (PM2.5) in Skopje urban area 63
Figure 30. Annual concentration of nickel (Ni) in particulate matter (PM2.5) in Skopje urban area 64
Figure 31. Annual concentration of nickel (Ni) in particulate matter (PM2.5) in Skopje urban area 64
Figure 32. Arsenic average monthly concentrations at Karposh monitoring site 64
Figure 33. Arsenic average monthly concentrations at Novo Lisiche monitoring site 65
Figure 34. Average annual metals concentrations in Skopje urban area 65
Figure 35. Free software US-EPA PMF 5.0 version 5.0.14 – splash screen 67
Figure 36. PMF screenshot - Base model run setting for Novo Lisiche site 69
Figure 37. PMF screenshot - Base model run setting for Karposh site 69
Figure 38. PM 2.5 observed vs. predicted concentration for Karposh site 70
Figure 39. Uncertainty-scaled residuals for total variable PM 2.5 70
Figure 40. PMF screenshot – FPEAK rotation 71
Figure 41. Factor fingerprint for Novo Lisiche dataset 72
Figure 42. Biomass burning factor profiles 73
Figure 43. Traffic associated factors for Karposh dataset 74
Figure 44. Traffic associated factors for Novo Lisiche dataset 74
Figure 45. De -icing salt and Road Dust factors associated with traffic (Novo Lisiche dataset) 74
Figure 46. Fuel/residual oil factor profiles 75
Figure 47. Soil/mineral dust factor profiles 76
Figure 48. Open fire burning factor profile 76

Figure 49. General industrial emissions factor profile 77
Figure 50. Secondary Aerosols factor profile 77
Figure 51. Average monthly contributions to total particulate mass (PM 2.5) – Karposh urban background site 78
Figure 52. Monthly contributions to total particulate mass (PM 2.5) – Novo Lisiche urban traffic exposed site 78
Figure 53. Relative monthly contribution – Kaprosh urban background site 79
Figure 54. Relative monthly contribution – Novo Lisiche urban traffic exposed site 80
Figure 55. Relative annual contribution of PM 2.5 sources at Kaprosh urban background site 80
Figure 56. Relative annual contribution of PM 2.5 sources at Novo Lisiche urban traffic exposed site 81

List of tables

Table 1. Municipalities of Skopje - general information's 21
Table 2. Number of registered vehicles in Skopje classified according to the type and fuel used 26
Table 3. Energy plants located in Skopje [8] 27
Table 4. Total emissions from heat and energy production sector 28
Table 5. Largest industrial installation with significant emissions [8] 28
Table 6. Emissions associated with industrial production [8] 28
Table 7. Total emissions from the road transportation sector [8] 28
Table 8. Annual consumption of fuels 29
Table 9. Total emissions from domestic heating sector [8] 29
Table 10. Emissions from waste management sector 29
Table 11. Emissions from construction activities 30
Table 12. Emissions from agriculture 30
Table 13. Total emissions for Skopje Region (reference year 2014) [8] 30
Table 14. Total emissions for City of Skopje (reference year 2019)[9] 31
Table 15. Results of control quality – EDXRF NEX CG 47
Table 16. QC results of control quality – Spectroquant Prove 600 49
Table 17. Statistical evaluation – Karposh dataset 51
Table 18. Statistical evaluation – Novo Lisiche dataset 53
Table 19. Statistical evaluation – GP – Hrom dataset 55
Table 20. Statistical evaluation – GP Volkovo dataset 57
Table 21. Statistical analysis – Gazi baba dataset 59
Table 22. Statistical evaluation of PM 2.5 mass concentration in Skopje urban area 61
Table 23. Major contribution of PM2.5 in urban areas (%) [26] 63

Terms, definitions, symbols, and abbreviations

For the purposes of this document, the following terms and definitions apply.

Ambient air – is outdoor air in the troposphere, excluding workplaces as defined by Directive 89/654/EEC [12] where provisions concerning health and safety at work apply and to which members of the public do not have regular access.

Calibration - operation that, under specified conditions, in a first step, establishes a relation between the quantity values with measurement uncertainties provided by measurement standards and corresponding indications with associated measurement uncertainties and, in a second step, uses this information to establish a relation for obtaining a measurement result from an indication.

Calibration Standard (CAL) - A solution prepared from the stock standard solution(s) which is used to calibrate the instrument response with respect to analyte concentration.

Certified reference material (CRM) is defined as a "reference material characterized by a metrologically valid procedure for one or more specified properties, accompanied by a reference material certificate that provides the value of the specified property, its associated uncertainty, and a statement of metrological traceability".

Combined standard uncertainty - standard uncertainty of the result of a measurement when that result is obtained from the values of a number of other quantities, equal to the positive square root of a sum of terms, the terms being the variances or covariances of these other quantities weighted according to how the measurement result varies with changes in these quantities.

Coverage factor - numerical factor used as a multiplier of the combined standard uncertainty in order to obtain an expanded uncertainty.

Expanded uncertainty - quantity defining an interval about the result of a measurement that may be expected to encompass a large fraction of the distribution of values that could reasonably be attributed to the measurand.

Field blank - filter that undergoes the same procedures of conditioning and weighing as a sample filter, including transport to and from, and storage in the field, but is not used for sampling air, and it has the same treatment like samples.

Instrument Detection Limit (IDL) - The concentration equivalent of the analyte signal, which is equal to three times the standard deviation of the blank signal at the selected analytical mass(es).

Internal Standard - Pure analyte(s) added to a solution in known amount(s) and used to measure the relative responses of other method analytes that are components of the same solution. The internal standard must be an analyte that is not a sample component.

Laboratory Reagent Blank (LRB) (Preparation Blank) - An aliquot of reagent water that is treated exactly as a sample including exposure to all labware, equipment, solvents, reagents, and internal standards that are used with other samples. The LRB is used to determine if method analytes or other interferences are present in the laboratory environment, the reagents or apparatus.

Linear Dynamic Range (LDR) - The concentration range over which the analytical working curve remains linear.

Limit value - level fixed on the basis of scientific knowledge, with the aim of avoiding, preventing or reducing harmful effects on human health and/or the environment as a whole, to be attained within a given period and not to be exceeded once attained.

Method Detection Limit (MDL) - The minimum concentration of an analyte that can be identified, measured and reported with 99% confidence that the analyte concentration is greater than zero. MDLs are intended as a guide to instrumental limits typical of a system optimized for multi-element determinations and employing commercial instrumentation and pneumatic nebulization sample introduction. However, actual MDLs and linear working ranges will be dependent on the sample matrix, instrumentation and selected operating conditions.

Performance characteristic - one of the parameters assigned to a sampler in order to define its performance.

Performance criterion - limiting quantitative numerical value assigned to a performance characteristic, to which conformance is tested.

Period of unattended operation - time period over which the sampler can be operated without requiring operator intervention.

PMx - particulate matter suspended in air which is small enough to pass through a size-selective inlet with a 50 % efficiency cut-off at x µm aerodynamic diameter.

Quality Control Sample (QCS) - A solution containing known concentrations of method analytes which is used to fortify an aliquot of LRB matrix. The QCS is obtained from a source external to the laboratory and is used to check laboratory performance.

RM – (reference method) - measurement method(ology) which, by convention, gives the accepted reference value of the measurand.

Sampled air - ambient air that has been sampled through the sampling inlet and sampling system.

Sampling inlet - entrance to the sampling system where ambient air is collected from the atmosphere.

Standard uncertainty - uncertainty of the result of a measurement expressed as a standard deviation.

Stock Standards Solutions - A concentrated solution containing one or more analytes prepared in the laboratory using assayed reference compounds or purchased from a reputable commercial source.

Suspended particulate matter - notion of all particles surrounded by air in a given, undisturbed volume of air.

Tuning Solution - A solution used to determine acceptable instrument performance prior to calibration and sample analyses.

Time coverage - percentage of the reference period of the relevant limit value for which valid data for aggregation have been collected.

Uncertainty (of measurement) - parameter associated with the result of a measurement that characterizes the dispersion of the values that could reasonably be attributed to the measurand

Weighing room blank - filter that undergoes the same procedures of conditioning and weighing as a sample filter, but is stored in the weighing room

For the purposes of this document, the following symbols and abbreviated terms apply.

- C Concentration of PM (µg/m^3) at ambient conditions
- GUM Guide to the Expression of Uncertainty in Measurement
- JCGM Joint Committee for Guides in Metrology
- PM Particulate Matter
- PTFE Polytetrafluoroethylene
- QA/QC Quality Assurance / Quality Control
- NIST National Institute of Standards and Technology
- QCS Quality Control Sample
- AQIP Academic Quality Improvement program
- EEA European Environment Agency
- TSP Total suspended particles
- NMVOC Non-methane volatile organic compounds
- MOEPP Ministry of environment and physical planning
- ED-XRF Energy dispersive X-ray fluorescence
- IC Ion chromatography
- OC Organic carbon
- EC Elemental carbon
- SA Source apportionment
- SD Standard deviation
- C.V. Coefficient of variation

Executive summary

Study Background

The Source Apportionment Study for Skopje Agglomeration was preprepared by AMBICON UGD Lab, as a part of Tackling Air Pollution in the City of Skopje Project, implemented by the United Nations Development Programme (UNDP) in partnership with the Ministry of Environment and Physical Planning and the City of Skopje. The project is financially supported by Sweden.

Main goal of Source Apportionment (SA) study for Skopje Agglomeration was to derive information about pollution sources and the amount they contribute to ambient air pollution levels, as essential tool in design of air quality policies as required explicitly or implicitly for the implementation of the Air Quality Directives (Directive 2008/50/EC and Directive 2004/107/EC).

The project preparations and field works set up were started during the late October 2020 and officially commenced from start of January 2021, and included following activities:

- Selection of representative receptors/monitoring sites,
- Sampling and chemical speciation,
- Construction of multivariate receptor model for all receptors,
- Source Apportionment study compilation.

Particulate matter sampling

Considering the SA study goals, current data availability, the project document requirements and guidelines for air pollution source apportionment with receptor models [11], in total five (5) specific receptors/sampling points were selected and set within Skopje agglomeration. As agreed in close consultations with all stakeholders involved and with support of MOEPP technical teams, the sampling points include two permanent (full year coverage) sites:

- Karposh state network monitoring site (our code MP1-AQP), as a representative for urban background (no direct exposure to significant sources),
- Novo Lisiche state network monitoring site (our code MP2-AQP), as a representative for urban site, exposed to mixture of sources in the area (traffic, residential heating, and mixed industrial sources).

In addition, and in order to improve source impact zone delineation and increase data quality, as an input for RM development, three indicative monitoring sites (partial coverage in each season) were set as follow:

- Primary school “Dimitar Pop Gergiev - Berovski in Gorce Petrov as a site under possible influx of pollution along the Vardar and Treska rivers valleys (our code MP3-AQT).
- Primary school “Joakim Krcovski” in Volkovo as a site under possible influx of pollution along the Lepenec river valley (our code MP4-AQT).
- Gazi Baba state network monitoring site (our code MP5-AQT), as a representative for specific industrial exposure.

Sampling programs were simultaneously launched at two permanent and one indicative site on 29.10.2020 and ended on 04.12.2021. During this period a total of 376 samples were taken at Karposh sampling site (MP1-AQP), 367 at Lisiche sampling site (MP2-AQP) and 60 samples at each of the temporary sampling sites (MP3-AQT, MP4-AQT and MP5-AQT). Details of monitoring sites are given bellow.

Sampling process was performed fully in line with the requirements of standard gravimetric measurement method for determination of the PM10/PM2,5 mass concentration of suspended particulate matter (EN 12341:2014). Sampling was performed on 47 mm PTFE filters (Advantec depth

filter PF 020 and PF 040), according to Standard Operating Procedure of the UGD AMBICON Lab, an ISO 17025 accredited for environment and samples from the environment testing (https://iarm.gov.mk/en/2021/07/01/lt-052-university-goce-delcev-shtip/).

Chemical speciation

The elemental analysis of PM2.5 of aerosols was conducted using energy dispersive X-ray fluorescence spectrometer NEX CG produced by Rigaku. Analyses were carried out in the AMBICON Lab, at Goce Delchev University in Shtip, North Macedonia, according to the EPA/625/R-96/010a Compendium of Methods, Method IO-3.3: determination of metals in ambient particulate matter using x-ray fluorescence (XRF) spectroscopy published by U.S. Environmental Protection Agency.

Water-soluble ions were extracted from the aerosol filters using sonication and shaking as recommended in the standard operating procedure for PM2.5 cation Analysis [25]. Water-soluble ions, including sulphates (SO_4^{2-}), nitrates (NO_3^-) and ammonium (NH_4^+) were photometrically analyzed using Spectroquant® Prove 600 spectrophotometer by Merck.

Black Carbon or Elemental Carbon was determined using Magee Scientific, SootScan™ Model OT21 Optical Transmissometer with dual wavelength light source (880nm providing the quantitative measurement of Elemental Carbon in PM, and a 370 nm for qualitative assessment of certain aromatic organic compounds), by applying EPA empirical EC relation for Teflon FRM filters.

Results summarized present daily variations in mass concentrations and chemical composition of PM with respect to various chemical species including carbon fraction (elemental carbon), crustal elements (Al, Si, Ca, Ti and Fe), water soluble ions (NH_4^+, SO_4^{2-}, NO_3^-) and larger group of other elements (Na, S, K, Cr, Mn, Co, Ni, Cu, Zn, As, Sc, V, Rb, Sb, Ba, Ce, Sm, W, Pb, Th, Cl, Se, Cd).

The collected data indicates that the daily average PM2.5 concentrations measured at all monitoring sites in the urban area of Skopje, exhibit significant seasonal and spatial variability, exceeding all of the European Union's limit, target, and threshold values for the protection of human health.

The highest mass concentrations were measured in Gazi Baba (46.62 ± 34.20 µg/m^3), followed by Novo Lisiche (45.68 ± 28.85 µg/m^3), Gorce Petrov – Hrom (43.98 ± 30.26 µg/m^3), Karposh (36.40 ± 24.18 µg/m^3) and Gorce Petrov – Volkovo (35.75 ± 23.58 µg/m^3). The particulate mass (PM 2.5) concentrations measured in Skopje, were among the highest reported in the Europe (PM2.5 annual average concentrations observed in Europe were found from 3 to 35 µg/m^3) [26].

Percentage of days exceeding annual limit values for PM 2.5 (25 µg/m^3) was 62.30 % for Novo Lisiche (195 out 313 valid daily values) and 58.97 % for Karposh site (194 out 329 valid daily values), with significantly higher concentrations recorded during the cold months.

Average PM 2.5 concentrations recorded at Karposh urban background site during the cold season (November, December, January February and March) were 54.26 µg/m^3, and only 24.79 µg/m^3 during the warm season (May, June, July, August and September). Similar variations were found for all monitoring sites in Skopje urban area.

The chemical compositions of PM2.5 differ across Europe and on average, Central Europe has more carbonaceous matter in PM2.5, North-western Europe has more nitrate, and southern Europe has more mineral dust in all fractions [26].

Due to the fact that the majority of the pollutant concentrations in the Skopje valley originate from local emissions and are exacerbated by the local topography, along with poor atmospheric mixing

conditions, this urban area typically displays an extremely homogeneous pollution field, both spatially and by component [27].

Contribution of soil (mineral) dust observed in Skopje is similar to the values found in other parts of Europe [26], and starts from 4.9 % in Novo Lisiche, 4.8 % in Kapros, 4.46 % in GP- Volkovo, and slightly lower 3.2 % in GP-Hrom and 3.18% in Gazi Baba. Elements like Mg, Al, Si, Ca, Ti and Fe, usually used as tracers for soil dust, are well corelated, indicating common source for these elements and providing clear identification of this source in subsequent factor analysis.

Sea salt contributions are negligible, as would be expected for a typically continental location, and smaller amounts found could be attributed more to de-icing salt suspension, than to long range transport.

Sulphates and nitrates contributions are within the lower range of values recorded across Europe, and were found similar to the values recorded in Southern Europe [26]. Although this could be attributed to several factors, a relatively low average concentrations of their gaseous precursors like sulphuric and nitrous oxides must be noted. Average sulphate contribution to total particulate mass is 12.42 % in GP-Volkovo, 12.26 % in GP-Hrom, 11.51 % in Gazi Baba, 10.17 % in Karposh and 9.5 % in Novo Lisiche, while average nitrate contribution reach 4.85 % in GP-Hrom, 4.4% in Karposh, 4.29 % in Gazi Baba, 4.15 % in GP-Volkovo and 3.7% in Novo Lisiche.

However, elemental carbon (EC) contributions found in the urban area of Skopje are higher than European averages and fall within the range of those found in Central Europe, likely reflecting the mix of local sources, where wood combustion was identified as the most significant single source of particulate matter emission [8, 9] for all receptors, and traffic in particular for the Novo Lisiche site.

EC contributions to total particulate mass range from 33.7 % at Novo Lisiche (site exposed to traffic and residential heating emissions), 25.6 % at Gazi Baba, 21.6 % at GP-Hrom, 18.8 % at GP – Volkovo and 16.5 % at Karposh urban background site. Elemental carbon was shown to be correlated with K, Cl, Rb, ammonium, and nitrate ions, mostly associated with biomass burning emissions. All those elements corelate well with total particulate mass, indicating that biomass burning is a significant contributor to particulate mass.

According to the results of the assessment of regulated metals including lead, arsenic and nickel, it was determined that concentrations found were within the annual limit, upper assessment threshold, and lower assessment threshold values as specified in Directives 2008/51/EC and 2004/71/EC. However, the concentrations of As found at two sites (Volkovo and Gorce Petrov) were at or above the lower assessment target. Cadmium was excluded from the evaluation because more than 80 percent of the readings were close to or below the method limit detection.

Further investigation into metal concentrations found higher levels of a specific set of metals (Cr, Co, Ni, As, Sc. Ce. Sm. W and Th) at the Volkovo site as compared to other locations, showing that this receptor is being influenced by a specific source. Increased metal concentrations are usually linked to anthropogenic sources, however further investigation is required to make a correct identification.

Positive Matrix Factorisation

In this study, the free software US-EPA PMF 5.0 version 5.0.14 (Norris and Duvall, 2014), implementing the ME-2 algorithm developed by Paatero (1999), was used.

Because the number of samples for indicative monitoring sites was limited, only data sets from Karpsoh and Novo Lisiche were subjected to comprehensive PMF analysis.

Species lists for both sites included water soluble ions NH_4, SO_4, NO_3, elemental carbon (EC), and following elements; Na, Mg, Al, Si, S, K, Ca, Ti, Cr, Mn, Fe, Co, Ni, Cu, Zn, As, Sc, V, Rb, Sb, Ba, Ce, Sm, W, Pb, Th, Cl, Se and Cd.

Because the number of samples for indicative monitoring sites was limited, only data sets from Karpsoh and Novo Lisiche were subjected to comprehensive PMF analysis.

Following the EU protocol for receptor models [11], the data were first treated to remove values that potentially decrease the analysis quality. After data validation, original datasets included 34 species for both sites and 256 daily samples Novo Lisiche and 332 daily samples for Karposh.

Species with high noise were down-weighted based on their signal-to-noise (S/N) ratio to reduce the influence of poor variables on the PMF analysis. Species with S/N lower than 0.5 were considered as bad variables and excluded from the analysis, and species with S/N between 0.5 and 1 were defined as weak variables and down-weighted by increasing the uncertainty as recommended in the PMF users guideline. After additional validation and outlier's filtration, 23 samples were excluded from the Karposh data set and 5 from Novo Lisiche data set, and percentage of modelled data ranged from 93.1 % for Karposh and 98.1 % Novo Lisiche.

Because each entry is weighted according to its uncertainty, uncertainty estimation is especially important in PMF analysis. The analytical uncertainty indicated in the original dataset included expanded analytical uncertainty calculated according to SOPs following GUM approach and accounting all sources of uncertainties, and therefore only 10 % extra modelling uncertainty was added, using the methodology that is described from Ammato et. al [42].

Number of factors was determined through examination of Q-values and scaled residuals. A first estimate of the number of factors p was made by examining the Q values of several runs with increasing numbers of factors from 5 to 12 and final solution for both data sets included 10 factors.

At least 100 base model runs in robust mode were performed for datasets from each site with start seed value set as random.

Achieved Q robust/Q true was 0.67% for Novo Lisiche data set and 0.9% for Karposh data set (Figures 36 and 37). A comparison between observed (input data) values and predicted (modeled) values was used to determine if the model fits the individual species well. Species that do not have a strong correlation (coefficient of determination r2 is < 0.5) between observed and predicted values were evaluated and a decision was made whether they should be down-weighted as week or excluded from the model. For Karposh dataset, only Sc and Cd were down-weighted to weak, while Sc, Sb, Ba, and Cd were down-weighted to weak for Novo Lisiche data set. Coefficient of determination (r2) values between observed and predicted values for total variable (PM 2.5) were 0.87 for Karposh and 0.83 for Novo Lisiche data set.

In addition, the uncertainty-scaled residuals were evaluated in order to determine how well the model fits each species. The species accounted as well-modeled if all residuals are between +3 and -3 and they are normally distributed.

The rotational ambiguity of PMF solutions was investigated using the FPEAK tool for a variety of parameter values (ranging from 1 to +1). Small rotations had no significant effect on Q values, F and G matrices, and scaled residuals for both datasets.

The factor analytical solutions were analyzed using error estimation (EE) methods contained in the US-EPA PMF 5.0 software. The Bootstrap (BS) method was used for detecting and estimating probable

random mistakes caused by disproportionate effects of a small number of data on the solution. To ensure the statistics' robustness, each dataset was subjected to 100 BS runs, with the 5th and 95th percentiles serving as the BS uncertainty range for each factor profile. The block size was to 3 and the minimum correlation value to 0.6 [5].

By examining the broadest range of source profile values without a notable rise in the Q-value, Displacement (DISP) was utilized to investigate the rotational ambiguity in the solutions more explicitly.

The Base Model Displacement Error Method was used to explore the rotational ambiguity in the PMF final solutions. With that methodology it is possible to estimate the effect of a small set of observations in the dataset has on the solution. The number of Bootstraps was set to 100, block size to 3 and the minimum correlation value to 0.6 [56].

Factor attribution to sources

Final PMF solution for both datasets included 10 factors. Factors were attributed to their sources though a quantitative and qualitative comparisons of the factor chemical profile with PM profiles reported EC-JRC SPECIEUROPE data base and profiles from previous source apportionment studies available in the literature. In addition, the standardised identity distance (SID) and the Pearson coefficient, expressed as Pearson distance (PD = 1 - r), were used to calculate the similarity between the factors and the reference source profiles available in the public datasets: EC-JRC SPECIEUROPE and US-EPA SPECIATE (Simon et al., 2010). The Delta SA tool (http://source-apportionment.jrc.ec.europa.eu/) was used to complete the work.

For Karposh- urban background site, 10 factors were attributed to; secondary aerosols, traffic 1, traffic 2, metal processing, industry 1, industry 2, fuel/residual oil, soil/road dust, open fire burning and biomass burning. Similarly, for Novo Lisiche – urban traffic site, factors were attributed to secondary aerosols, traffic 1, traffic 2, metal processing, industry, fuel/residual oil, soil dust, road dust, open fire burning, biomass burning and de-icing salt.

Biomass burning incorporate emissions from different types of woodburning stoves and boilers used mostly in residential heating. Key species found is this factor include EC, K, Cl, NO3- and Rb. K is produced from the combustion of wood lignin [60,61]. Although this element can be emitted from other sources, such as soil dust [62], K has been used extensively as an inorganic tracer to apportion biomass burning contributions to ambient aerosol. Cl can be emitted from biomass burning and also from coal combustion, especially during the cold period [63]. It is also associated with biomass burning in PMF source profiles in Belgrade and Banja Luka [5]. In addition, NO3-, and NH4+ also contributed significantly to the biomass burning factor. Biomass burning is an important natural source of NH3 [65] which rapidly reacts with HNO3 to form NH4NO3 aerosols. The presence of NH4NO3 aerosols in biomass burning plumes, has also been reported previously [65,66].

Traffic includes particles from several different sources including vehicles exhaust, mechanical abrasions of brakes and tires, road (resuspended) dust and road salting. All sources associated have their own specific fingerprints, and can be identified by EC, Ba, Cu, Mn, Pb and Zn, as well as crustal species like Mg, Al, Si, Ca, Fe, and Ti, or Na and Cl in the case of winter road salting.

The vehicle exhaust, including diesel and gasoline, consist high percentage of organic and elemental carbon, Fe, Pb, Zn, Al, Cu and sulphate. Zn is a major additive to lubricant oil. Zn and Fe can also originate from tire abrasion, brake linings, lubricants and corrosion of vehicular parts and tailpipe emission [54-37]. As the use of Pb additives in gasoline has been banned, the observed Pb emissions may be associated with wear (tyre/brake) rather than fuel combustion [58]. Fe and Al is likely

associated with vehicles part wear, such as tyre/brake wear and road abrasion, and are common species in case sampling sites are located close to major roads.

De-icing salt profile exhibit high percentage of Na and Cl (30 and 55%, respectively) and specific temporal pattern, associated with snowfalls occurrence during the cold season.

Although elemental composition of particulate emissions associated with traffic can significantly vary due to differences in traffic volume and patterns, vehicle fleet characteristics, the climate and geology of the region [59]. Similar elements (Cu, Mn, Zn, Pb, Fe and EC) were identified as key species in PMF source profiles in most European and Central Asia urban areas [5].

Fuel and residual oil combustion is a stand-alone factor that includes emissions from a wide range of sources, the majority of which are larger buildings heating systems (schools, hospitals, and other public institutions), industrial combustion emissions and to some extent older diesel-powered vehicles emissions, principally composed of EC, V, Cd and Ni [65, 66].

Organic carbon, sodium, and water-soluble ions including nitrates and sulphates are common key species for fuel oil emissions. The presence of V and Ni is also common marker. Water-soluble ions, V, Fe, and Ni are also important species for residual oil combustion, but increased quantities of elemental carbon, rather than organic carbon, are common for this source. Vanadium, either alone or in conjunction with nickel, is a prevalent marker in PMF source profiles, in most European and Central Asian urban areas [5].

Soil or mineral dust usually originates from construction/demolition activities, dust resuspension and wind erosion processes. This source is commonly identified with so called crustal elements like Mg, Al, Si, Ca, Fe and Ti [51]. Silicon and Ca are usually most abundant elements, followed by Fe, Al, Mg, and Ti, with variations due to local geology. Other research studies also reported significant contribution of soil dust to PM2.5 mass, suggesting that soil dust is an important contributor to PM2.5 mass especially in summertime [52,53]. Similar elements (Ca, Fe, Al, Si, Ba, Na and Ti) were identified as key species in PMF source profiles in most European and Central Asia urban areas [5].

Silicon and calcium are also prevalent species in the construction related source's chemical profile. Chemical profile of construction source also includes Si, Ca, Al and Fe, but also OC, EC and sulphates have significant contribution.

All types of low efficiency burning of agricultural and garden waste, as well as other types of waste, are classified as open fire burning. This factor is identified by high contribution EC, As and Rb, but also includes some specific metals like Cu and Ni. Elemental carbon, Br, Co, V, Ti, and As were also found as important species in an analysis of agricultural waste open burning profiles, conducted in the Thessaloniki area in Northern Greece (SPECIEUROPE data base).

Industrial emission includes complex mixture of stationary and diffuse emissions, associated with the various process and operations, mostly identified by a mixture of several metallic species Mn, Fe, Pb, Zn, Cu, and Cr, with consistent contribution over the year. Although those elements can be emitted from various sources, metals are commonly associated with anthropogenic sources and therefore used as tracers to apportion industrial sources.

Rather than being discharged directly into the atmosphere by a single source, secondary aerosols are generated in the atmosphere as a result of complicated chemical and physical transformations of gaseous precursors to particulate matter. SA are mainly recognised by their high S and ion content (SO4 and NH4). Secondary aerosols contribute the most during the coldest and warmest months, when there are high levels of gaseous percussors in the winter and high temperatures in the summer.

Source contribution

Using the data from measurements and modelling exercise, contribution of each source to total particulate mass (PM 2.5) was calculated. To provide most "real world" plausible solution, traffic and industry related factors were grouped in complex sources, thus producing 7 major sources for both sites. The major sources identified for Karposh urban background site include; biomass burning, open fire burning, secondary aerosols, soil/mineral dust and fuel/residual oil burning. Traffic contribution was calculated as a sum of 2 factors associated (traffic 1 and 2) and industry as a complex source with 3 factors associated (industry 1 and 2 + metal processing industry). The major sources identified for Novo Lisiche urban traffic exposed site include; biomass burning, open fire burning, secondary aerosols, industry, soil/mineral dust and fuel/residual oil burning, while traffic contribution was calculated as a sum of 4 factors associated, including traffic 1, traffic 2, road dust and road salt factors.

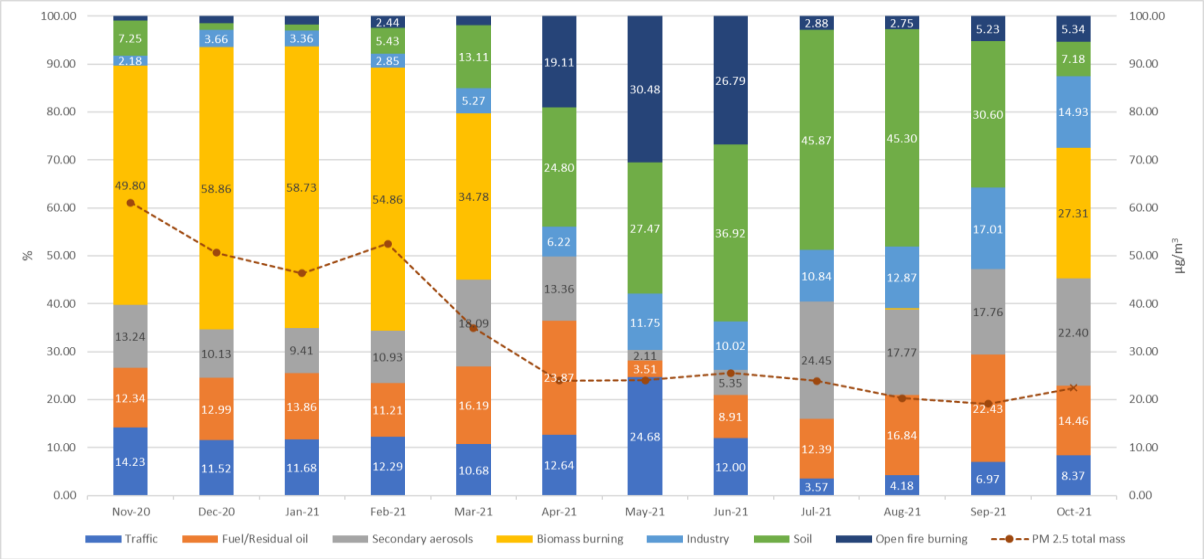

Figure 1- ES. Relative monthly contribution – Karposh urban background site

Biomass burning relative contributions (%) in total particulate mass exhibit high seasonal variability and during the cold season (Nov, Dec, Jan, Feb and March), this is a major source at both sites, with contribution ranging from 15 to 57 % at Novo Lisiche site, and from 27 to 59 % at Karposh site. Despite being completely seasonal, biomass burning has the highest annual relative contribution, reaching 32% for Novo Lisiche and 33 % for Karposh (Figures 55 and 56).

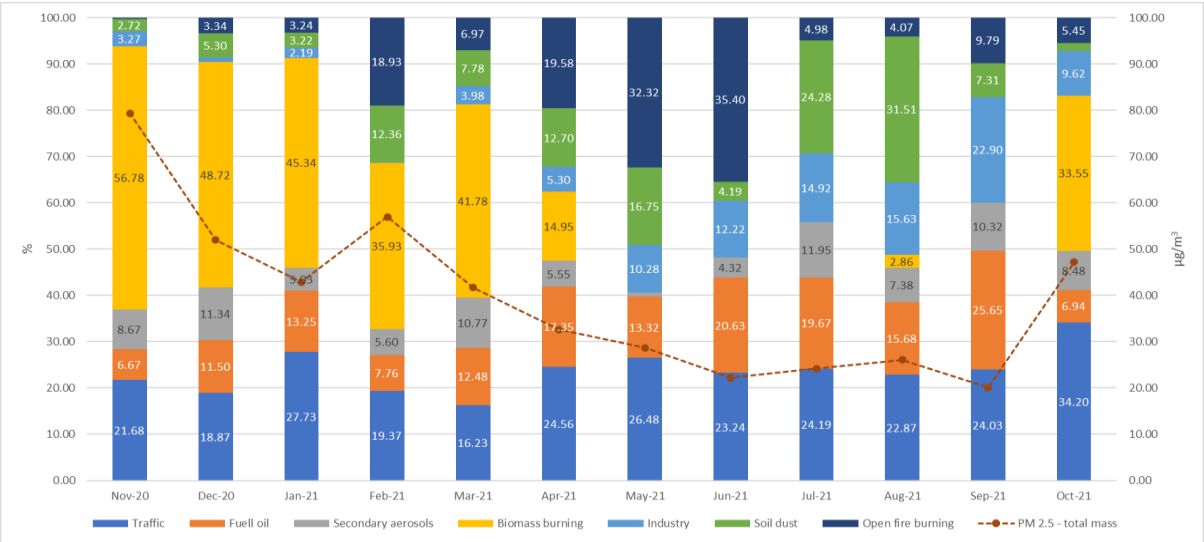

Figure 2- ES. Relative monthly contribution – Novo Lisiche urban traffic exposed site

Traffic annual relative contribution accounted for 18 % of the total particulate mass (PM 2.5) at Karposh site and 23 % at Novo Lisiche (Figures 55 and 56), with monthly relative contribution ranging from 4 to 25 % at Karposh site and from 16 to 34 % at Novo Lisiche site (Figures 53 and 54). This source exhibit relatively consistent contribution over the year, especially at Novo Lisiche urban exposed sites.

Annual relative contribution of fuel/residual oil combustion accounted for 5 % of the total particulate mass (PM 2.5) mass at Karposh site and 12% at Novo Lisiche site (Figures 55 and 56). Relative monthly contribution at Karposh site ranged from 4 to 24 % and from 7 to 26 % at Novo Lisiche, exhibiting relatively consistent contribution over the year at both sites (Figures 53 and 54).

Industrial sources also exhibit consistent contribution over the year, reaching annual relative contribution of 9 % at Karposh site and 6 % at Novo Lisiche site (Figures 55 and 56). Monthly relative contribution ranges from 0.05 to 23% at Novo Lisiche site and from 2 to 17% at Karposh site (Figures 53 and 54).

Soil/mineral dust have also significant contribution to total particulate mass (PM2.5) especially during the warm season. Relative monthly contributions of this source varies from 1 % to significant 46 % at Karposh site and from 2 to 32 % at Novo Lisiche site, but for this traffic exposed site, road dust is identified as a separate factor attributed to traffic source (Figures 53 and 54). Annual relative contribution reaches 15 % at Kaprosh site and 9 % at Novo Lisiche site (Figures 55 and 56).

All types of low efficiency open burning of agricultural and garden waste, as well as other types of waste, classified as open fire burning, exhibit strongest contribution during the spring and early summer months (April, May and June) with relative monthly contribution from 1 to 30 % at Karposh, and from 0.2 to 35 % at Novo Lisiche site (Figures 53 and 54). Relative annual contribution of this source was 7 % for Karposh site and 10 % for Novo Lisiche site (Figures 55 and 56).

Secondary aerosols exhibit specific seasonal pattern, with largest contributions during the coldest and warmest months, associated with high levels of gaseous percussors during the winter months and high temperatures over the summer months. Annual relative contribution of secondary aerosols was 13% of the total particulate mass (PM2.5) at Karposh and 8% at Novo Lisiche sites. Relative monthly contributions exhibit large variation and reach between 2 and 24 % at Karposh site and between 1 and 12 % at Novo Lisiche site.

Conclusions

Biomass burning remain the largest single source of ambient air pollution, and due to specific temporal distribution, probably the main driver of extreme wintertime pollution episodes. During the winter months (Nov, Dec, Jan, Feb and March) biomass burning was a major source at both sites, with contribution ranging between 36 and 57 % at Novo Lisiche, and from 27 to 59% at Karposh background. Therefore, strong commitment in reducing wood burning for residential heating in Skopje urban and suburban areas should remain imperative for all further air quality improvement plans.

However, there are other significant sources, especially fuel/residual oil burning, soil dust and open fire burning, that can and must be tackled in much shorter time frame.

Fuel and residual oils burning includes emissions from a wide range of sources, the majority of which are larger buildings heating systems (schools, hospitals, and other public institutions), industrial combustion emissions and to some extent older diesel-powered vehicles emissions. Rapid plan for reducing this fuels usage could be easily justified with their clear economic and environmental benefits.

Soil dust usually originates from construction/demolition activities, dust resuspension and wind erosion, thus exhibiting high seasonal variation. Specific policies for reduction of fugitive dust during construction and simple street cleaning/washing in combination with long term measures like increased urban vegetation could significantly reduce soil/road dust emissions.

Open fire burning is among the sources that exhibit strongest contribution during the spring and early summer months. Zero tolerance to agricultural/garden waste burning and improved waste management practices could virtually eliminate this source.

For the future improvement of air quality in Skopje's urban and suburban areas, it is necessary to draft targeted and well-detailed air quality management plans based on existing scientific data, and to commit strongly to their execution.

This page is intentionally left blank

1. Introduction

During the last few decades, urban air pollution and especially high particulate matter concertation's become major environmental concern, due to adverse effects on human's health, climate, visibility and ecosystems [1]. Outdoor and indoor air pollution are environmental risk factors that have been linked to a variety of health conditions such as cardiovascular disease, stroke, respiratory disease, and cancer, resulting in approximately 7 million deaths worldwide [2], including about half a million in the European Union (EU) in 2016 [3]. High ambient particulate matter concertation remains highest health concern, leading to 374,000 non-accidental premature deaths attributed to air pollution in EU [3].

Globally, the concentration of fine particulate matter PM2.5 (particulate matter 2.5 micrometres or less in diameter; an indicator of ambient or outdoor air pollution exposure) was 34.7 $\mu g/m^3$ in 2016, which is several times higher than the WHO annual mean limit of 10 $\mu g/m^3$. The lowest annual mean PM2.5 concentrations were reported in the Americas Region (11.6 $\mu g/m^3$) and the European Region (12.8 $\mu g/m^3$), while highest were reported in the South-East Asia Region (54.3 $\mu g/m^3$) and the Eastern Mediterranean Region (51.1 $\mu g/m^3$), confirming extensive regional variations [2].

And small, landlocked North Macedonia is well fitted in this grim picture, as the largest urban areas are often high on the various pollution lists, while capitol Skopje was pointed as one of the most polluted capitols in Europe [4]. During the 2015/16 IAEA Source Apportionment exercise [5], Skopje exhibited highest PM 2.5 annual mean concentrations (58 $\mu g/m^3$) among the regional capitols including Tirana (20 $\mu g/m^3$), Belgrade (20 $\mu g/m^3$), Sofia (34 $\mu g/m^3$) and Banja Luka (30 $\mu g/m^3$), while according to the EEA Annual Air Quality Statistic, annual mean concentrations (PM 10) for last 10 years (2012-2021) for Karposh and Novo Lisiche monitoring stations averaged 57.44 ± 8.23 $\mu g/m^3$ and 75.82 ± 18.73 $\mu g/m^3$ respectively.

Most Danube and Western Balkans countries, including Bosnia and Herzegovina, Bulgaria, Albania, Montenegro, Serbia and North Macedonia, are included among those having the highest mortality due to household and ambient air pollution in Europe [6]. Age-standardized mortality rate attributed to household and ambient air pollution for 2016 in North Macedonia, Bosnia and Herzegovina, Montenegro, Albania, Serbia and Bulgaria reach 82.2, 79.8, 78.6, 68, 62.5 and 61.8 deaths per 100.000 inhabitants, respectively. Mortality rates for North Macedonia, Monte Negro and Albania are more than double compared to European Region average mortality rate (36.3), or more than six (6) times higher when compared with average mortality rate attributed to household and ambient air pollution (12.86) in five (5) largest economies in EU (Germany, France, Italy, Spain and Netherlands) [2].

Although this is not a new problem, limited in scope and temporally scattered data about pollution sources, leave room for dubious discussions, that hamper any efforts to implement proper abatement strategies.

Though at regional and local level significantly different, dominant anthropogenic sources of air pollution usually include large and small-scale combustion, industrial processes, transportation, waste disposal, agriculture and forest and land-use change.

Current scientific data available for Skopje agglomeration, point to residential wood combustion as probably most significant air pollution source [4, 5, 8 and 9].

The Source Apportionment Study for Skopje Agglomeration was preprepared by AMBICON UGD Lab, as a part of Tackling Air Pollution in the City of Skopje Project, implemented by the United Nations Development Programme (UNDP) in partnership with the Ministry of Environment and Physical Planning and the City of Skopje. The project is financially supported by Sweden.

The project aims to demonstrate a multi-pronged intervention to tackle air pollution in the City of Skopje linked to the residential sector and include four main components.

- Component -1: Develop a comprehensive monitoring system for the pilot area, and a coordination platform to tackle air pollution;
- Component - 2: Implement regulatory changes necessary to transitions towards a lower emission household energy system;
- Component - 3: Demonstration of measures that address the causes of pollution for household heating, and
- Component – 4: Build public awareness.

Main goal of Source Apportionment (SA) study for Skopje Agglomeration was to derive information about pollution sources and the amount they contribute to ambient air pollution levels, as essential tool in design of air quality policies as required explicitly or implicitly for the implementation of the Air Quality Directives (Directive 2008/50/EC and Directive 2004/107/EC).

The project preparations and field works set up were started during the late October 2020 and officially commenced from start of January 2021, and included following activities:

- Selection of representative receptors/monitoring sites:
    - Two permanent monitoring sites (24 hours interval over 365 days) with more that 90% coverage over the year.
    - Three indicative monitoring sites (24 hours interval over 14 consecutive days per season or more than 56 days per year) with more that 95% temporal coverage over the year
- Sampling and chemical speciation:
    - gravimetric sampling on PTFE filters in accordance with EN 12341:2014, and
    - determination of chemical composition of ambient particulate matter collected on filter in accordance to the EPA/625/R-96/010a Compendium of methods for the determination of inorganic compounds in ambient air, method IO-3.3: determination of metals in ambient particulate matter using x-ray fluorescence (XRF) spectroscopy,
    - determination of Black Carbon (BC) or Elemental Carbon (EC) using optical transmissometer through application of EPA empirical EC relation for Teflon FRM filters, and
    - determination of water - soluble ions, including sulphate (SO_4^{2-}), nitrate (NO_3^-), ammonium (NH_4^+), using internally developed extraction procedure and referent photometric methods.
- Construction of multivariate receptor model for all receptors:
    - compilation of concentrations and uncertainty data matrices,
    - data modelling using robust Positive Matrix Factorization (PMF).
- Source Apportionment study compilation:
    - reporting site specifics, source inventories, source profiles, time series for pollutant of interest,
    - reporting results and methodology.

This research is one of the first attempts to offer quantitative information on the contributions of pollution sources to ambient PM2.5 in Skopje urban area, that has been carried out to date. As a result, the study generated unique data set that may be used to address air pollution mitigation techniques and to develop air quality plans with the goal of improving air quality and increasing public health.

2. Background information's

2.1. Skopje urban area

The City of Skopje serves as the country's capital and is home to a substantial amount of business and industrial activity. The urban area of Skopje itself is subdivided into ten municipalities (Centar, Aerodrom, Cair, Karposh, Gazi Baba, Kisela Voda, Gjorce Petrov, Butel and Shuto Orizari). According to the latest census (2021), the total population of the urban area is 526 502 inhabitants and 171 171 households [7].

Table 1. Municipalities of Skopje - general information's

Municipalities	Inhabitants	Households
Aerodrom	77 735	27 895
Butel	37 968	10 968
Gazi Baba	69 626	22 509
Gorce Petrov	44 844	15 524
Karposh	63 760	24 589
Kisela Voda	61 965	22 096
Saraj	38 399	8 639
Centar	43 893	17 068
Cair	62 586	15 779
Suto Orizari	25 726	6 104

2.1.1. Topography

Located in the heart of the Balkan Peninsula, the City of Skopje is a major economic center and the capital of the Republic of North Macedonia. The City of Skopje is located in the Skopje valley and is oriented on a west-east axis, parallel to the flow of the Vardar River. The city is limited to the south and north with mountains, (Vodno and Skopska Crna Gora) stretching 9 km in north-south direction and 22 km in northwest-southeast direction. The urban expansion of Skopje is restricted by these mountain ranges, which run along the Vardar River and the Serava, a small river that originates in the north. Skopje is roughly 245 meters above sea level and covers area of 571 km^2. The urbanized area has a total size of 337 km^2.

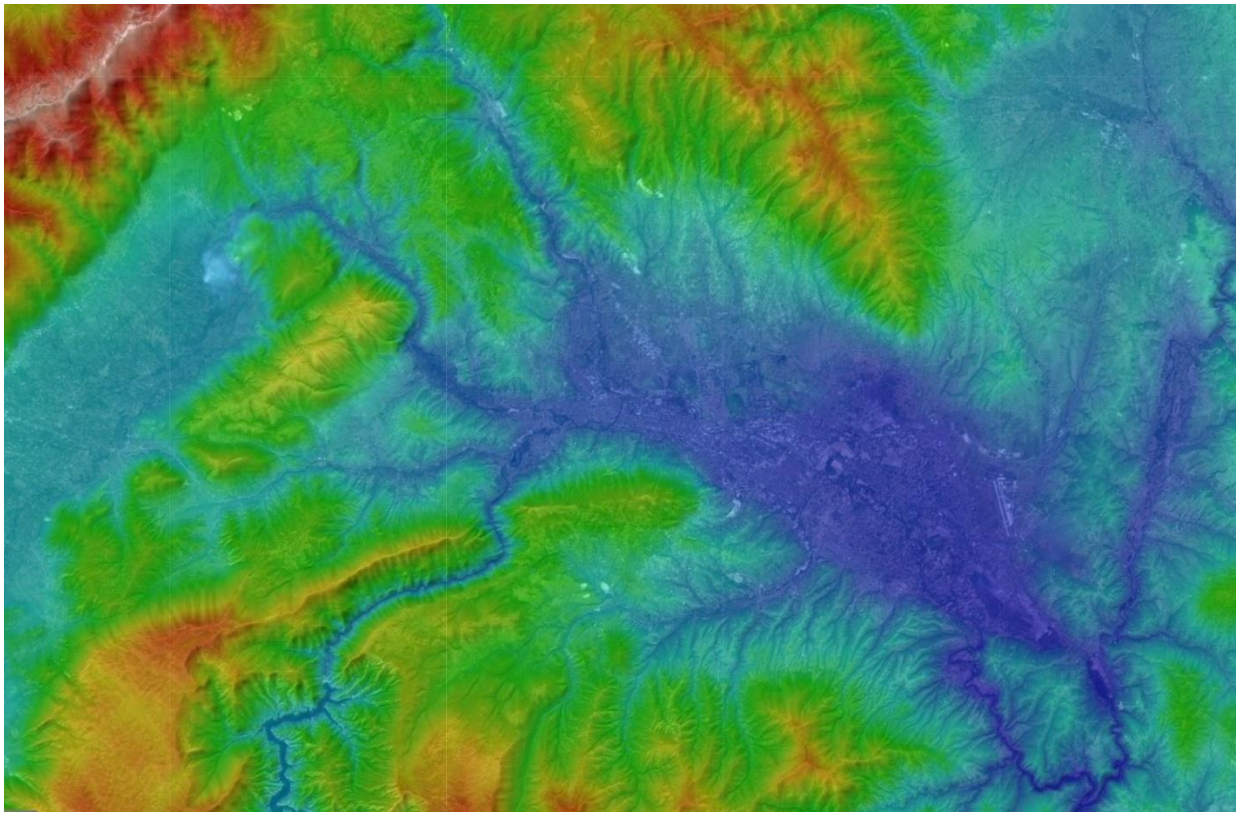

Figure 1. Skopje topography (ESRI digital elevation map)

The Skopje valley is surrounded by mountains on all sides, on the western side, the Skopje valley is flanked by the Sar Mountains; on the southern side, by the Jakupica range; on the eastern side, by hills belonging to the Osogovo range; and on the northern side, by the Skopska Crna Gora. Mount Vodno, the highest peak within the city borders, stands at 1066 meters above sea level and is a part of the Jakupice mountain range. Despite the fact that Skopje is situated at the foot of Mount Vodno, the metropolitan area is primarily flat. Many minor hills, most of which are covered with trees and parks, such as Gazi Baba hill (325 m), Zajcev Rid (327 m), and the foothills of Mount Vodno, are located within the city boundaries (lowest between 350 and 400 m high).

The 1963 earthquake, which devastated 80% of the city and the subsequent restoration, had a significant impact on Skopje's urban morphology. Neighbourhoods, for example, were constructed in such a way that the population density remained low in order to reduce the impact of future earthquakes. The south bank of the Vardar River is mostly made up of high-rise tower blocks, including the sprawling Karposh neighborhood west of the city center, which was erected in the 1970s. The new municipality of Aerodom, to the east, was planned in the 1980s to accommodate 80,000 people on the site of the former airport. The city center is located between Karposh and Aerodrom.

The City of Skopje comprises a number of settlements outside of the main region. Some of them are transforming into suburbs, such as Singelikj, which is located on the route to Belgrade and has over 23,000 residents, and Dracevo, which has about 20,000 residents. Other sizable settlements, such as Radisani, with 9,000 residents, are located north of the city, while smaller villages may be found on Mount Vodno or in Saraj municipality, the most rural of the ten municipalities that make up the City of Skopje. Outside of the city borders, several areas, mainly in the municipalities of Ilinden and Petrovec, are developing into suburbs. They benefit from the proximity of major highways, trains, and the Petrovec Airport.

Food and beverage manufacturing (bread, baked goods, and meat), textile industry, printing, cement and metal processing are the most important industries in the Skopje region. The majority of the industrial districts are in the municipality of Gazi Baba, along major highways and rail lines leading to

Belgrade and Thessaloniki. The Arcelor Mittal and Makstil steel mills, as well as the Skopje Brewery, are all located there. Other industrial zones can be found along the railway to Greece between Aerodrom and Kisela Voda. Alkaloid Skopje (pharmaceuticals), Rade Koncar (electrical supply), Imperial Tobacco, and Usje Cemenet Plant are among these zones. There are also two special economic zones around the airport and the Okta refinery.

2.1.2. Climate

Climate in Skopje is typically described as continental sub-Mediterranean or even hot continental climate, depending on the season. Long, hot, and humid summers characterize the region, although the winters are short and quite cold. Even though snowfalls are typical during the winter months, major snow accumulation is rare, and the snow cover lasts only for a few days on average.

In order to provide more representative data for entire Skopje urban area, ERA 5 reanalysis data set were used. This data set combines model data with real time observations for specific area (ERA5 is the fifth generation reanalysis package for the global climate and weather from European Centre for Medium-Range Weather Forecasts).

During the summer, temperatures frequently exceed 30°C and, on rare occasions, exceed 40°C. July and August are the warmest months of the year, with average temperatures exceeding 20 degrees Celsius. Temperatures range from 15 to 24 degrees Celsius in the spring and autumn. During the winter, daytime temperatures average roughly 6 degrees Celsius, but nighttime temperatures frequently fall below 0 degrees Celsius and occasionally below -10 degrees Celsius. Temperatures average barely a few degrees above zero in the coldest months of January and December, which are also the wettest.

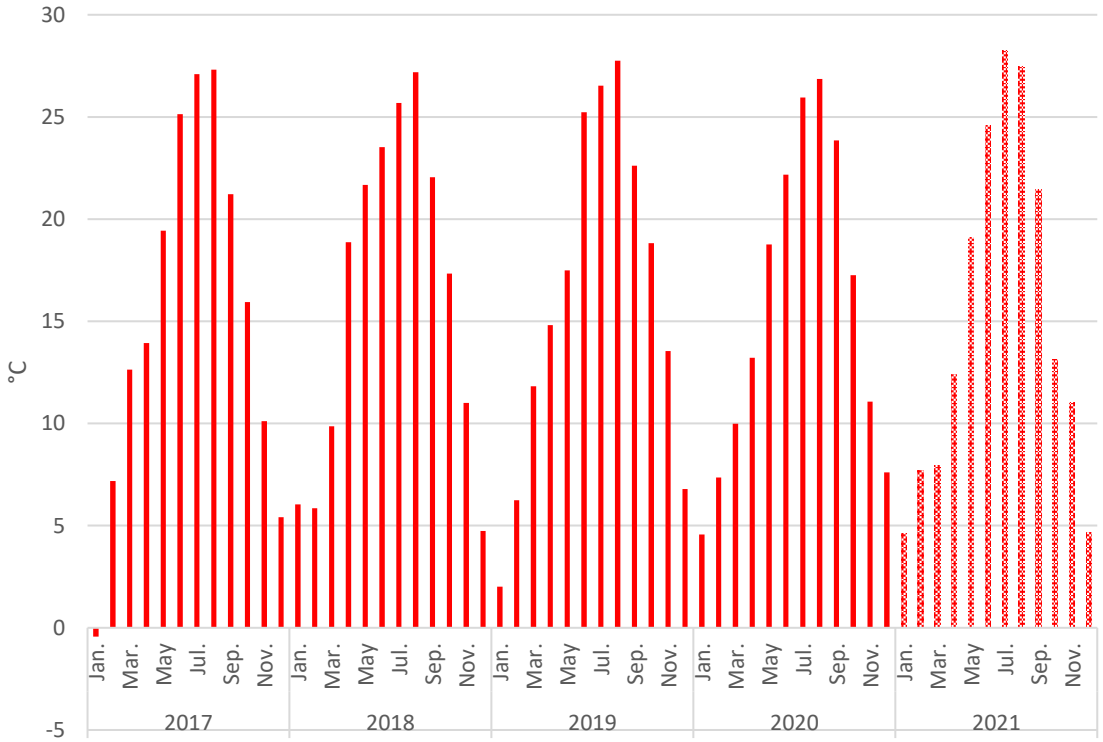

Figure 2. Monthly averaged temperatures in Skopje (2017-2021)

Because to the prominent rain shadow cast by the Prokletije Mountains to the northwest, precipitation is comparatively low, with precipitation being just a fraction of that obtained on the Adriatic Sea shore at the same latitude. The annual average precipitation is 357 mm (in the five-year period). March, April and May are often the wettest months of the year. From October to December

and from April to June, the highest precipitation is frequently experienced. Figure 3 depicts the monthly precipitation totals for the years 2017-2021.

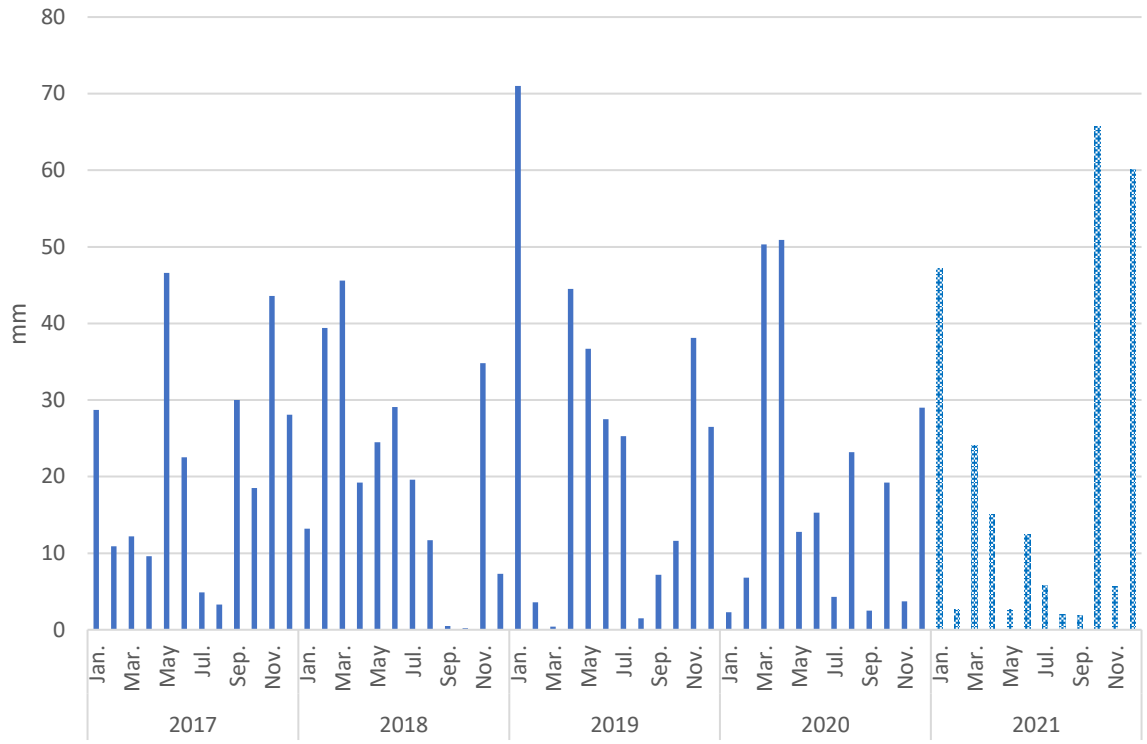

Figure 3. Monthly precipitation in Skopje urban area (2017-2021)

The total amount of sunshine that falls in the Skopje valley each year is approximately 2100 hours.

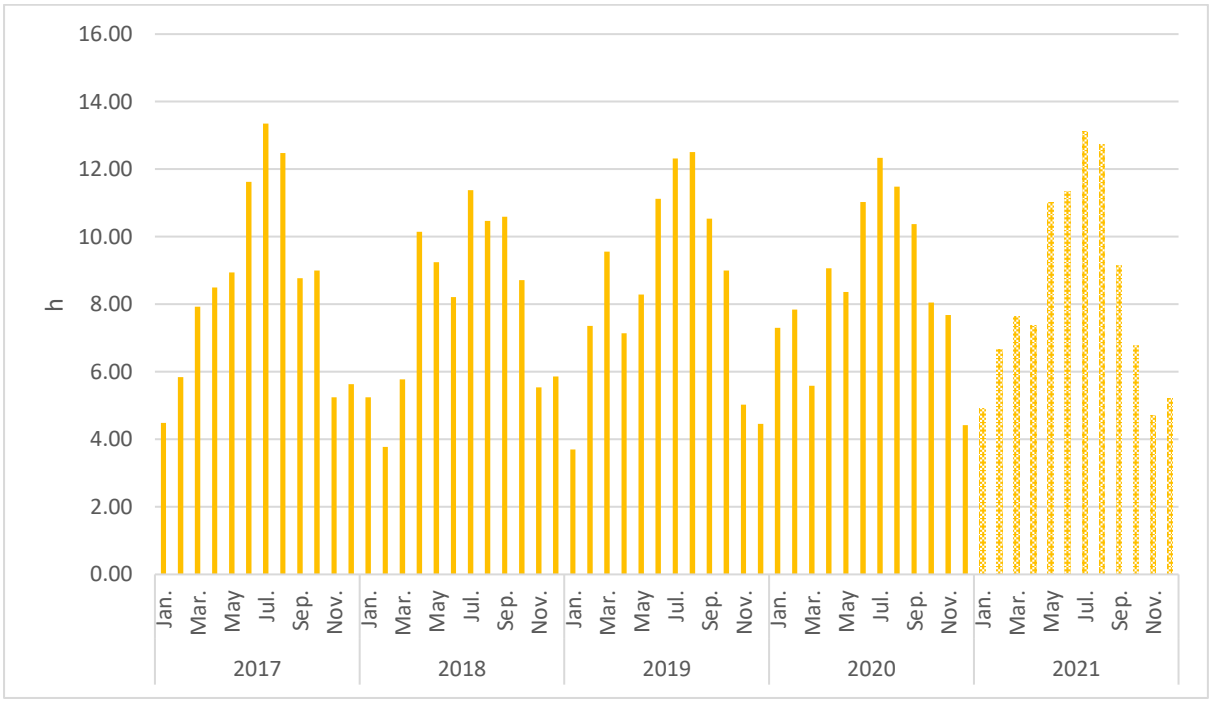

Figure 4. Monthly averaged sunshine hours for Skopje urban area (2017-2021)

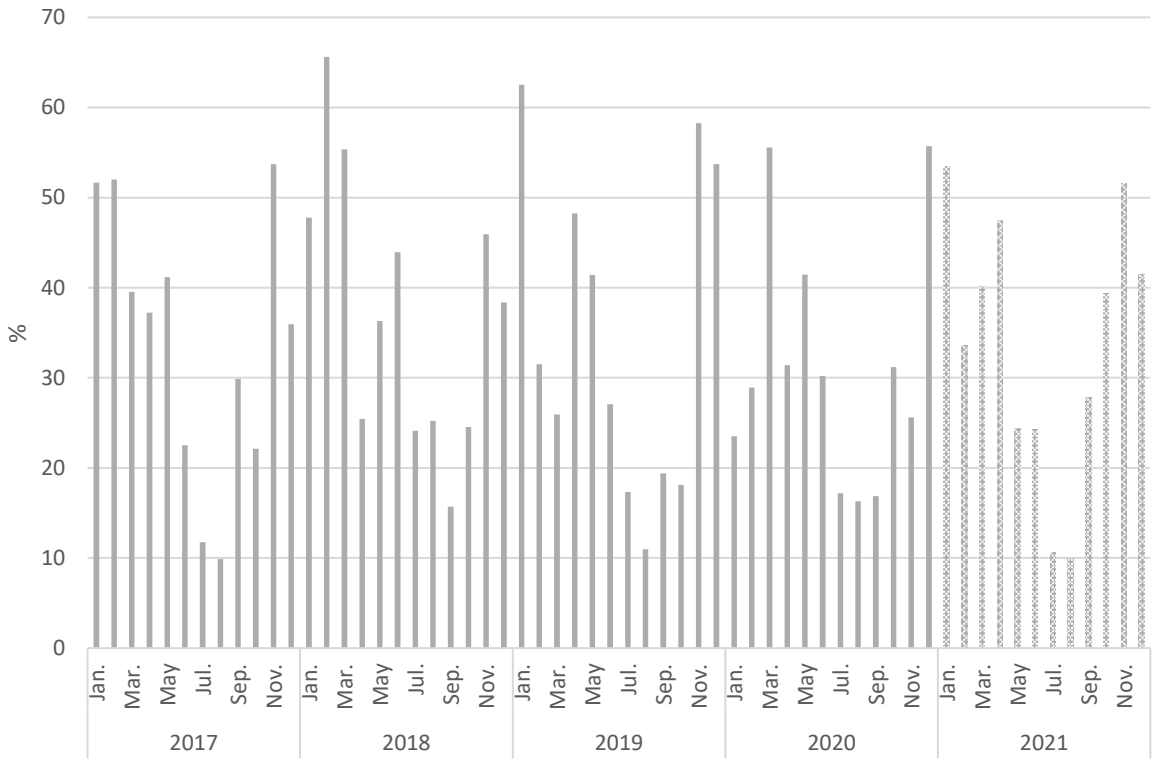

Figure 5. Monthly averaged percentage of cloud covers for Skopje urban area (2017-2021)

In accordance with the ERA 5 data model, the most frequent wind directions are westward and north-westward. As depicted in Figure 6, the wind speed and direction are indicated by a wind rose. Each sector of the wind rose is represented by a number of occurrences of the average wind sectors (from which the wind is blowing) and the average wind speed (meters per second) represented by a number of occurrences of each sector.

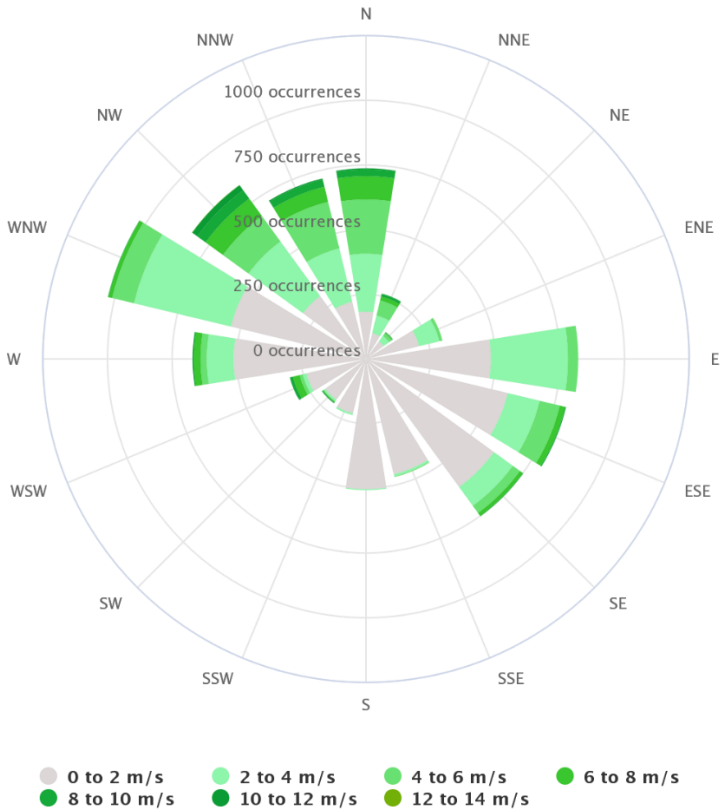

Figure 6. The wind rose in 2015, reflecting the average wind speed and direction in Skopje.

It is reasonable to assume that meteorology plays a significant role in the incidence of air pollution in Skopje. During the winter, extremely high levels of air pollution are recorded. During stable atmospheric conditions, high quantities are recorded, with released chemicals collecting in the valley. Due to lengthy periods of weak winds, minimal rain, and the development of temperature inversions, there is less circulation in the atmosphere during these periods. It also should be noted that all parameters for 2021, are within the average from previous 5 years, and this include temperature, humidity, precipitation, wind speed and direction, cloud cover and insolation hours.

2.1.3. Transportation and energy infrastructure

There are two major highways, the M3 and M4, that run along the northern and western banks of the river Vardar, respectively, and connect the south and north as well as the east and west. A ring road connects the northern part of the city to the southern part of the city. The total length of roads in the Skopje region is 919 kilometres, and the length of roads in the city of Skopje is 533 kilometres [9].

In 2020, there were 178 618 vehicles registered in Skopje, which is a record high. Table 2, shows the number of different types of vehicles registered in Skopje, as well as the segmentation of the vehicles fleet according to the type of fuels used [7].

Table 2. Number of registered vehicles in Skopje classified according to the type and fuel used

	Motorcycles	Passenger cars	Busses	Trucks	Light duty vehicles	Heavy duty vehicles
Petrol	4 261	79 247	52	3 514	30	71
Diesel	140	74 113	743	12 664	212	1 543
Mix	27	38	2	13	0	0
Methane/LPG	2	1 744	36	64	0	10
Electric	36	53	0	3	0	0

International rail connections connect Skopje with Belgrade in the north, Thessaloniki in the south, and Pristina in the west.

Skopje public transport is served by a bus system that is administered by the city and operated by several public and private companies.

In the Skopje region, all of the electric power utilized is supplied by the national power network. Power generation within Skopje boundaries is negligible.

In the City of Skopje, there is a city gas pipeline network of approximately 19 km in length, which supplies natural gas to industries and the energy sector. Approximately 70 000 m^3/h of capacity is provided by the network [8].

The heating network, which has a total length of 170 kilometres, serves the central areas of the City of Skopje. Five different heating plants provide the heat (hot water capacities of 295 MW, 230 MW, 100 MW, 70 MW and 28 MW). As of 2016, approximately 51 000 residences in Skopje are connected to the network, serving more than 33% of the city's total population. Approximately 4% of the households have their own boilers, with the remaining 63 percent being heated by other sources [8].

3. Major emission sources

Major emission sources in Skopje urban area were assessed and their respective emission estimated within several officially published documents, including but not limited to AQIP for Skopje agglomeration [8] and Integrated Polluters Inventory for Skopje [9].

3.1. Emission inventory

The following were the most significant sectors included in the emission estimation:

- Energy production,
- Industry,
- Traffic,
- Domestic heating,
- Waste management,
- Construction sites,
- Agriculture, and
- Transportation.

The information on the emissions from energy plants and industries that are associated with each pollutant were gathered from the stack measurements (emission measurements), which were performed in accordance with the emission permit requirements. Emissions from other sectors were estimated using a top-down method, as is the case with transportation. In accordance with the EEA emission estimating Guidebook, one or more activity indicators were specified for each emission sector. The majority of the information's pertaining to activity data were obtained from local or national statistics that have been suitably scaled to the area of interest (Skopje urban area) and emissions for particular pollutants were estimated by multiplying the activity data by emission factors given in the Guidebook.

3.1.1. Heat and energy production

As already mentioned, largest share of all of the electric power utilized in Skopje urban area is supplied by the national power grid. However, there are a number of heating plants that are connected to the district heating system that serves the entire metropolitan city center. The heat energy supplied by those plants provides approximately 30 % of the entire heating requirements of the city of Skopje [8].

Table 3. Energy plants located in Skopje [8]

Plant	Power capacity (MW)
TE-TO AD Skopje	230
AD ELEM Energetika, Skopje	100
Balkan Energy - Toplana ISTOK	295
Balkan Energy - Toplana ZAPAD	70
Balkan Energy - Toplana 11 Oktomvri	28
KOGEL	26.5 (thermal) 31 (electrical)

Table 4 shows the emissions associated with energy and heat generation in the City of Skopje, based on measurements taken in the plants in 2014[8]. The gradual replacement of heavy oil with natural gas as the primary fuel for district heating during the last several years, as well as the installation of low NOx burners in district heating facilities, has resulted in a major reduction of emissions into the environment from this sector.

Table 4. Total emissions from heat and energy production sector

	Pollutants (in t/year)			
Heat and Energy production sector	TSP	SO_x	NO_x	CO
Total emissions	4	8	182	10

3.1.2. Industry

Among the major industrial infrastructures in the Skopje Region are ferrous and nonferrous metal processing plants, chemical factories, a cement processing plant, asphalt and concrete production plants, and firms engaged in the production of food and beverages. List of identified industrial installations with significant emissions in Skopje [8] is given in the Table 5.

Table 5. Largest industrial installation with significant emissions [8]

Name of Company	Industry type
Makstil	Iron and steel
Arcelor Mittal	Iron and steel
RZ Institut	Non-ferrous metal
Johnson Matthey	Chemical
Alkaloid	Chemical
Titan USJE	Cement
JP Ulici i patista	Road paving with asphalt
Rade Koncar	Electrical supplies
Duropack	Packaging production
Pivara	Food and beverages
Imperial Tobacco	Tobacco

Table 6 lists the emissions associated with industrial production in the City of Skopje, based on data from the emission measurements taken in 2014 [8].

Table 6. Emissions associated with industrial production [8]

	Pollutants (in t/year)			
Industrial Production Sector	TSP	SO_x	NO_x	CO
Total emission	25	159	1528	2816

3.1.3. Traffic emissions

Emissions from the transportation sector include the exhaust emissions and non-exhaust part, which is caused by vehicle tyre and brake wear, as well as road surface wear. Emission assessment was performed in accordance with the European Environment Agency's manual on emission assessment, based on the information on the vehicles fleet for Skopje region (for 2014) that are generally believed to be a decent representation of the actual circulating fleet [8].

Table 7. Total emissions from the road transportation sector [8]

	Pollutants (in t/year)					
Road transport sector	CO	NH_3	NMVOC	NO_x	PM (exhaust + non-exhaust)	SO_2
Passenger Cars	3166	37	309	572	43	197
Light Duty Vehicles	270	2	27	105	12	21
Heavy Duty Vehicles	805	0	83	294	13	30
Buses	137	0	34	577	25	16
Motorcycles	50	0	11	2	0	2
Total emission	4428	39	464	1549	93	265

The total amount of emissions for the road traffic sector is summarized in Table 7 based on the data calculated for each class of vehicles and the total amount of emissions for each class of vehicles.

3.1.4. Domestic heating

The emissions from the domestic heating were estimated using the information of the annual fuel consumption in Skopje area and emission factors for small combustion residential plants [8]. The emission calculated does not include the electric energy consumption or the district heating related energy, because they are already included in the "energy production sector". Annual consumption of fuels used for estimation of emissions from the domestic heating sector in given below.

Table 8. Annual consumption of fuels

Fuel	Annual consumption of fuels	
wood	234 978	m^3
coal	1 275	t
heating oil	754	t
LPG	525 466	kg

Table 9 summarizes the total amount of estimated emissions for the household heating sector, where wood burning emissions accounts for nearly all (99%) of the overall emissions from domestic heating.

Table 9. Total emissions from domestic heating sector [8]

	Pollutants (in t/year)					
Domestic heating sector	CO	NH_3	NMVOC	NO_x	SO_x	PM
Biomass	10 247	179	1 537	128	28	2 049
Coal	39	0	4	1	8	4
LPG	0	Na	0	1	2	0
Heavy oil, liquid oil	2	0	0	2	2	0
TOTAL	10 289	179	1 541	132	41	2 053

3.1.5. Waste management

Emissions from waste management activities included waste incineration and waste disposal activities at Drisla Regional Landfill. Both the medical waste incineration and solid waste disposal emissions were calculated using the fundamental approach outlined in the EEA Guidebook 2013[8]. Estimation presented is based on data from MOEPP and Drisla Regional Landfill operator for 2014, and include landfilling activities for 153732 tons of municipal solid waste, and incineration of approximately 711 tons of medical waste. Table 10 shows the estimated emissions associated with these activities.

Table 10. Emissions from waste management sector

Waste management	Pollutants (in t/year)				
Type of treatment	CO	NMVOC	NO_x	PM	SO_x
Waste incineration	0.1	0.5	1.6	12.1	0.4
Waste disposal	na	239.8	na	0.1	na
TOTAL	0.1	240.3	1.6	12.2	0.4

3.1.6. Construction

The emissions from construction sites (for particulate matter) were estimated according to the basic approach included in the EEA Guidebook 2013, assuming construction of approximately 168 866 m^2 of dwellings during the 2014 [8]. No data for other construction activities were included (infrastructure, commercial buildings etc.). The estimated emission related to these activities are listed in Table 11.

Table 11. Emissions from construction activities

	Pollutants (in t/year)
Construction sector	PM_{10}
Construction sites	27
TOTAL	27

3.1.7. Agriculture

Emissions from agricultural practices include manure management (animal husbandry and emissions associated with manure application to land), as well as the use of synthetic fertilizers. Estimations are based on data for animals bred in 2014, while emission associated with the usage of synthetic fertilizers were evaluated using the fundamental approach outlined in the EEA Guidebook 2013 [8]. Estimations assume 80 598 hectares of arable land and 84 tonnes of nitrogen used as fertilizer. Table 12 summarizes the overall emissions associated with agricultural activities.

Table 12. Emissions from agriculture

	Pollutants (in t/year)			
Agriculture	NH_3	NMVOC	NO_x	PM
Manure management	809	346	5	50
Use of fertilizers	6	69	2	na
TOTAL	815	416	7	50

3.2. Total emissions

The total emissions estimated for CO, NH3, NMVOC, NOx, SOx, and PM10, grouped by emission sector, are listed in Table 13 [8].

Table 13. Total emissions for Skopje Region (reference year 2014) [8]

	Emission estimation (in t/year)					
Sources	CO	NH_3	NMVOC	NO_x	SO_x	PM
Traffic	4 428	39	464	1 549	265	93
Industrial production	2 816	na	na	1 528	159	25
Energy plants	10	na	na	182	8	4
Domestic heating	10 289	179	1 541	132	41	2 053
Waste management	0	na	240	2	0	12
Agriculture activities	na	815	416	7	na	50
Construction sites	0	na	0	0	0	27
GRAND TOTAL	17 543	1 033	2 661	3 400	473	2 264

Emissions summarized in Air quality improvement plan for Skopje agglomeration [8] differ from the estimations presented in updated Integrated Polluters Inventory for Skopje [9], mostly due to different approach in data organisation and calculations, as much as different reference years (2014 vs 2019).

Air quality improvement plan for Skopje agglomeration does not include carbon dioxide emissions (CO_2), while Integrated Polluters Inventory for Skopje, does not include ammonia emissions for (NH_3). The emissions of the majority of pollutants assessed in the Skopje Integrated Polluters Inventory [9] are much greater than those estimated in the Air quality improvement plan for Skopje agglomeration [8], particularly particulate matter, carbon monoxide, and NMVOC emissions.

Table 14. Total emissions for City of Skopje (reference year 2019)[9]

	Emission estimation (t/year)					
	SO_x	CO	CO_2	NO_x	TSP	NMVOC
Stationary sources	37	1 187	1 164 243	1 911	84	147
Residential sources	72	36 882	1 022 796	475	7 172	5 601
Mobile sources	6	8 911	706 839	3 957	312	1 241
Fugitive emissions						594
GRAND TOTAL	116	46 979	2 893 879	6 344	7 568	7 583

However, both documents' point residential heating as a single important source of particulate matter emissions, responsible for more than 90 % of total particulate emissions.

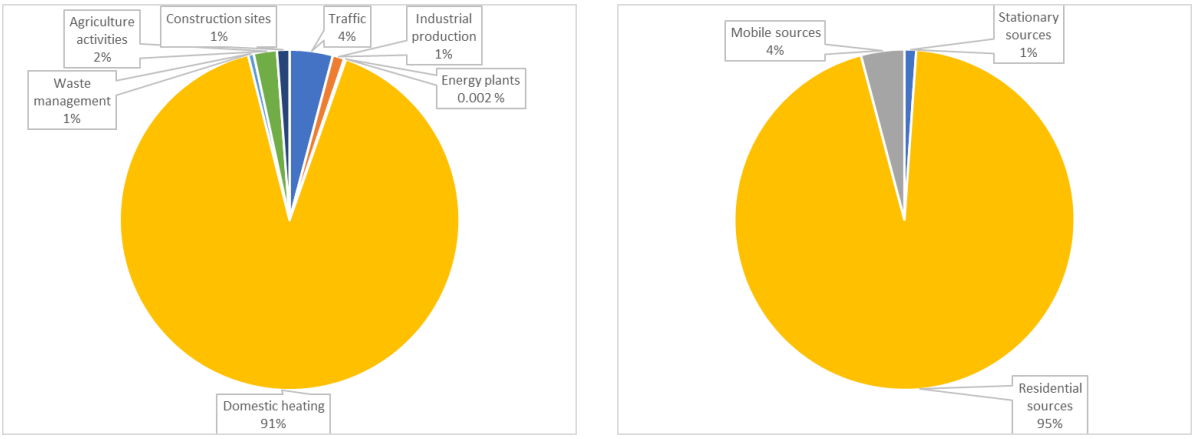

a. Particulate matter emssions AQIP-2014 [8] b. Particulate matter emissions IPI -2019 [9]

Figure 7. Particulate matter emission contribution by sources in Skopje

3.3. Source profiles

Chemical profiles of the sources identified in the inventory were obtained using the data published in SPECIEUROPE, a repository of source profiles developed by the JRC in the framework of FAIRMODE project [10]. SPECIEUROPE comprises chemical profiles of particulate matter, both organic and inorganic, derived from measurements of European sources and source apportionment investigations conducted in Europe.

Based on data given in the emission inventories, chemical profiles for following sources are included:

- Cement industry,
- Still works –arc furnace
- Biomass burning
- Open burning of crop residues
- Construction
- Traffic urban + Vehicle Exhaust
- Soil dust + Road dust
- De-icing Salt
- Fuel oil + Residual oil

A brief description of the source, sampling and analytical procedures that were employed, geographical location, elemental composition (relative mass of the elements), and bibliography are provided in the sections that follow.

Selected cement industry profile is based on grab sample from cement plant in Volos, Greece. Sample was resuspended in chamber and analysed using energy dispersive X-ray fluorescence (ED-XRF) for

elemental composition and ion chromatography (IC) for water soluble ions analysis. Calcium is by far most abundant element (36.02 %), followed by Si (3.93 %), Fe (1.7 %) and Al (1.59 %). Ammonium (6.36 %) and nitrates (2.85 %) are most abundant ions.

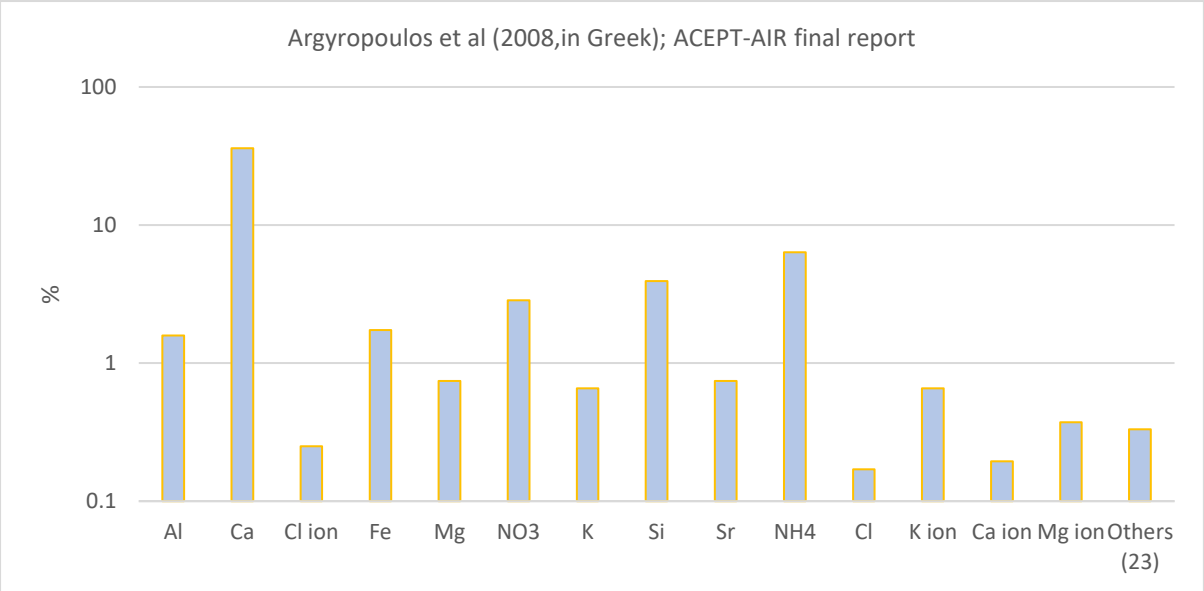

Figure 8. Cement industry chemical profile

Still production industry profile is based on grab sample from Still processing plant that include arc furnace smelting in Volos, Greece. Sample was resuspended in chamber and analysed using energy dispersive X-ray fluorescence (ED-XRF) for elemental composition and ion chromatography (IC) for water soluble ions analysis. Iron (Fe) is most abundant element (34.92 %), followed by Sn (7.69%), Mn (7,69%), Si (6.82 %), Ba (4.03 %), Ca (4.03 %), Cd (3.144%), Zn (2.59 %) and Cr (1.64 %). Nitrates (2.85 %) are most abundant ion.

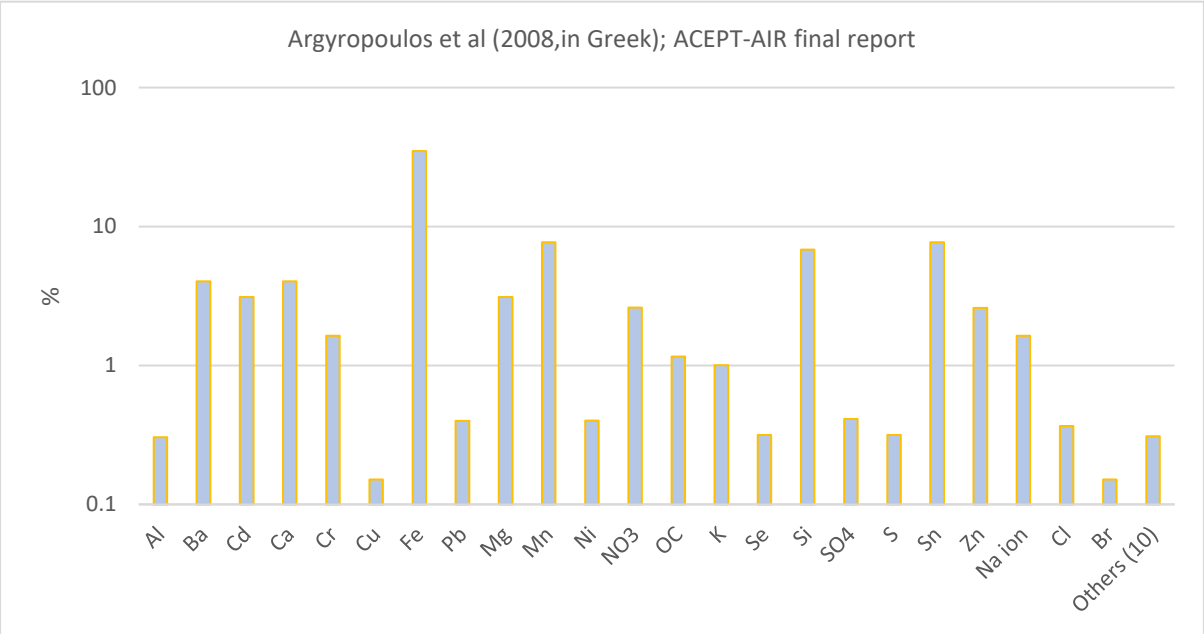

Figure 9. Still production industry chemical profile

Biomass burning profile is based on JRC data, referencing closed fireplace wood combustion in Krakow, Poland. Elemental analysis was performed using particle induced x-ray emission (PIXE), photometric and ion chromatography (IC) methods are used for water soluble ions analysis, thermal optical analysis (TOT) was used for OC and EC analysis, and gas chromatography-mass spectrometry

(GC-MS) for organic compounds. Organic carbon (OC) and elemental carbon (EC) are by far most abundant compounds (89.63 and 6.65 % respectively), followed by K (1.11 %) and Cl (0,43%). Sulphates (0.87%) and nitrates (0.25 %) are most abundant ions.

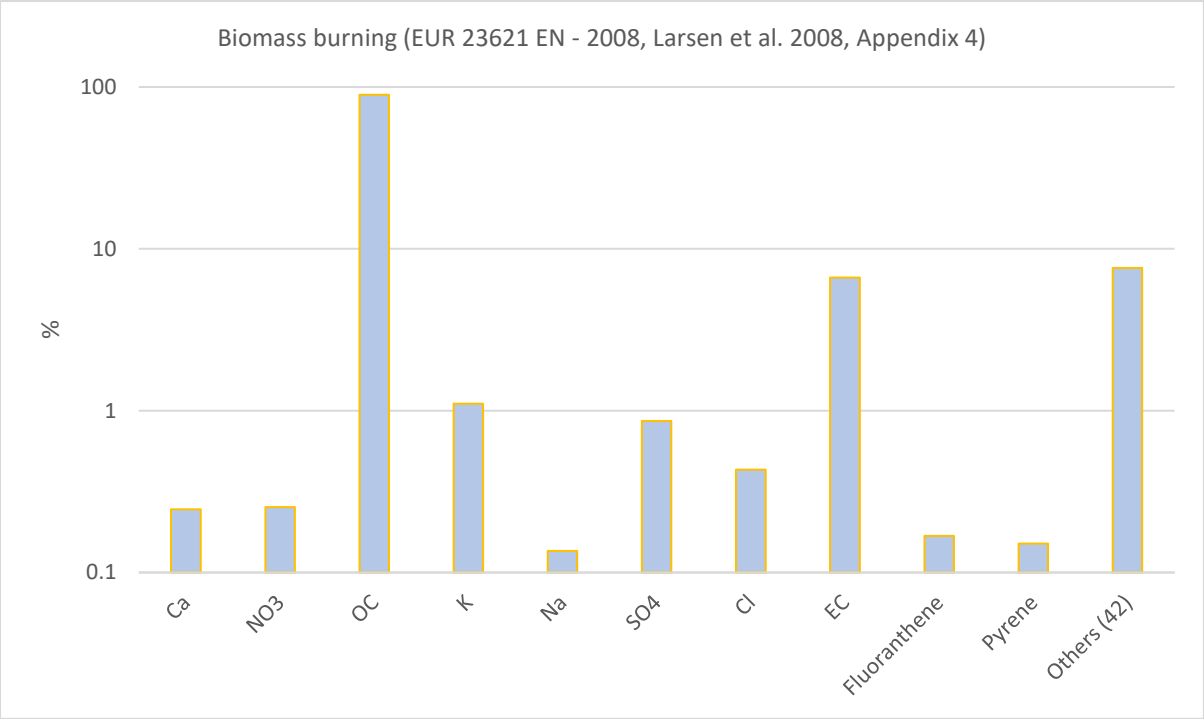

Figure 10. Biomass burning in closed fireplace chemical profile

Open burning of crop residues, or agricultural fields burning profile is based on direct on filter samples from Thessaloniki area in Northern Greece. Samples were analysed using energy dispersive X-ray fluorescence (ED-XRF) for elemental composition and ion chromatography (IC) for water soluble ions analysis. Bromine is most abundant element (9.43 %), followed by EC (9.0 %) and Co (9,0%). Other metals including V (8.133 %), Ti (4.83 %) and As (1.1 %) also have significant concentrations. Sulphates (8.13 %) are by far most abundant ion.

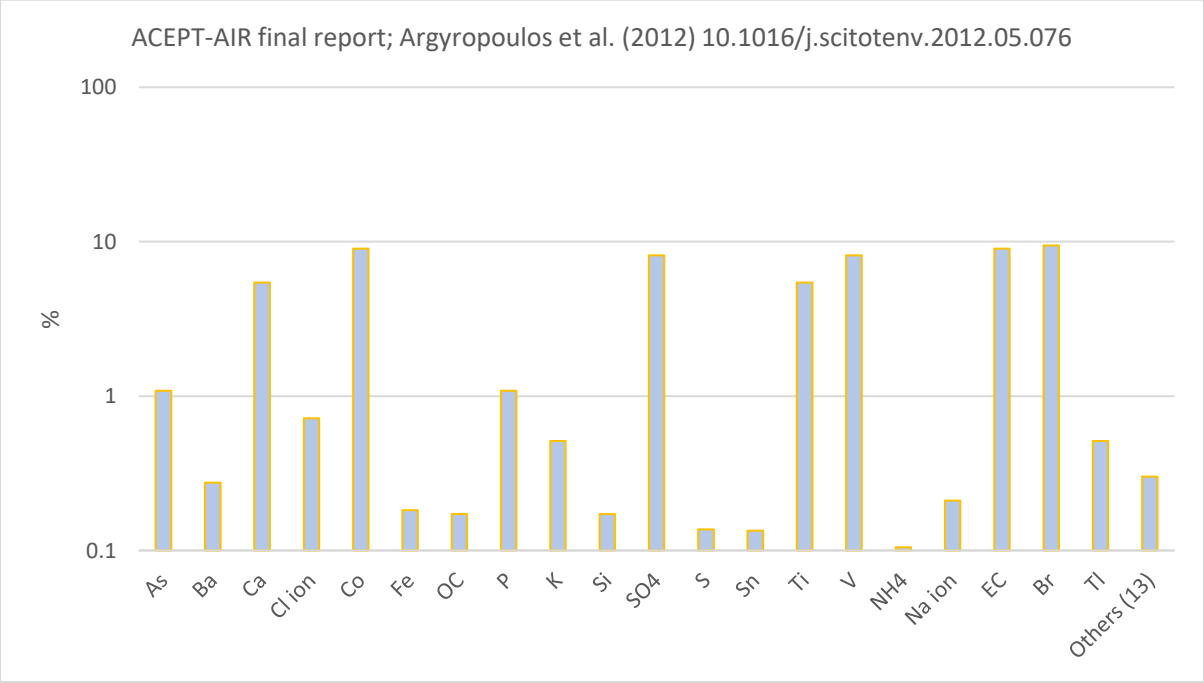

Figure 11. Open burning of crop residues chemical profile

Construction activities source profile is based on data obtained from Milan, Italy. Specific information's about sampling and analytical procedures used, were not provided. Calcium is most abundant element (19.85 %), closely followed by OC (17.9 %) and Si (12,55 %). Other metals including Ni (7,66 %), Al (3.78 %), Fe (1.91 %) and K (1.71 %) also have significant concentrations. Sulphates (9.14 %) and ammonium (1.96 %) are most abundant ions.

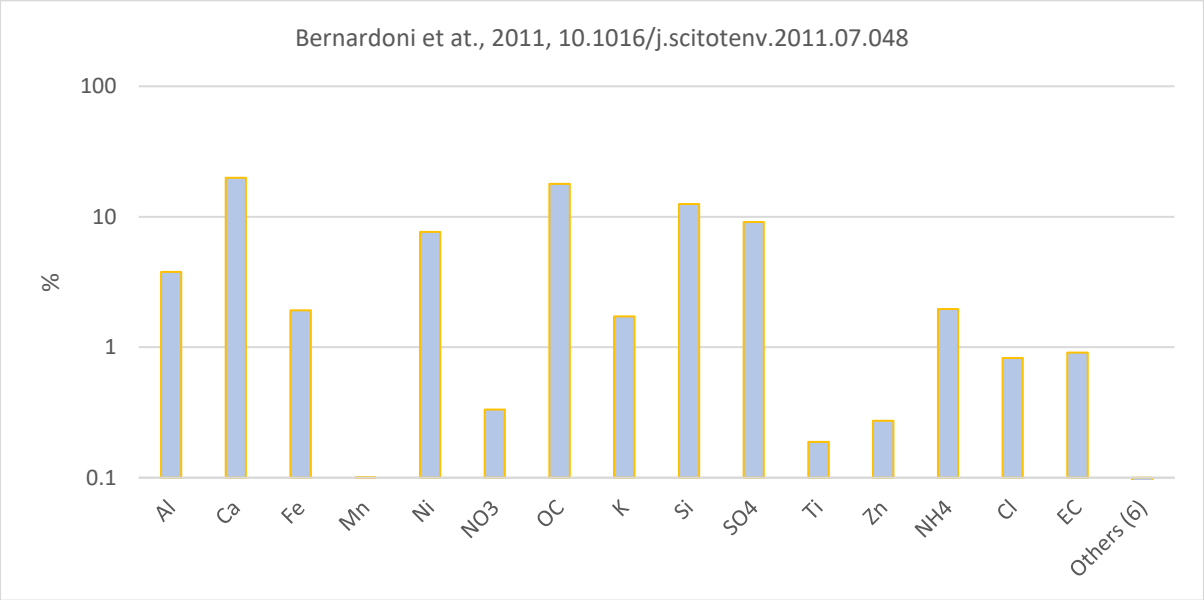

Figure 12. Construction activities chemical profile

Traffic source profile include two separate profiles, exhaust diesel and gasoline and urban traffic profile, based on data from PMF exercises in Valtellina, Po Valley, and Genoa Corso, Firenze in Italy. Specific information's about sampling and analytical procedures used, were not provided. OC and EC are most abundant compounds in both profiles, OC (53.59 and 35.1 %) and EC (30.46 and 23.04%) respectively. Some metals including Fe (13.56 and 2.34%), Cu (1.1%) and Si (0.89 %) in mixed exhaust and Ca (1.89 %) in urban traffic mix, also have significant concentrations. Sulphates (5.05 %) are by far most abundant ion in mixed exhaust, while ammonium (1.68 %) and nitrates (1.51 %) are most abundant ions in urban traffic mix.

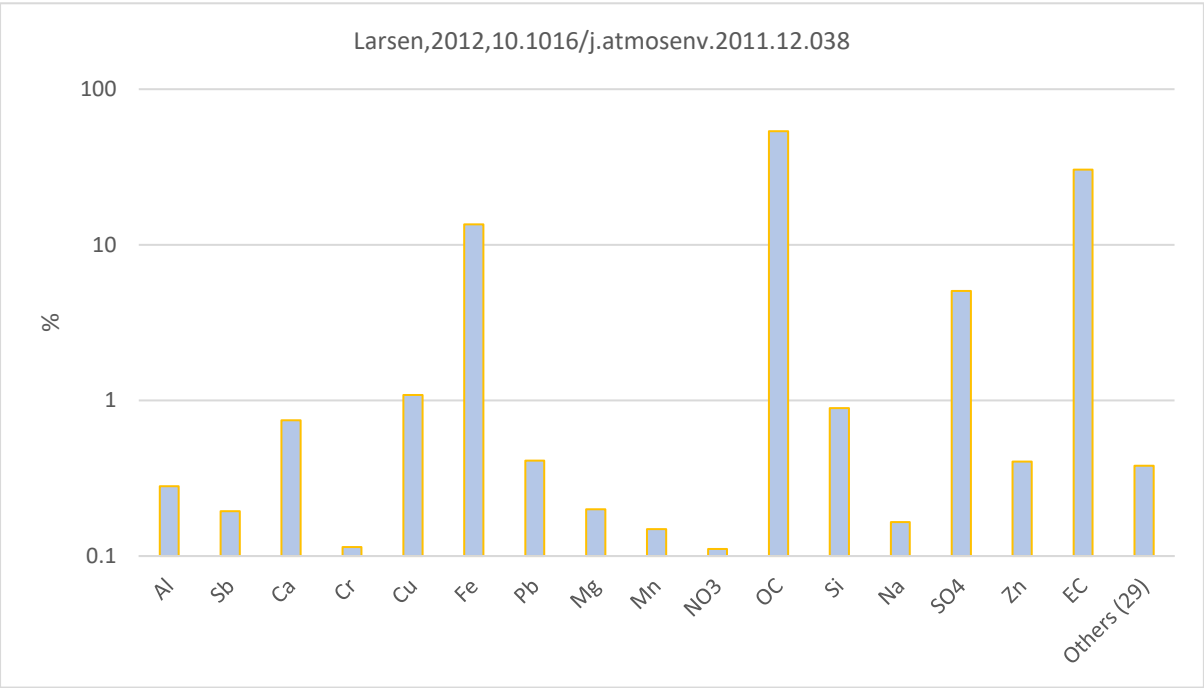

Figure 13. Exhaust diesel and gasoline chemical profile

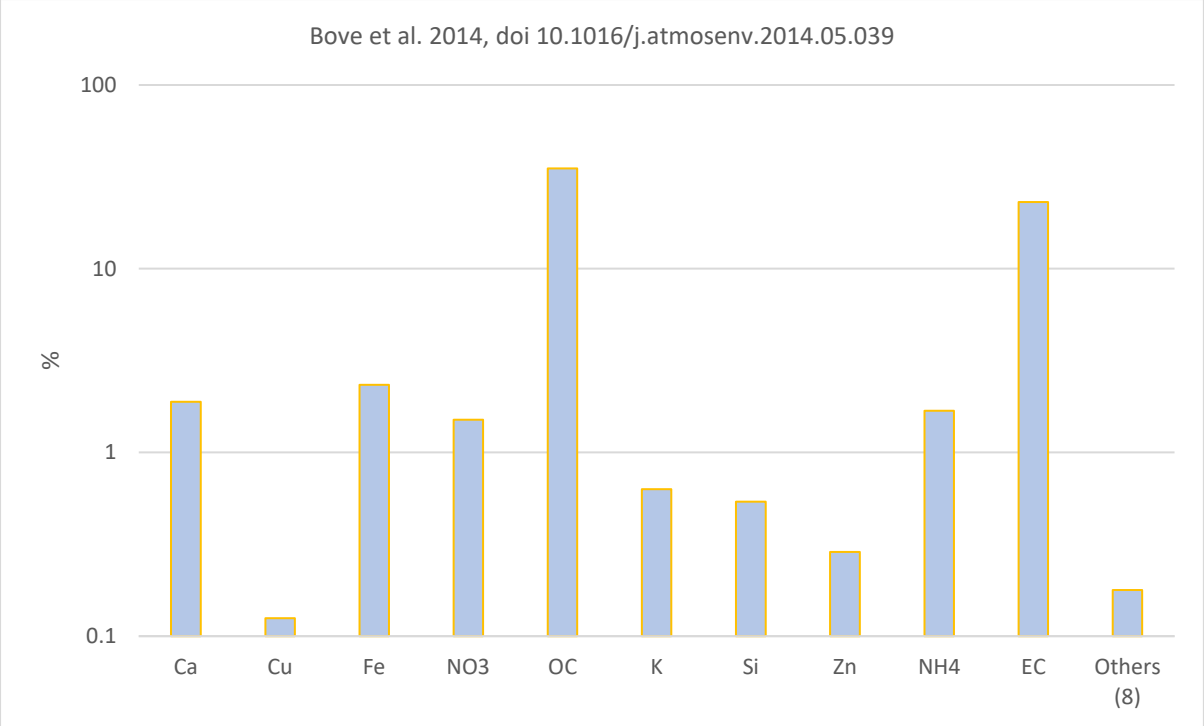

Figure 14. Urban traffic chemical profile

Road dust is another profile associated with traffic emissions. The profile selected is based on data from PMF exercises in Valtellina, Po Valley in Italy. Description of sampling and analytical procedures used, was not included. Silica is most abundant elements (15.63 %), followed from OC (7.25 %), Al (7,07 %), Fe (4.19 %), Ca (2.41 %), Mg (1.37%) and K (1.43 %). No significant concentrations of water-soluble ions were reported.

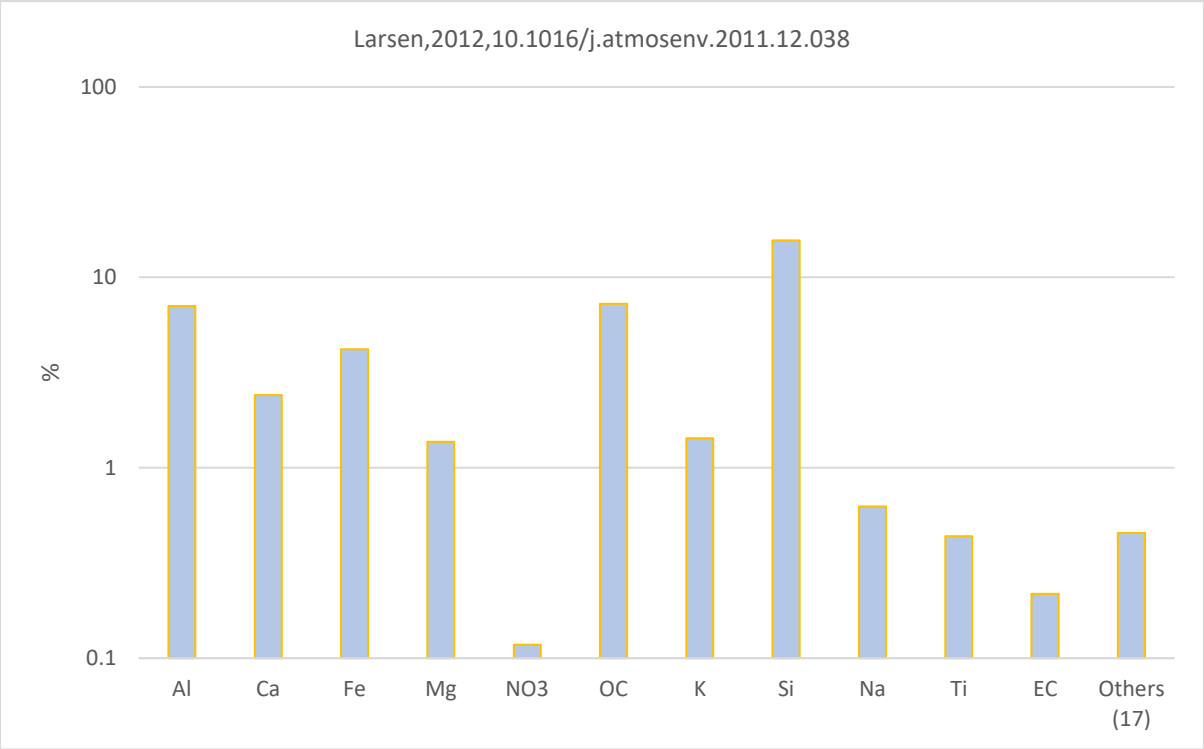

Figure 15. Road dust chemical profile

Soil dust profile is based on grab dust samples collected from the fabric filter from Thessaloniki area in Northern Greece. Samples were dried and resuspended in a puff of clen air, then sampled with PM10 inlet with LVS, and analysed using energy dispersive X-ray fluorescence (ED-XRF) for elemental

composition and ion chromatography (IC) for water soluble ions analysis. Silica is most abundant element (20.9 %), followed by Al (5.65 %), Fe (4,36 %), Ca (3.20 %), Mg (1.56 %), K (1.37%) and Ti (0.41 %). No significant concentrations of water-soluble ions were reported.

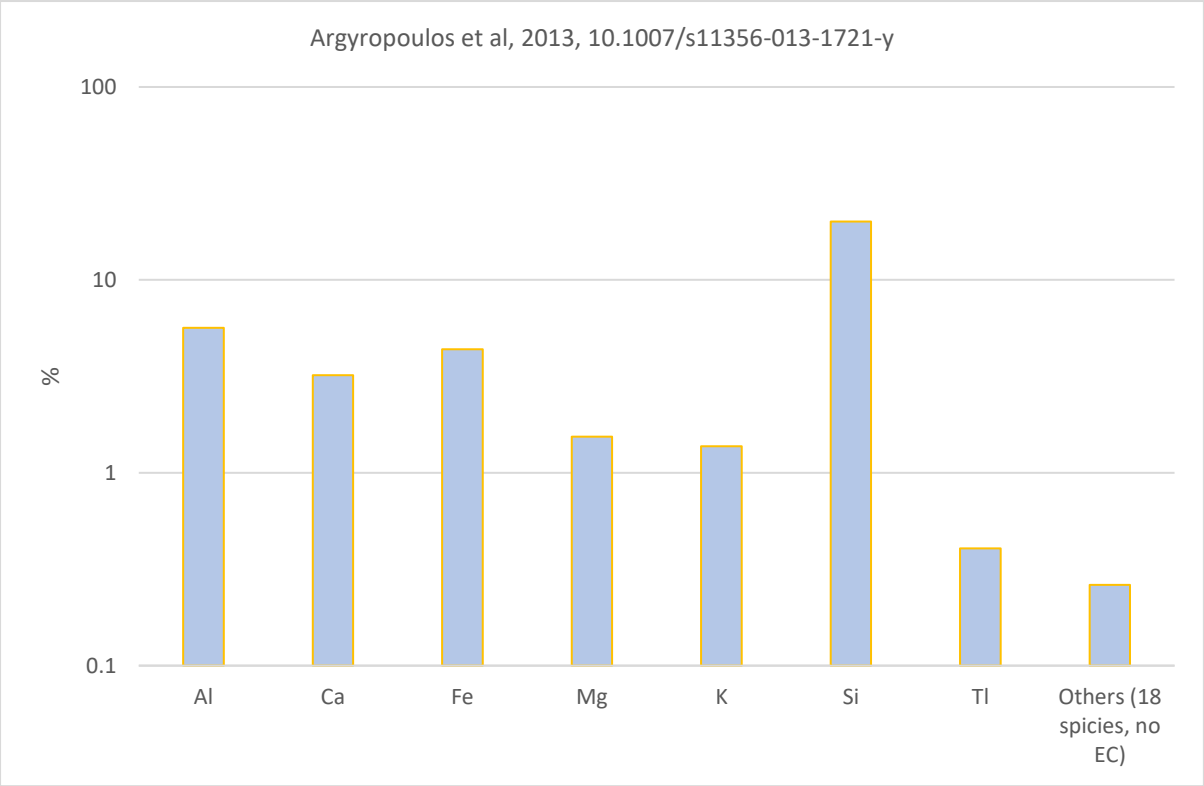

Figure 16. Soil dust chemical profile

Fuel and residual oils burning includes emissions from a wide range of sources, the majority of which are larger buildings heating systems (schools, hospitals, and other public institutions), industrial combustion emissions and to some extent older diesel-powered vehicles emissions.

Residual oil chemical profile is based on data from PMF exercise in Genoa Corso, Firenze in Italy. Samples were analysed using energy dispersive X-ray fluorescence (ED-XRF) for elemental composition, ion chromatography (IC) for water soluble ions analysis, and thermal optical analysis (TOT) for OC\EC analysis. Elemental carbon is by far most abundant compound (31.3 %), followed by sulphates and ammonium ions (23 and 5.75% respectively). As of metals, iron and vanadium exhibit highest concentrations (0.98 and 0.76 % respectively), followed by Ni (0.28 %), K (0.128 %) and Ca (0.10 %).

Fuel oil chemical profile is based on JRC data on small (<5MW) fuel oil boilers emission in Krakow, Poland. Specific information's about sampling and analytical procedures used, were not provided. Organic carbon is most abundant compound (25.3 %), followed by nitrates (18.53 %) and sulphates (13.78 %). Other elements include Ca (1.2 %), Cl (1.16 %), Mg (0.57 %), Al (0.42 %), V (0.16 %) and Ni (0.14 %).

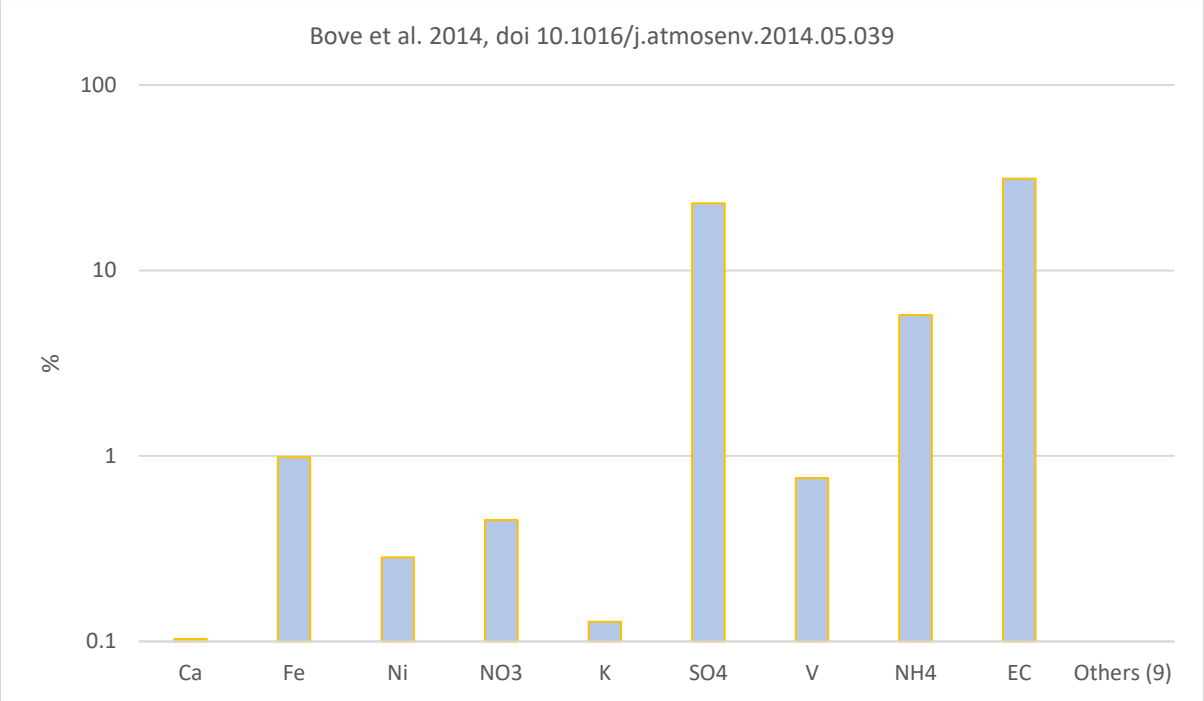

Figure 17. Residual oil chemical profile

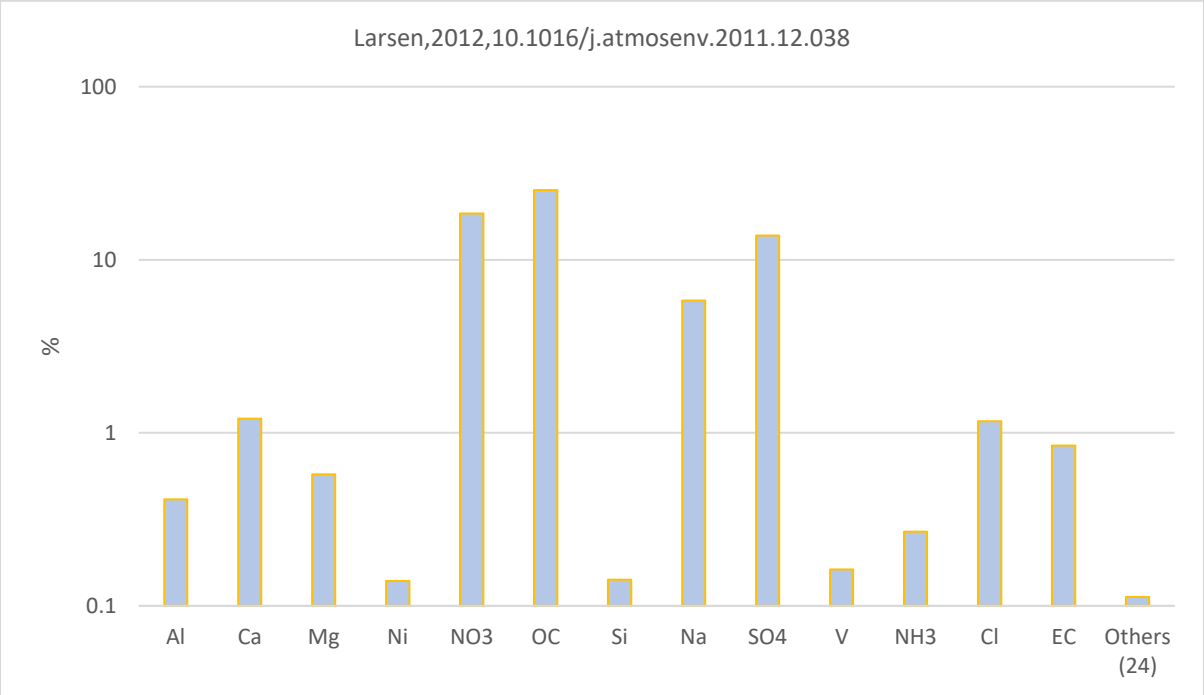

Figure 18. Fuel oil chemical profile

The source profiles outlined above were utilized to assign source categories to factors generated during positive matrix factorization. This procedure was supported with quantitative and descriptive comparison of the factor chemical profiles with those measured at the source and profiles from previous source apportionment studies in the literature, as given above.

4. Particulate matter sampling and analysis

Considering the SA study goals, current data availability, the project document requirements guidelines for air pollution source apportionment with receptor models [11], in total five (5) specific receptors/sampling points were selected and set within Skopje agglomeration. As agreed in close consultations with all stakeholders involved and with support of MOEPP technical teams, the sampling points include two permanent (full year coverage) sites:

- Karposh state network monitoring site (our code MP1-AQP), as a representative for urban background (no direct exposure to significant sources),
- Novo Lisiche state network monitoring site (our code MP2-AQP), as a representative for urban site, exposed to mixture of sources in the area (traffic, residential heating, and mixed industrial sources).

In addition, and in order to improve source impact zone delineation and increase data quality, as an input for RM development, three indicative monitoring sites (partial coverage in each season) were set as follow:

- Primary school “Dimitar Pop Gergiev - Berovski in Gorce Petrov as a site under possible influx of pollution along the Vardar and Treska rivers valleys (our code MP3-AQT).
- Primary school “Joakim Krcovski” in Volkovo as a site under possible influx of pollution along the Lepenec river valley (our code MP4-AQT).
- Gazi Baba state network monitoring site (our code MP5-AQT), as a representative for specific industrial exposure.

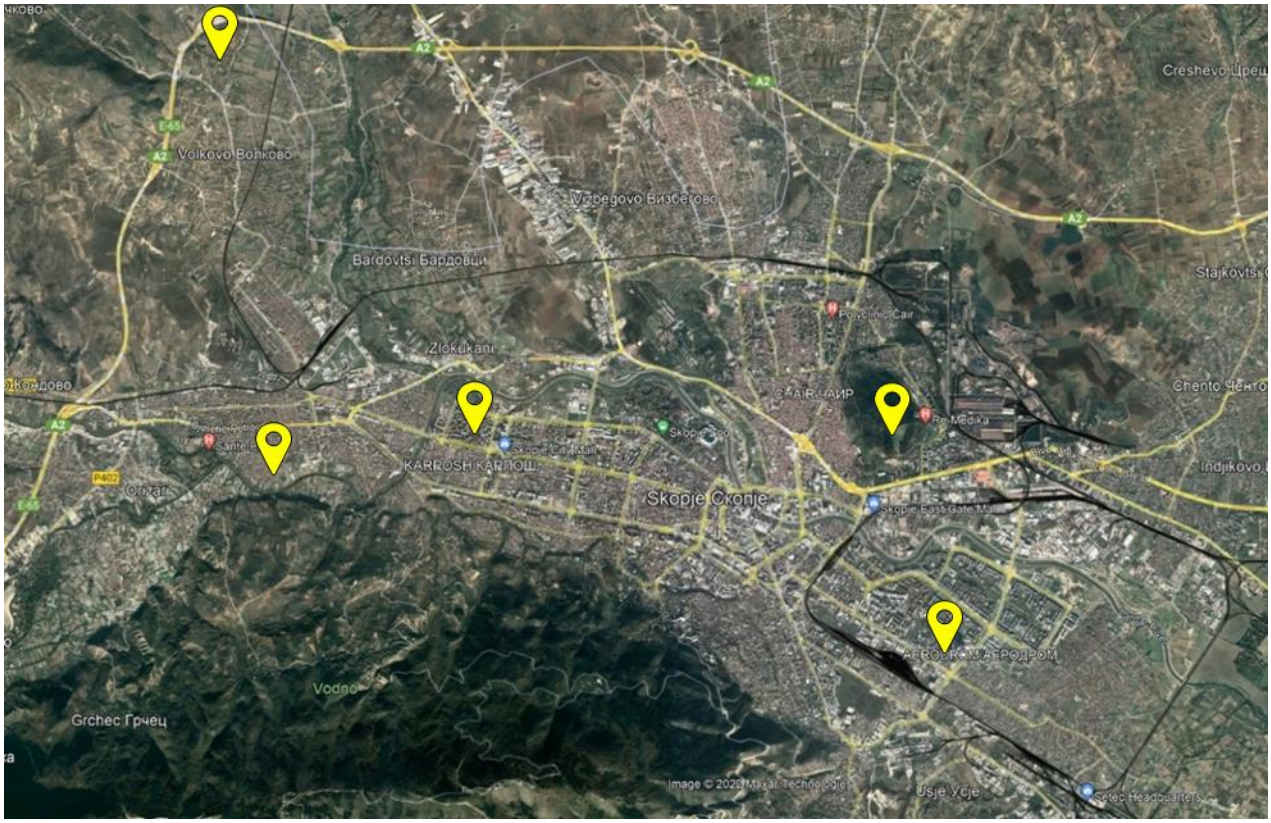

Figure 19. Monitoring sites map

Sampling programs were simultaneously launched at two permanent and one indicative site on 29.10.2020 and ended on 04.12.2021. During this period a total of 376 samples were taken at Karposh sampling site (MP1-AQP), 367 at Lisiche sampling site (MP2-AQP) and 60 samples at each of the temporary sampling sites (MP3-AQT, MP4-AQT and MP5-AQT). Details of monitoring sites are given bellow.

Novo Lisiche - permanent monitoring site (MP1-AQP)

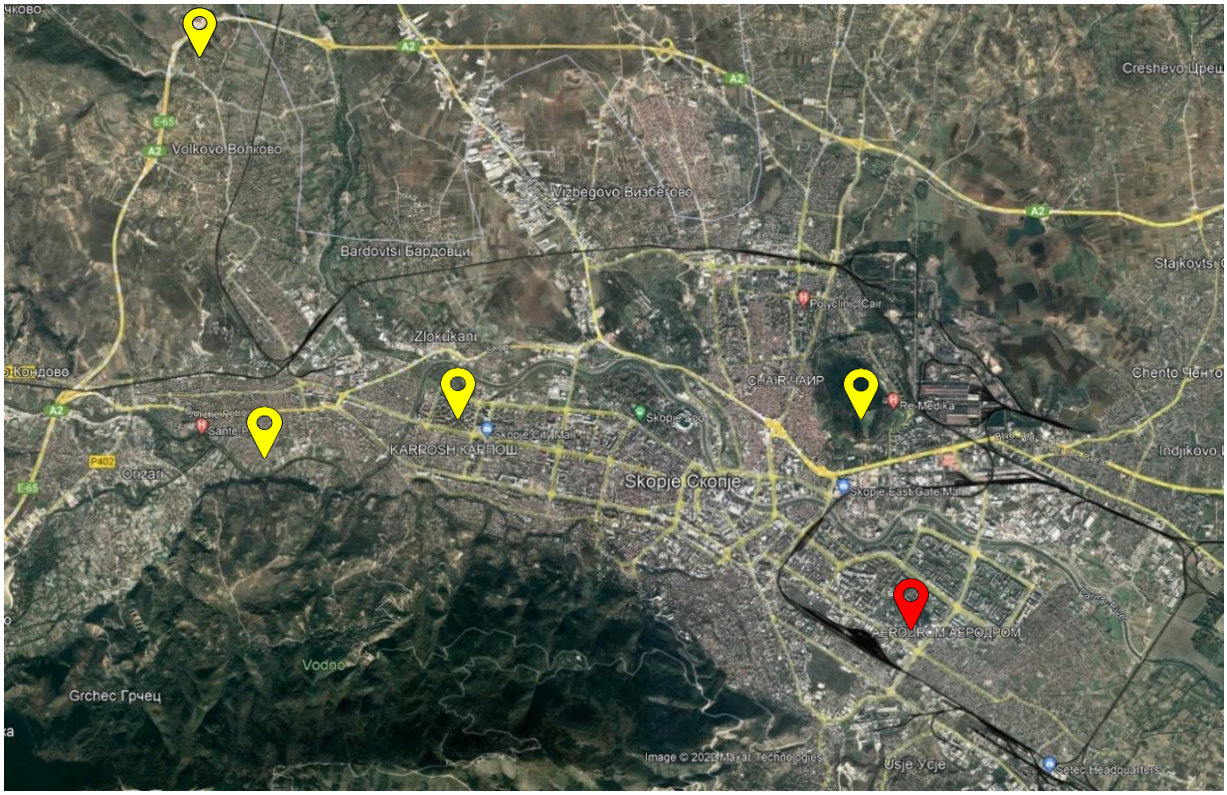

Monitoring site is positioned close to a major intersection. The distance to the nearest street is 45 m and to the intersection 70 m. A cement factory is located 1.2 km in the south-west direction to the station and a marl quarry at a distance of 1.8 km. Area surrounding immediate vicinity of the site represent mix of commercial and residential zones.

Site photo

GPS coordinates: Y = 7.538.493; X = 4.647.405

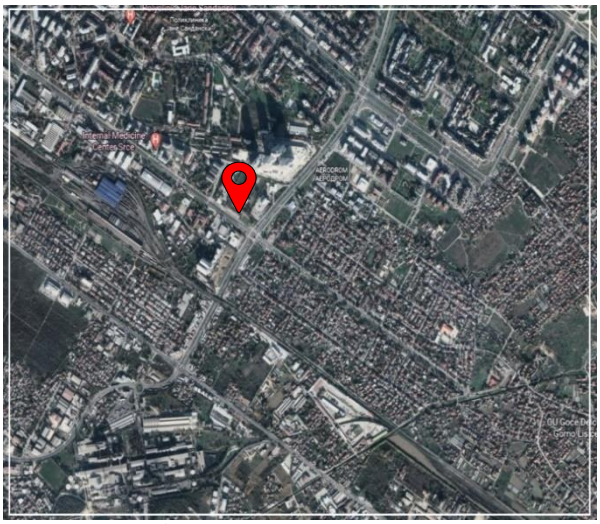

2 x 2 km^2 Area around the Monitoring Site

Karposh - permanent monitoring site (MP2-AQP)

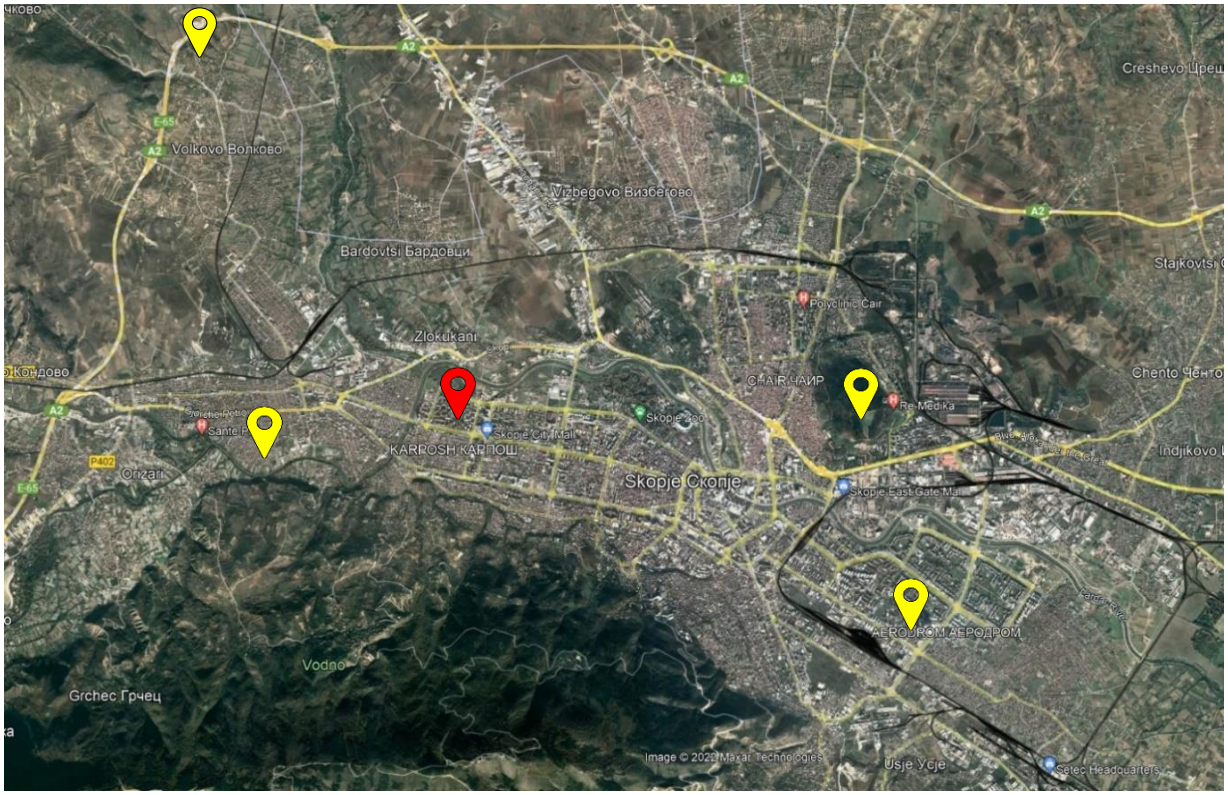

Monitoring site is positioned in a school yard in the middle of an urban residential area in the western part of Skopje. The nearest low-speed residential roads are 20–120 m away and major boulevards are located approximately 250 m away. This urban background station represents the overall city background concentrations.

Site photo

GPS coordinates – Y - 7.532.044 X - 4.650.585

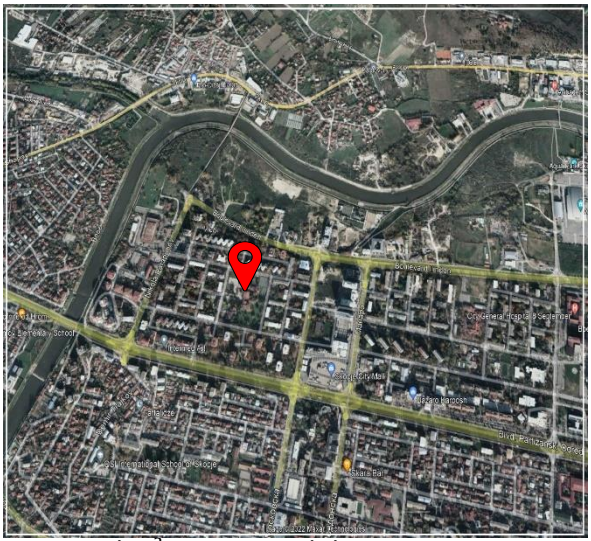

2 x 2 km^2 Area around the Monitoring Site

Gorce Petrov (Hrom) - indicative monitoring site (MP3-AQT)

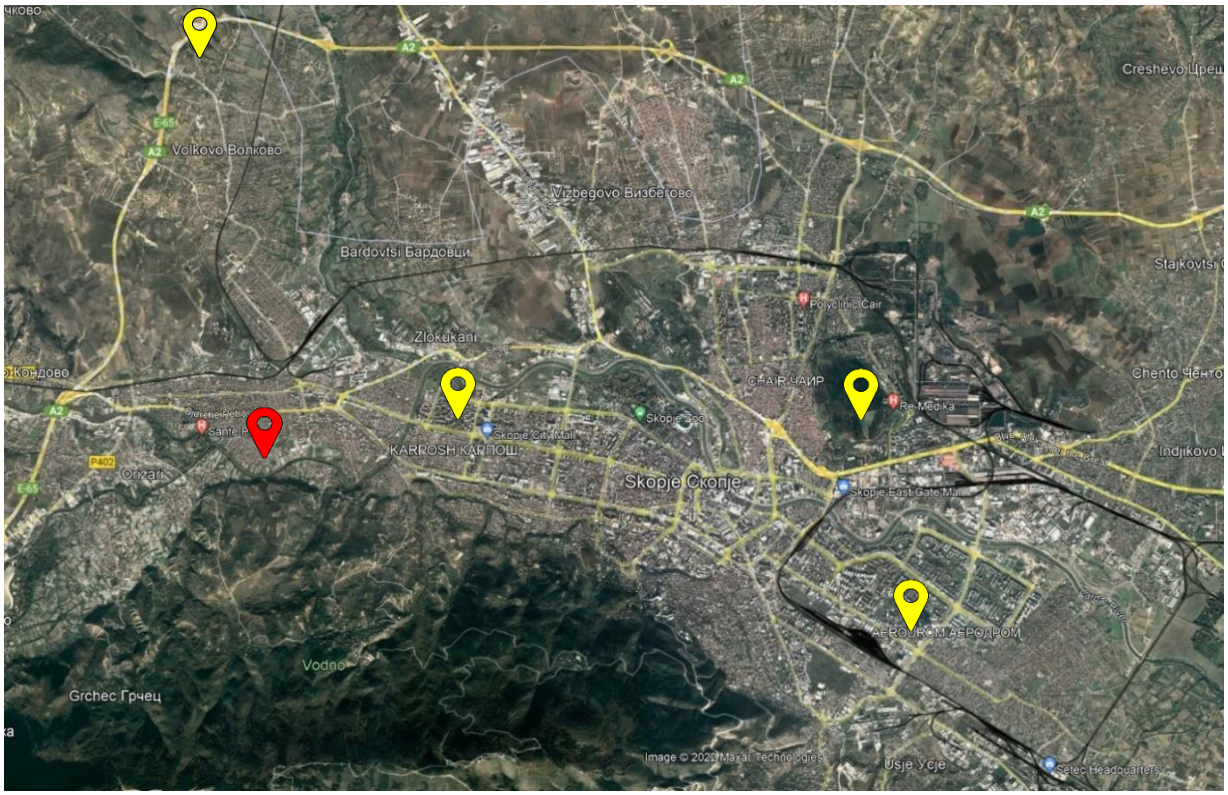

The site is located in urban area with low speed streets and mostly individual housing in the backyard of “Dimitar Pop Georgiev – Berovski” primary school.

Site photo

GPS coordinates – Y - 7.529.605 X - 4.650.217

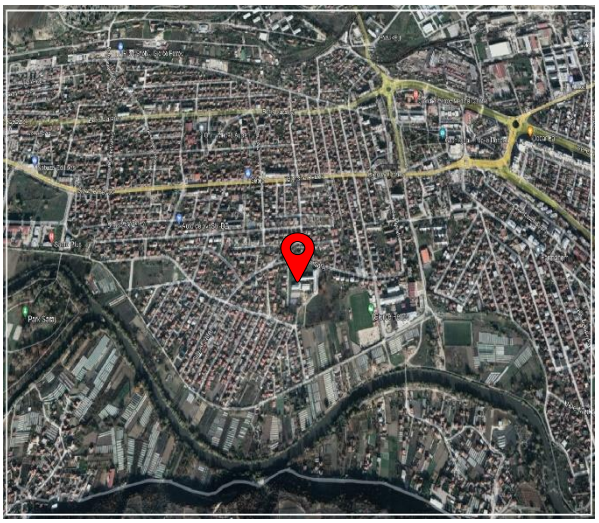

2 x 2 km^2 Area around the Monitoring Site

Gorce Petrov (Volkovo) - indicative monitoring site (MP4-AQT)

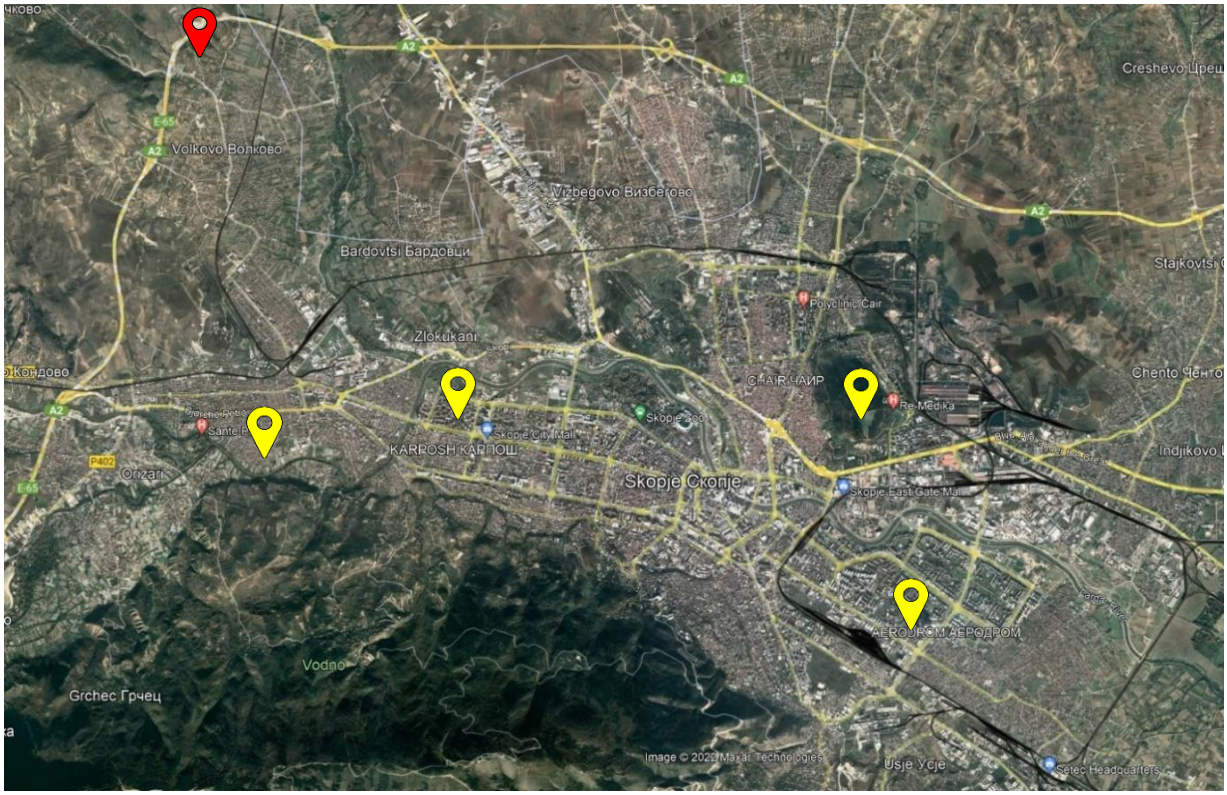

The site located in the backyard of "Joakim Krcovski" primary school, surrounded mostly by rural area and opened to the Lepenec river valley to the north. There are no major local sources, with exclusion of the Skopje ring road, located few hundreds meter to the north.

Site photo

GPS coordinates – Y - 7.528.864 X - 4.655.902

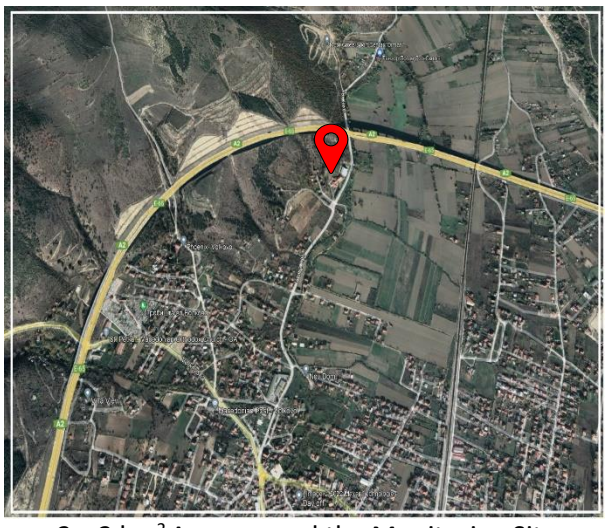

2 x 2 km^2 Area around the Monitoring Site

Gazi Baba - indicative monitoring site (MP5-AQT)

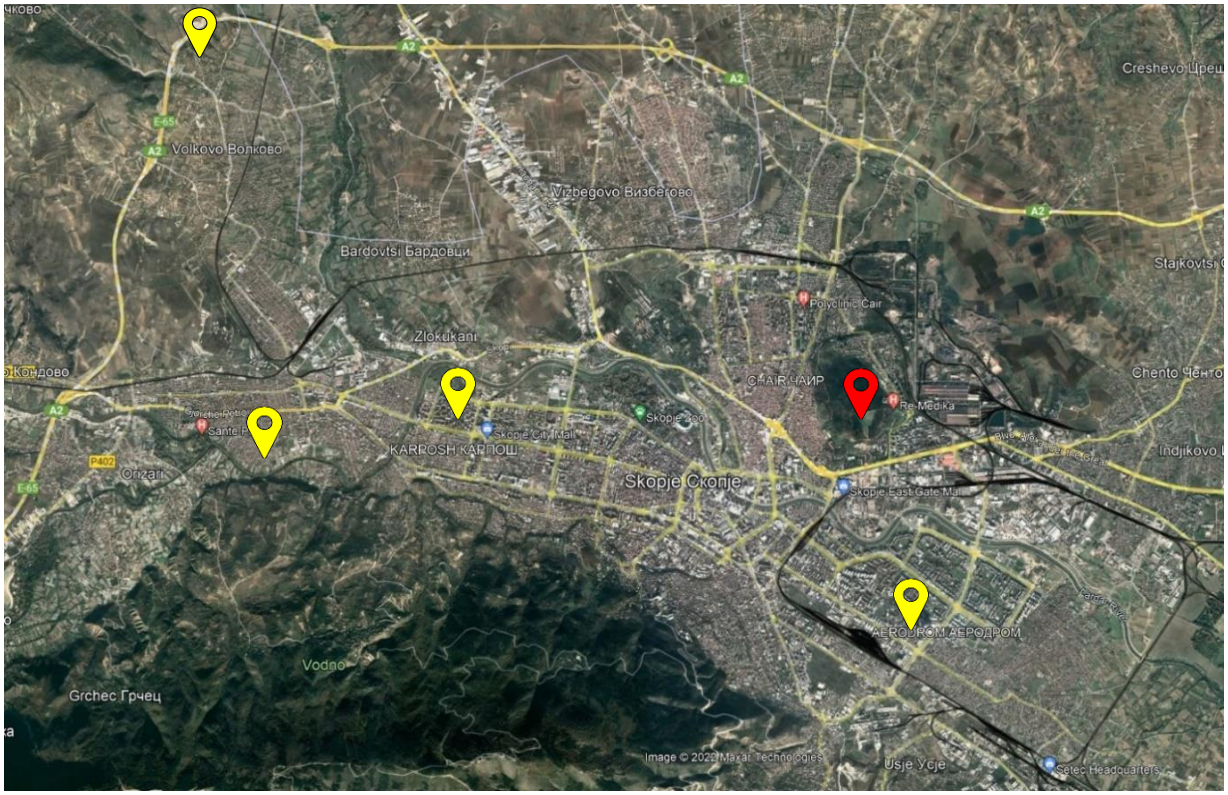

The site is in a forest, close to major still processing industrial area and no other local sources in the site vicinity.

Site photo

GPS coordinates – Y - 7.537.379 X - 4.650.125

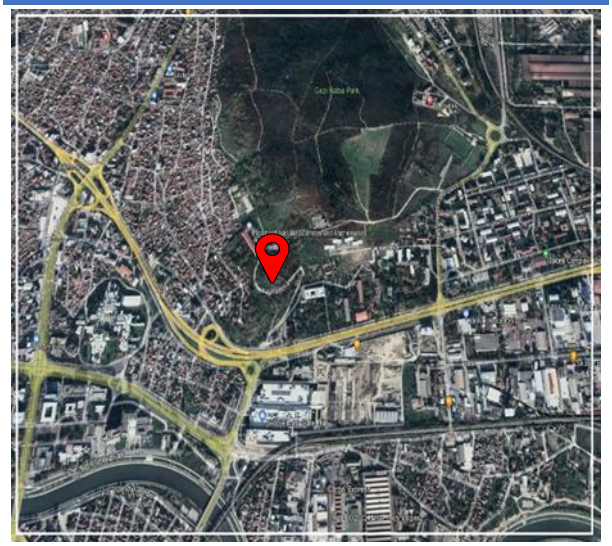

2 x 2 km^2 Area around the Monitoring Site

4.1. Sampling and determination of mass concentration of ambient particulate matter (PM2.5)

Sampling process was performed fully in line with the requirements of standard gravimetric measurement method for determination of the PM10/PM2,5 mass concentration of suspended particulate matter (EN 12341:2014). Sampling was performed on 47 mm PTFE filters (Advantec depth filter PF 020 and PF 040), according to Standard Operating Procedure of the UGD AMBICON Lab, an ISO 17025 accredited for environment and samples from the environment testing (https://iarm.gov.mk/en/2021/07/01/lt-052-university-goce-delcev-shtip/).

4.1.1. Sampling procedure

All sampling sites were equipped with low/medium volume sequential sampling systems (PNS 18T-DM-6.1, Comde Derenda, Germany), certified as a reference device for PM2.5 sampling according to EN 12341:2014.

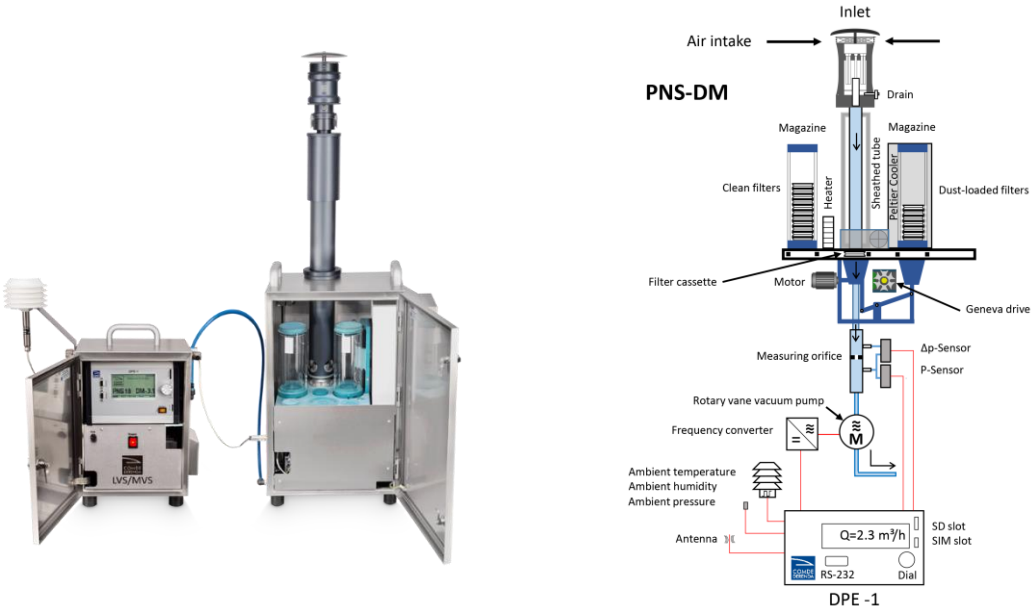

Figure 20. Sequential sampling system PNS 18T-DM 6.1

Sequential sampling systems provide fully automatic sampling according to pre-set parameters. Session from 14 to 16 days were set for each site. Each initial magazine was loaded in the AMBICON Lab premises with 16 to 18 filters, of which top one was not used for sampling, but as a protection in order to collect possible passive particle deposits. Additional one was transferred to the storage magazine without exposure and used as a field blank.

All monitoring data were electronically recorded, including sample ID, pump runtime, time of measurement, motor speed, actual flow, normalized flow, volume sampled-actual, volume sampled-normalized, filter pressure, ambient air pressure, outdoor temp, filter temp, chamber temp and relative humidity.

During each filter magazine change operation or at a period of 14 to 16 days, several quality assurance and control procedures were performed, including:

- sampling head cleaning,
- reading accuracy check for all sensors, and
- leak tightness test.

Sampling head, including inside of the tubular casing, the intake side of the multijet unit, the impaction plate and the jet tubes will be cleaned with alcohol and wiped with dry cloth. Impaction plate will be greased with silicone spray lubricant. The insect screen will be checked for obstructions and cleaned if necessary. Notes about cleaning and visual inspection were recorded in lab sampling logbook.

Reading accuracy of all sensors will be checked through a short sampling test cycle, all the while, readings of the sensors was compared against external calibrated standards, including:

- test of flow rate set, against the reading of calibrated external flow meter (with certificate issued from ISO 17025 calibration lab),
- test of system temperature, humidity and ambient pressure readings, against calibrated external ambient Temp, RH and Ambient Pressure meter (with certificate issued from ISO 17025 calibration lab),

Data about readings from all sensors were recorded in separate form of lab sampling logbook.

Leak tightness test of the system was performed through a low-pressure method, fully according to section 5.1.7.2 of the EN 12431:2014. The system has integrated leak test procedure, where pump is run, with closed calibration adapter until 400 hPa under-pressure in chamber is reached. The pump is switched of, and after 5 minutes pressure is read from the screen. If the value of under-pressure in the chamber is above 210 hPa, the system has passed the run test. According to above norm requirements, the test was repeated 3 times (total 3 runs). Data from the test runs were recorded in separate sheet of lab sampling logbook.

4.1.2. Filters handling and weighing

Prior to sampling, all filters were uniquely identified and conditioned at 19 °C to 21 °C and 45 to 50 % RH in climate chamber (ICH 110, Memmert, Germany) for ≥ 48 h, and weighted twice with at least 12 hours reconditioning period, to confirm mass stabilization (qualified difference < 40 µg). For each batch, two (2) blank filters are left to serve as a weighing room blanks.

Figure 21. Weighing room- AMBICON UGD Lab

After each sampling session, storage and initial magazine were removed from the housing. Protective reference filter was removed from the magazine and discarded, while empty magazine was fixed as new storage magazine. As soon as removed from the housing, storage magazine was sealed with cap and parafilm and stored in transportation "cool box".

Sampled filters after exposure were returned to the weighing room and conditioned in a controlled temperature and humidity chamber for more than 48 hours and weighted. After additional conditioning period of minimum 24 hours, filters were re-weighted and accepted as stabilized if difference between results is ≤ 60 µg. Same conditions was applied for filed blanks.

Weighing was performed with electronically controlled micro balance Radwag MYA5.3Y.F (resolution d = 1 µg), installed within controlled temperature and humidity room and completed with antistatic ionizer. Weighing data set and room conditions were electronically recorded.

Ongoing quality control were performed fully in line with the requirements of standard gravimetric measurement method for determination of the PM10/PM2,5 mass concentration of suspended particulate matter (EN 12341:2014), according to standard operating procedure of UGD AMBICON Lab, an ISO 17025 accredited for environment and samples from the environment testing areas.

Measurement uncertainties were calculated following GUM concept (JCGM 100) and included all individual uncertainty sources.

Mass concentration of ambient particulate matter was calculated as the difference in mass between the sampled and unsampled filter, divided by the sampled volume of air, determined as the flow rate multiplied by the sampling time. Measurement results are expressed as µg/m^3, where the volume of air is that at the ambient conditions near the inlet during sampling.

Data collected and comments are included in each filter testing results, given as supplementary material to this report (A – 1 Mass concentration of ambient particulate matter).

4.2. Chemical speciation

Elemental analysis of atmospheric aerosols, particularly PM2.5, is a useful tool for determining their source and environmental impact. It can be done in a variety of ways. Some analytical procedures are highly costly, while others are time-consuming, and some methods destroy the material. Currently, several different methods are used to determine elemental concentrations in the aerosols, such as scanning electron microscopy [12,13], energy dispersive X-ray fluorescence (ED-XRF) [14,15], ion chromatography [15,16], inductively couple plasma atomic emission spectrometry (ICP-AES) [17-19], ICP-mass spectrometry [19], atomic absorption spectroscopy (AAS) [15,16], particle induced X-ray emission (PIXE) [16,20], thermal optical transmittance (TOT) method [16], ion-selective electrode method [17], gas chromatography-mass spectrometry [21], capillary electrophoresis [22], and spectrophotometry [23].

4.2.1. Elemental analysis using energy dispersive X-ray fluorescence spectrometry

The elemental analysis of PM2.5 of aerosols was conducted using energy dispersive X-ray fluorescence spectrometer NEX CG produced by Rigaku. The secondary targets of the NEX CG substantially improve detection limits for elements in highly scattering matrices including water, hydrocarbons, and biological materials, and a unique close-coupled Cartesian Geometry optical kernel significantly increases signal-to-noise. The spectrometer is capable of routine trace element analysis even in filter samples, thanks to the remarkable reduction in background noise and corresponding increase in element peaks [24].

Figure 22. NEX CG by Rigaku

Analyses were carried out in the AMBICON Lab, at Goce Delchev University in Shtip, North Macedonia, according to the EPA/625/R-96/010a Compendium of Methods, Method IO-3.3: determination of metals in ambient particulate matter using x-ray fluorescence (XRF) spectroscopy published by U.S. Environmental Protection Agency.

The calibration curve on the NEX CG was produced using the certificated standard reference material SRM 2783 from the National Institute of Standards and Technology (NIST) in one point, having in mind the instrument upgrades. Single element certified reference materials from Micromatter, such as KCl and CdSe, were used to calibrate the elements that were not included in the SRM 2783.

Results from ongoing quality control (daily analysis of certificated reference filter - SRM 2783) are given in the table below.

Table 15. Results of control quality – EDXRF NEX CG

Chemical Element	Certified reference concentration		Average	Standard deviation	Coefficient of variation (%)	Recovery (%)
	ng/cm^2	Certified reference material				
Na	187,0	SRM 2783	171,8	42,2	24,5	100,00
Mg	865,0		840,2	49,8	5,9	100,00
Al	2330,0		2078,8	63,3	3,0	100,00
Si	5884,0		5401,2	259,1	4,8	100,00
S	105,0		99,7	8,9	8,9	100,00
K	530,0		488,0	45,6	9,3	100,00
Ca	1325,0		1312,9	144,9	11,0	100,00
Ti	150,0		124,2	14,2	11,4	100,00
Cr	13,6		19,8	2,4	12,0	100,00
Mn	32,0		29,1	1,8	6,1	100,00

Fe	2661,0		2572,4	267,5	10,4	100,00
Co	0,8		0,5	0,1	12,7	100,00
Ni	6,8		6,6	0,5	8,3	100,00
Cu	41,0		38,3	2,3	6,1	100,00
Zn	180,0		172,5	10,9	6,3	100,00
As	1,2		1,3	0,1	5,3	100,00
Sc	0,4		11,0	2,8	25,3	99,73
V	4,9		7,4	1,7	22,5	99,99
Rb	2,4		2,2	0,15	6,8	100,00
Sb	7,2		5,8	1,6	27,1	100,00
Ba	33,6		26,5	7,9	29,7	100,00
Ce	2,3		1,1	0,3	26,2	100,01
Sm	0,2		0,2	0,012	7,2	100,00
W	0,5		0,4	0,04	10,4	100,00
Pb	32,0		30,5	1,6	5,2	100,00
Th	0,3		0,3	0,02	9,0	100,00
Cl	856,8	KCl 47546 Micromatter	827,4	61,3	7,4	100,00
Se	1073,8	CdSe 47569 Micromatter	1004,4	16,8	1,7	100,00
Cd	1526,2		1523,8	56,3	3,7	100,00

4.2.2. Analysis of water-soluble ions

Water-soluble ions were extracted from the aerosol filters using sonication and shaking as recommended in the standard operating procedure for PM2.5 cation Analysis [25]. The filters were cut in half using ceramic scissors and the mass of the filters was determined using electronically controlled micro balance with resolution of 1 µg. Half of the filter is placed in plastic centrifuge tubes filled with 25 mL ultra-pure water (> 18MΩ-cm) and sonicated on room temperature in the ultrasonic bath (GT Sonic Pro, UK) for 60 minutes. Ice was added in the ultrasonic bath to keep the temperature below 27°C. After the sonication, the centrifuge tubes were shaken for 9 hours at 640 rpm using IKA KS 130 orbital shaker. After the procedure is completed, and in order to provide time for sample stabilization, the samples were stored in refrigerator overnight.

Water-soluble ions, including sulphates (SO_4^{2-}), nitrates (NO_3^-) and ammonium (NH_4^+) were photometrically analyzed using Spectroquant® Prove 600 spectrophotometer by Merck.

Figure 23. Spectroquant® Prove 600, Merck

Ammonium ions were analyzed using 1.14752.0001 Spectroquant® cell test analogous to EPA 350.1, ISO 7150-1 and DIN 38406-5 methods and detection limit of 0.015 mg/l NH_4^+. Quality control was provided using Certipur - certified reference solution of NH_4Cl in H_2O (1000 mg/l NH_4^+) traceable to NIST.

The sulphate ions were analyzed using 1.01812.0001 Spectroquant® cell test analogous to EPA 375.4, APHA 4500-SO_4^{2-}E, and ASTM D516-16 methods and detection limit of 0.5 mg/l SO_4^{2-}. Quality control was provided using Certipur - certified reference solution of Na_2SO_4 in H_2O (1000 mg/l SO_4) traceable to NIST.

Nitrate ions were analyzed using 1.09713.0001 Spectroquant® cell test analogous to DIN 38405-9in method and detection limit of 0.2 mg/l NO_3^-. Quality control was provided using Certipur - certified reference solution of $NaNO_3$ in H_2O (1000 mg/l NO_3^-) traceable to NIST.

Table 16. QC results of control quality – Spectroquant Prove 600

Ion	Concentration in certified reference sollution		Average	Standard deviation	Coefficient of variation (%)	Recovery (%)
	mg/l	Certified reference solution				
NH_4^+	0.1	NH_4Cl in H_2O (1000 mg/l NH_4^+), Certipur	0.099	0.01	14.8	100.0
SO_4^{2-}	10	Na_2SO_4 in H_2O (1000 mg/l SO_4), Certipur	9.849	0.49	5.0	100.0
NO_3^-	10	$NaNO_3$ in H_2O (1000 mg/l NO_3^-), Certipur	9.921	0.33	3.3	100.0

4.2.3. Elemental Carbon analysis

Black Carbon or Elemental Carbon was determined using Magee Scientific, SootScan™ Model OT21 Optical Transmissometer with dual wavelength light source (880nm providing the quantitative measurement of Elemental Carbon in PM, and a 370 nm for qualitative assessment of certain aromatic organic compounds), by applying EPA empirical EC relation for Teflon FRM filters.

Figure 24. Magee Scientific, SootScan™ Model OT21 Optical Transmissometer

Validation of the reproducibility of the photometric detector will be provided with use of Neutral Density Optical Kit traceable to NIST and as recommended from the producer.

4.3. Observations and results

This sections present observations from the monitoring programs conducted at 5 locations in Skopje, staring from October 2020 and ending October 2021. Results present daily variations in mass concentrations and chemical composition of PM with respect to various chemical species including carbon fraction (elemental carbon), crustal elements (Al, Si, Ca, Ti and Fe), water soluble ions (NH_4^+, SO_4^{2-}, NO_3^-) and larger group of other elements (Na, S, K, Cr, Mn, Co, Ni, Cu, Zn, As, Sc, V, Rb, Sb, Ba, Ce, Sm, W, Pb, Th, Cl, Se, Cd).

The full dataset from the chemical analysis is included as supplemental material in this report (A - 2 Particulate matter chemical speciation), whereas the description of the data and findings based on statistical analysis are described in this chapter.

4.3.1. Statistical evaluation

Descriptive statistics helps us to summarize, describe and illustrate the data in a more meaningful fashion, making data interpretation easier. Therefore, a summary of descriptive coefficients for data sets collected for each of the sites included in the monitoring program is given below.

Descriptive statistical analysis presented, include both categories: measurements of central tendency and measures of variability (or variation).

Measures of central tendency are techniques of describing the position of the centre of a frequency distribution given a set of data. Although a multitude of statistics such as the mode, median, and mean, can be used for this purpose, the middle position in this case is described with arithmetic mean.

Measures of variability are a means of summarizing a set of data by indicating how widely the results observed are distributed. Several statistics to explain this spread are used, including minimum, maximum, quartiles, variance, and standard deviation.

Descriptive coefficients are combined with tabular and graphical descriptions, as much as the comments and discussion of the results.

In addition, a correlation matrix illustrating relationship between all values in the dataset is also given, as a basic tool for summarizing massive datasets and identifying and visualizing data trends.

The corelation matrix table contain the correlation coefficients between each variable based on Pearson parametric correlation test and its colour coded for correlation values above ± 0.6.

In this specific case, correlation matrixes present relationships between the species, indicating their common sources, but also serves as an input for exploratory factor analysis and data quality control.

Table 17. Statistical evaluation – Karposh dataset

	Units	N	Mean	SD	Minimum	Maximum	C.V.	95 th %	5 th %
PM2.5	µg/m^3	331	36.40	24.18	3.30	167.35	0.66	87.81	11.69
Na		331	10.425	9.143	1.070	87.353	0.877	27.943	5.176
Mg		331	35.095	39.657	0.519	271.873	1.130	97.926	1.863
Al		331	107.718	140.459	1.536	928.900	1.304	338.586	7.892
Si		331	286.289	329.589	1.460	2212.996	1.151	844.820	19.509
S		331	158.655	75.975	19.358	467.932	0.479	319.400	68.170
K		331	305.563	296.774	32.398	1570.100	0.971	872.200	55.809
Ca		331	683.073	481.733	7.955	3247.775	0.705	1532.248	71.644
Ti		331	14.016	15.260	0.608	111.611	1.089	40.119	2.032
Cr		331	0.825	0.671	0.025	4.053	0.813	2.127	0.151
Mn		331	3.993	2.351	0.050	15.422	0.589	7.930	0.579
Fe		331	266.110	211.006	14.097	1540.138	0.793	620.022	48.082
Co		331	0.031	0.020	0.003	0.113	0.646	0.077	0.014
Ni		331	0.388	0.327	0.025	1.435	0.841	1.007	0.076
Cu		331	5.700	4.374	0.101	25.627	0.767	13.291	0.234
Zn		331	36.834	34.976	3.474	253.341	0.950	102.608	8.761
As		331	1.486	3.123	0.327	15.608	2.101	10.686	0.375
Sc	ng/m^3	331	1.618	0.134	0.692	3.723	0.083	1.610	1.610
V		331	1.789	0.793	0.442	5.337	0.443	3.159	0.533
Rb		331	0.394	0.320	0.008	1.276	0.811	0.988	0.050
Sb		331	1.603	0.598	0.305	3.122	0.373	2.769	0.501
Ba		331	3.553	4.171	0.039	65.199	1.174	8.521	1.762
Ce		331	0.150	0.110	0.003	1.697	0.735	0.288	0.031
Sm		331	0.007	0.006	0.001	0.030	0.845	0.021	0.002
W		331	0.059	0.066	0.003	0.282	1.113	0.209	0.008
Pb		331	8.671	5.245	0.176	38.176	0.605	17.848	2.291
Th		331	0.036	0.044	0.000	0.146	1.233	0.126	0.003
Cl		331	80.930	88.546	0.207	628.315	1.094	239.502	4.040
Se		331	0.708	0.575	0.025	3.776	0.812	2.064	0.201
Cd		331	4.576	1.448	0.503	12.990	0.316	6.445	2.643
EC		331	6022.96	2931.34	389.68	14844.52	0.487	10829.35	1703.23
NH_4		331	1056.23	829.85	45.45	4234.07	0.786	2901.27	145.43
SO_4		331	5664.07	9937.10	9.09	44267.09	1.754	36904.06	418.12
NO_3		331	2156.86	3050.58	9.09	17204.40	1.414	8821.60	25.45

Table. 17- a . Corelation matrix – Karposh dataset

	PM2.5	Na	Mg	Al	Si	S	K	Ca	Ti	Cr	Mn	Fe	Co	Ni	Cu	Zn	As	Sc	V	Rb	Sb	Ba	Ce	Sm	W	Pb	Th	Cl	Se	Cd	EC	NH4	SO4	NO3
PM2.5	1.00																																
Na	0.10	1.00																															
Mg	0.07	0.42	1.00																														
Al	0.05	0.41	0.97	1.00																													
Si	0.05	0.43	0.98	1.00	1.00																												
S	0.55	0.01	0.05	0.04	0.04	1.00																											
K	0.89	0.13	0.06	0.05	0.05	0.54	1.00																										
Ca	0.09	0.45	0.89	0.83	0.87	0.10	0.07	1.00																									
Ti	0.05	0.43	0.97	0.99	0.99	0.04	0.06	0.85	1.00																								
Cr	0.03	0.26	0.61	0.53	0.56	-0.05	0.01	0.65	0.55	1.00																							
Mn	0.15	0.30	0.59	0.55	0.57	0.09	0.16	0.59	0.56	0.51	1.00																						
Fe	0.19	0.41	0.96	0.95	0.96	0.15	0.20	0.89	0.96	0.60	0.66	1.00																					
Co	-0.19	0.12	0.20	0.17	0.20	-0.21	-0.20	0.25	0.19	0.33	0.32	0.20	1.00																				
Ni	-0.25	0.22	0.35	0.32	0.35	-0.21	-0.29	0.40	0.34	0.43	0.52	0.34	0.65	1.00																			
Cu	0.16	0.15	0.13	0.05	0.09	-0.04	0.13	0.24	0.07	0.33	0.44	0.19	0.55	0.56	1.00																		
Zn	0.50	0.03	-0.09	-0.13	-0.12	0.29	0.54	-0.07	-0.11	0.04	0.53	0.04	-0.02	-0.01	0.32	1.00																	
As	-0.19	0.16	-0.05	0.07	0.08	-0.20	-0.22	0.09	0.06	0.04	0.06	0.01	0.25	0.42	0.19	-0.19	1.00																
Sc	0.10	0.01	-0.04	-0.03	-0.03	0.20	0.10	-0.04	-0.03	0.05	0.14	0.01	0.07	0.14	0.09	0.16	-0.01	1.00															
V	0.24	0.30	0.43	0.41	0.42	0.16	0.22	0.44	0.42	0.32	0.29	0.43	0.19	0.14	0.16	0.07	0.02	0.12	1.00														
Rb	0.25	0.35	0.23	0.21	0.24	-0.07	0.23	0.31	0.22	0.27	0.42	0.27	0.50	0.62	0.70	0.25	0.39	0.08	0.24	1.00													
Sb	-0.04	0.05	0.30	0.26	0.28	0.18	-0.01	0.39	0.28	0.30	0.24	0.31	0.01	0.13	0.06	-0.03	-0.05	0.10	0.24	-0.03	1.00												
Ba	0.19	0.02	0.10	0.06	0.06	0.04	0.20	0.14	0.03	0.16	0.13	0.09	-0.02	-0.01	0.15	0.09	-0.04	-0.01	0.25	0.08	0.06	1.00											
Ce	-0.03	0.03	0.10	0.09	0.09	-0.01	0.00	0.11	0.10	0.09	0.09	0.10	0.02	0.08	0.03	-0.02	0.03	0.01	0.04	0.04	0.21	-0.04	1.00										
Sm	-0.39	0.01	-0.12	-0.14	-0.12	-0.21	-0.40	-0.09	-0.13	0.07	0.12	-0.17	0.44	0.58	0.32	-0.14	0.33	0.14	-0.13	0.29	-0.01	-0.09	0.01	1.00									
W	-0.25	0.23	0.10	0.07	0.11	-0.34	-0.32	0.20	0.09	0.28	0.27	0.07	0.68	0.75	0.63	-0.09	0.53	0.10	0.12	0.73	-0.04	-0.02	0.03	0.60	1.00								
Pb	0.40	0.11	0.09	0.00	0.02	0.18	0.39	0.12	0.02	0.17	0.47	0.15	0.26	0.28	0.59	0.65	-0.17	0.10	0.15	0.55	0.00	0.12	-0.01	0.07	0.26	1.00							
Th	-0.21	0.26	0.16	0.14	0.17	-0.34	-0.29	0.25	0.14	0.28	0.34	0.13	0.63	0.77	0.64	-0.02	0.50	0.05	0.15	0.80	-0.05	0.05	0.02	0.52	0.91	0.35	1.00						
Cl	0.78	0.32	-0.06	-0.09	-0.08	0.42	0.85	0.03	-0.07	-0.01	0.16	0.06	-0.05	-0.14	0.36	0.56	-0.08	0.04	0.23	0.44	-0.05	0.15	-0.02	-0.24	-0.06	0.55	-0.01	1.00					
Se	-0.15	0.22	0.12	0.09	0.12	-0.29	-0.20	0.19	0.10	0.20	0.30	0.09	0.52	0.61	0.54	0.01	0.31	-0.04	0.13	0.64	-0.03	-0.01	0.04	0.39	0.70	0.31	0.75	0.02	1.00				
Cd	0.00	-0.01	0.00	-0.01	0.00	0.12	0.03	0.03	-0.01	0.06	0.10	0.02	0.01	0.06	-0.02	0.13	-0.03	0.19	0.10	-0.02	0.14	0.08	0.09	-0.01	-0.04	0.06	-0.02	-0.02	-0.04	1.00			
EC	0.58	0.14	0.00	-0.07	-0.05	0.16	0.57	0.05	-0.06	0.05	0.13	0.07	0.13	0.04	0.52	0.45	-0.07	-0.01	0.18	0.60	-0.17	0.14	-0.02	-0.15	0.19	0.55	0.28	0.67	0.27	-0.03	1.00		
NH4	0.66	-0.18	-0.30	-0.28	-0.30	0.74	0.65	-0.33	-0.29	-0.26	-0.14	-0.19	-0.34	-0.44	-0.10	0.41	-0.28	0.20	0.00	-0.10	-0.04	-0.05	-0.05	-0.32	-0.43	0.21	-0.44	0.55	-0.34	0.05	0.30	1.00	
SO4	0.01	0.06	0.04	-0.01	0.01	0.04	0.00	0.10	0.00	0.01	0.09	0.02	0.10	0.12	0.19	0.09	0.01	-0.09	-0.02	0.24	-0.05	0.00	0.04	0.06	0.17	0.14	0.23	0.12	0.24	-0.02	0.23	-0.06	1.00
NO3	0.84	0.01	-0.16	-0.15	-0.16	0.54	0.89	-0.15	-0.15	-0.12	0.00	-0.02	-0.23	-0.36	0.07	0.51	-0.21	0.12	0.11	0.14	-0.09	0.08	-0.04	-0.36	-0.33	0.33	-0.32	0.78	-0.20	0.01	0.53	0.82	-0.02	1.00

Table 18. Statistical evaluation – Novo Lisiche dataset

	Units	N	Mean	SD	Minimum	Maximum	C.V.	95 th %	5 th %
PM2.5	µg/m³	255	45.68	28.85	10.51	165.61	0.63	104.47	16.03
Na		255	14.690	32.978	0.214	435.500	2.245	35.873	5.747
Mg		255	44.240	41.085	0.503	387.685	0.929	107.387	2.573
Al		255	124.186	129.011	2.366	1150.468	1.039	318.957	15.422
Si		255	340.465	306.990	3.977	2837.400	0.902	769.318	52.311
S		255	185.804	120.843	31.165	696.555	0.650	435.384	66.978
K		255	385.263	399.742	43.726	2432.802	1.038	1210.378	64.470
Ca		255	1158.023	737.345	5.186	5689.805	0.637	2372.790	222.834
Ti		255	16.328	13.686	0.514	119.671	0.838	37.929	3.940
Cr		255	1.356	1.121	0.025	8.509	0.827	3.094	0.176
Mn		255	4.898	2.438	0.298	15.885	0.498	8.985	1.604
Fe		255	430.872	256.085	27.692	2026.031	0.594	837.294	123.955
Co		255	0.029	0.021	0.003	0.143	0.702	0.070	0.005
Ni		255	0.452	0.414	0.025	4.167	0.915	1.158	0.095
Cu		255	7.632	5.790	0.176	64.861	0.759	16.036	1.453
Zn		255	47.279	38.891	4.557	264.099	0.823	127.433	12.285
As		255	1.420	3.132	0.101	16.866	2.205	11.328	0.375
Sc	ng/m³	255	1.636	0.156	0.201	2.653	0.095	1.841	1.610
V		255	2.068	0.863	0.496	4.934	0.417	3.557	0.609
Rb		255	0.485	0.381	0.023	1.810	0.785	1.199	0.068
Sb		255	1.792	0.723	0.356	5.639	0.403	2.986	0.795
Ba		255	6.382	4.800	0.157	35.999	0.752	14.002	1.859
Ce		255	0.206	0.999	0.003	16.071	4.849	0.222	0.027
Sm		255	0.006	0.004	0.001	0.022	0.749	0.014	0.003
W		255	0.057	0.063	0.003	0.234	1.105	0.195	0.008
Pb		255	9.116	5.534	0.831	42.645	0.607	18.442	2.233
Th		255	0.033	0.043	0.000	0.145	1.274	0.127	0.002
Cl		255	112.643	117.561	0.076	907.729	1.044	332.427	6.188
Se		255	0.799	0.778	0.025	4.657	0.974	2.517	0.250
Cd		255	4.748	1.307	0.831	11.504	0.275	7.592	3.653
EC		255	15436.51	8444.12	2490.00	38625.00	0.547	33083.14	4904.00
NH_4		255	868.70	794.15	27.27	4704.45	0.91	2298.82	118.17
SO_4		255	4126.41	6335.67	9.09	53938.79	1.54	11026.00	558.12
NO_3		255	2240.81	2969.53	9.09	18742.76	1.32	8000.85	25.45

Table. 18- a . Corelation matrix – Novo Lisiche dataset

	PM2.5	Na	Mg	Al	Si	S	K	Ca	Ti	Cr	Mn	Fe	Co	Ni	Cu	Zn	As	Sc	V	Rb	Sb	Ba	Ce	Sm	W	Pb	Th	Cl	Se	Cd	EC	NH4	SO4	NO3
PM2.5	1.00																																	
Na	0.00	1.00																																
Mg	0.09	0.12	1.00																															
Al	0.05	0.12	0.95	1.00																														
Si	0.07	0.14	0.97	0.98	1.00																													
S	0.57	-0.06	0.23	0.19	0.18	1.00																												
K	0.82	-0.03	0.17	0.12	0.12	0.76	1.00																											
Ca	0.18	0.14	0.88	0.80	0.86	0.25	0.23	1.00																										
Ti	0.10	0.14	0.93	0.95	0.97	0.13	0.12	0.85	1.00																									
Cr	0.16	0.06	0.63	0.62	0.60	0.17	0.21	0.69	0.61	1.00																								
Mn	0.30	0.01	0.63	0.61	0.61	0.26	0.28	0.64	0.63	0.62	1.00																							
Fe	0.34	0.09	0.89	0.85	0.88	0.35	0.39	0.90	0.90	0.72	0.77	1.00																						
Co	0.02	0.02	0.26	0.26	0.28	-0.13	-0.08	0.30	0.30	0.25	0.32	0.27	1.00																					
Ni	0.01	-0.01	0.30	0.37	0.30	0.00	0.03	0.32	0.34	0.52	0.49	0.37	0.41	1.00																				
Cu	0.31	-0.05	0.23	0.28	0.21	0.15	0.28	0.33	0.25	0.55	0.53	0.39	0.41	0.75	1.00																			
Zn	0.59	-0.05	0.01	-0.04	-0.05	0.41	0.55	0.07	0.00	0.18	0.53	0.25	0.00	0.10	0.36	1.00																		
As	-0.15	-0.02	-0.22	-0.09	-0.08	-0.21	-0.22	-0.13	-0.10	-0.11	-0.08	-0.18	0.28	0.20	0.06	-0.23	1.00																	
Sc	0.45	-0.01	0.05	0.04	0.04	0.52	0.54	0.10	0.03	0.07	0.08	0.16	0.02	0.07	0.16	0.21	0.00	1.00																
V	0.28	0.12	0.42	0.41	0.40	0.31	0.34	0.39	0.40	0.37	0.31	0.47	0.14	0.21	0.21	0.16	-0.20	0.25	1.00															
Rb	0.59	-0.02	0.11	0.09	0.11	0.19	0.50	0.26	0.19	0.28	0.41	0.34	0.43	0.47	0.64	0.39	0.17	0.29	0.24	1.00														
Sb	0.08	0.06	0.59	0.57	0.58	0.36	0.23	0.59	0.54	0.47	0.40	0.57	0.13	0.17	0.08	0.01	-0.09	0.20	0.27	-0.06	1.00													
Ba	0.29	0.00	0.53	0.46	0.46	0.43	0.45	0.55	0.42	0.47	0.41	0.61	0.10	0.17	0.23	0.19	-0.17	0.15	0.37	0.14	0.44	1.00												
Ce	-0.05	-0.01	0.04	0.02	0.02	0.02	-0.03	0.03	0.00	0.04	0.05	0.04	-0.03	0.06	0.06	0.00	-0.01	-0.01	-0.06	-0.04	0.02	0.05	1.00											
Sm	-0.28	-0.08	-0.18	-0.15	-0.16	-0.17	-0.29	-0.20	-0.19	-0.16	-0.08	-0.27	0.29	0.18	0.04	-0.20	0.27	-0.05	-0.12	0.03	-0.11	-0.17	0.00	1.00										
W	-0.11	-0.02	-0.03	-0.01	0.02	-0.37	-0.29	0.07	0.07	0.10	0.13	-0.02	0.59	0.50	0.46	-0.15	0.44	-0.05	-0.06	0.58	-0.23	-0.23	-0.05	0.37	1.00									
Pb	0.45	-0.03	0.08	0.01	0.02	0.22	0.39	0.17	0.08	0.26	0.43	0.26	0.23	0.30	0.55	0.66	-0.20	0.15	0.21	0.58	0.01	0.12	0.07	-0.05	0.21	1.00								
Th	-0.06	-0.04	-0.01	0.02	0.02	-0.34	-0.23	0.10	0.08	0.17	0.18	0.03	0.58	0.59	0.58	-0.07	0.43	-0.05	-0.02	0.65	-0.19	-0.13	0.00	0.35	0.91	0.31	1.00							
Cl	0.62	0.58	0.04	-0.02	0.02	0.35	0.65	0.18	0.04	0.13	0.16	0.23	-0.01	-0.02	0.26	0.42	-0.14	0.34	0.24	0.46	0.03	0.21	-0.05	-0.27	-0.09	0.39	-0.05	1.00						
Se	0.09	-0.03	0.03	0.02	0.06	-0.25	-0.13	0.15	0.14	0.14	0.23	0.12	0.57	0.43	0.45	0.00	0.24	-0.01	0.03	0.63	-0.15	-0.11	-0.02	0.22	0.76	0.33	0.76	0.03	1.00					
Cd	-0.02	-0.05	-0.08	-0.06	-0.10	0.15	0.08	-0.11	-0.10	0.07	-0.04	-0.06	-0.10	0.09	0.04	-0.05	-0.06	0.20	0.13	-0.03	0.11	0.08	0.24	0.08	-0.11	-0.03	-0.09	-0.03	-0.07	1.00				
EC	0.56	0.00	-0.13	-0.18	-0.15	-0.01	0.35	0.05	-0.06	0.16	0.23	0.15	0.16	0.12	0.41	0.52	-0.03	0.05	0.10	0.66	-0.26	0.08	-0.03	-0.19	0.23	0.53	0.31	0.47	0.38	-0.14	1.00			
NH4	0.63	-0.09	-0.23	-0.22	-0.24	0.65	0.63	-0.23	-0.22	-0.13	-0.01	-0.06	-0.19	-0.20	0.02	0.45	-0.19	0.47	0.15	0.25	-0.05	0.02	-0.03	-0.21	-0.31	0.27	-0.28	0.37	-0.13	0.12	0.26	1.00		
SO4	0.34	-0.04	0.07	0.06	0.07	0.37	0.38	0.09	0.06	0.11	0.08	0.16	-0.09	-0.10	0.05	0.15	-0.11	0.24	0.12	0.13	0.17	0.24	-0.02	-0.17	-0.18	0.12	-0.17	0.29	-0.07	0.05	0.09	0.36	1.00	
NO3	0.82	-0.04	-0.08	-0.11	-0.11	0.59	0.84	-0.02	-0.08	0.04	0.16	0.16	-0.09	-0.08	0.21	0.58	-0.18	0.50	0.26	0.51	0.00	0.20	-0.04	-0.28	-0.22	0.40	-0.17	0.60	-0.03	0.06	0.50	0.85	0.37	1.00

Table 19. Statistical evaluation – GP – Hrom dataset

	Units	N	Mean	SD	Minimum	Maximum	C.V.	95 th %	5 th %
PM2.5	µg/m³	60	43.98	30.26	8.81	129.87	0.69	102.29	10.67
Na	ng/m³	60	8.568	3.785	3.082	25.028	0.442	16.242	4.587
Mg		60	18.757	16.956	0.311	88.024	0.904	44.497	1.331
Al		60	51.576	41.331	2.314	202.521	0.801	124.849	9.447
Si		60	146.776	111.757	3.219	551.029	0.761	344.520	20.675
S		60	158.293	108.956	14.741	471.179	0.688	425.286	28.237
K		60	496.798	542.142	28.099	2145.060	1.091	1536.564	54.747
Ca		60	481.562	280.035	15.240	1381.118	0.582	919.356	52.533
Ti		60	8.341	5.247	0.392	27.003	0.629	20.851	2.172
Cr		60	0.519	0.273	0.101	1.610	0.525	1.016	0.126
Mn		60	4.116	2.452	0.226	12.040	0.596	9.455	0.734
Fe		60	179.811	98.162	20.111	479.855	0.546	422.680	55.052
Co		60	0.029	0.017	0.004	0.093	0.566	0.063	0.010
Ni		60	0.375	0.329	0.025	1.082	0.878	0.907	0.074
Cu		60	4.681	3.340	0.126	16.083	0.713	9.866	0.470
Zn		60	50.418	49.891	4.956	202.659	0.990	152.926	8.720
As		60	2.451	4.466	0.375	13.835	1.822	13.332	0.375
Sc		60	1.666	0.193	1.607	2.872	0.116	1.896	1.608
V		60	1.710	0.699	0.494	3.605	0.409	2.980	0.561
Rb		60	0.518	0.346	0.013	1.104	0.667	1.033	0.057
Sb		60	1.619	0.614	0.382	3.119	0.379	2.678	0.642
Ba		60	3.045	4.055	0.874	32.014	1.332	7.749	1.684
Ce		60	0.128	0.063	0.003	0.338	0.496	0.231	0.010
Sm		60	0.006	0.005	0.000	0.022	0.776	0.014	0.001
W		60	0.064	0.062	0.004	0.214	0.979	0.194	0.008
Pb		60	10.967	12.833	0.855	95.430	1.170	20.147	3.448
Th		60	0.041	0.050	0.001	0.206	1.241	0.133	0.003
Cl		60	109.593	110.229	0.207	460.891	1.006	341.902	0.207
Se		60	0.648	0.476	0.045	3.169	0.734	1.259	0.209
Cd		60	7.408	7.156	1.592	30.035	0.966	27.357	4.431
EC		60	9489.05	3596.01	3018.00	18105.00	0.38	15619.75	4673.25
NH_4		60	1181.89	998.60	127.14	3911.17	0.84	3146.46	270.20
SO_4		60	10583.58	16769.93	354.21	56111.65	1.58	44369.32	734.22
NO_3		60	3165.50	4023.08	9.08	13980.36	1.27	11708.48	25.43

Table. 19- a . Corelation matrix – GP Hrom dataset

	PM2.5	Na	Mg	Al	Si	S	K	Ca	Ti	Cr	Mn	Fe	Co	Ni	Cu	Zn	As	Sc	V	Rb	Sb	Ba	Ce	Sm	W	Pb	Th	Cl	Se	Cd	EC	NH4	SO4	NO3
PM2.5	1.00																																	
Na	0.28	1.00																																
Mg	-0.08	0.08	1.00																															
Al	-0.15	0.18	0.85	1.00																														
Si	-0.13	0.26	0.81	0.98	1.00																													
S	0.73	0.25	-0.07	-0.11	-0.06	1.00																												
K	0.92	0.18	-0.07	-0.20	-0.21	0.74	1.00																											
Ca	-0.14	0.28	0.78	0.83	0.87	-0.01	-0.21	1.00																										
Ti	-0.19	0.03	0.81	0.88	0.85	-0.19	-0.22	0.82	1.00																									
Cr	0.17	0.06	0.23	0.28	0.23	0.10	0.23	0.21	0.35	1.00																								
Mn	0.39	0.13	0.28	0.26	0.23	0.35	0.46	0.26	0.28	0.37	1.00																							
Fe	0.22	0.05	0.66	0.68	0.64	0.25	0.24	0.62	0.74	0.49	0.70	1.00																						
Co	-0.33	-0.10	-0.02	0.05	0.12	-0.22	-0.38	0.06	0.00	-0.22	-0.13	-0.18	1.00																					
Ni	-0.50	0.06	-0.03	0.10	0.16	-0.49	-0.57	0.14	0.12	-0.28	-0.09	-0.13	0.64	1.00																				
Cu	0.29	0.24	0.07	0.18	0.21	0.28	0.34	0.09	0.00	0.16	0.50	0.29	0.09	0.12	1.00																			
Zn	0.73	0.14	-0.07	-0.17	-0.18	0.56	0.78	-0.21	-0.22	0.28	0.74	0.31	-0.27	-0.39	0.40	1.00																		
As	-0.26	0.35	-0.24	0.18	0.25	-0.21	-0.35	0.22	0.08	-0.09	-0.06	-0.11	0.22	0.53	0.25	-0.32	1.00																	
Sc	0.53	0.26	-0.11	-0.14	-0.13	0.66	0.65	-0.14	-0.16	0.27	0.53	0.36	-0.19	-0.24	0.37	0.56	-0.13	1.00																
V	0.27	0.12	0.29	0.27	0.27	0.25	0.28	0.31	0.28	0.00	0.23	0.28	0.01	-0.06	0.29	0.13	-0.02	0.03	1.00															
Rb	0.48	0.45	-0.07	0.06	0.17	0.39	0.43	0.05	-0.15	-0.02	0.27	0.04	0.32	0.26	0.68	0.37	0.34	0.33	0.25	1.00														
Sb	-0.07	-0.25	0.19	0.11	0.09	0.01	-0.07	0.24	0.38	0.14	0.30	0.43	0.14	0.29	-0.12	-0.04	-0.07	0.17	0.16	-0.17	1.00													
Ba	0.18	0.04	0.18	0.04	-0.04	0.09	0.35	-0.01	0.02	0.16	0.31	0.09	-0.21	-0.15	0.43	0.22	-0.09	0.21	0.34	0.11	-0.07	1.00												
Ce	0.40	0.09	0.04	0.13	0.13	0.46	0.37	0.20	0.13	0.11	0.38	0.37	-0.12	-0.13	0.18	0.33	0.04	0.38	0.19	0.20	0.23	0.13	1.00											
Sm	-0.42	-0.04	0.05	0.21	0.27	-0.34	-0.51	0.17	0.14	-0.31	-0.15	-0.10	0.59	0.79	0.09	-0.42	0.46	-0.21	0.05	0.24	0.22	-0.21	-0.16	1.00										
W	-0.43	0.25	-0.02	0.21	0.29	-0.33	-0.54	0.18	0.07	-0.24	-0.13	-0.19	0.58	0.78	0.26	-0.43	0.66	-0.22	-0.13	0.41	0.02	-0.11	-0.22	0.70	1.00									
Pb	0.31	0.15	-0.02	-0.08	-0.04	0.22	0.23	-0.12	-0.18	-0.02	0.23	0.00	0.13	0.12	0.20	0.45	-0.19	0.23	0.07	0.36	0.08	0.02	0.12	0.01	0.04	1.00								
Th	-0.28	0.33	0.01	0.21	0.31	-0.24	-0.38	0.17	0.00	-0.16	-0.10	-0.21	0.52	0.71	0.41	-0.23	0.57	-0.13	-0.04	0.57	-0.12	0.03	-0.09	0.61	0.82	0.37	1.00							
Cl	0.90	0.34	-0.08	-0.15	-0.12	0.77	0.94	-0.15	-0.22	0.18	0.43	0.23	-0.23	-0.42	0.45	0.72	-0.21	0.70	0.31	0.59	-0.12	0.30	0.32	-0.36	-0.34	0.33	-0.16	1.00						
Se	-0.14	0.28	0.08	0.19	0.27	-0.21	-0.31	0.19	0.03	-0.15	-0.05	-0.12	0.36	0.51	0.23	-0.07	0.31	-0.20	0.08	0.37	0.00	-0.11	-0.04	0.46	0.50	0.61	0.72	-0.17	1.00					
Cd	-0.33	-0.34	0.02	-0.12	-0.19	-0.38	-0.26	-0.02	0.19	-0.09	0.06	0.16	0.12	0.39	-0.32	-0.20	-0.08	-0.05	-0.08	-0.44	0.61	0.00	-0.01	0.23	-0.02	-0.14	-0.23	-0.34	-0.16	1.00				
EC	0.73	0.14	-0.03	-0.06	-0.04	0.40	0.70	-0.18	-0.18	0.19	0.26	0.10	-0.12	-0.39	0.42	0.61	-0.17	0.21	0.26	0.55	-0.26	0.14	0.10	-0.27	-0.24	0.20	-0.11	0.69	-0.05	-0.48	1.00			
NH4	0.75	0.00	-0.27	-0.37	-0.36	0.81	0.76	-0.31	-0.30	0.08	0.31	0.17	-0.22	-0.43	0.15	0.61	-0.36	0.55	0.18	0.25	0.15	0.01	0.32	-0.34	-0.46	0.23	-0.42	0.75	-0.32	-0.07	0.45	1.00		
SO4	0.42	0.33	-0.03	-0.17	-0.13	0.54	0.40	0.10	-0.17	-0.03	0.09	-0.03	-0.16	-0.35	-0.25	0.30	-0.25	0.28	0.16	0.04	-0.10	-0.02	0.13	-0.30	-0.36	0.13	-0.30	0.40	-0.16	-0.21	0.09	0.39	1.00	
NO3	0.90	0.17	-0.20	-0.31	-0.29	0.81	0.94	-0.25	-0.31	0.15	0.38	0.18	-0.33	-0.56	0.24	0.75	-0.35	0.60	0.24	0.40	-0.05	0.17	0.35	-0.50	-0.54	0.27	-0.40	0.91	-0.31	-0.26	0.64	0.89	0.49	1.00

Table 20. Statistical evaluation – GP Volkovo dataset

	Units	N	Mean	SD	Minimum	Maximum	C.V.	95 th %	5 th %
PM2.5	µg/m³	60	35.75	23.58	7.68	111.32	0.66	85.95	8.44
Na		60	11.850	10.514	5.520	69.663	0.887	28.925	6.014
Mg		60	27.313	38.932	1.572	209.577	1.425	83.094	2.074
Al		60	87.142	160.246	5.551	852.899	1.839	373.833	8.827
Si		60	234.196	374.017	14.907	2020.539	1.597	893.828	31.750
S		60	135.604	64.495	44.479	326.596	0.476	251.375	57.235
K		60	248.286	207.786	41.684	805.869	0.837	651.803	50.721
Ca		60	558.882	466.797	37.427	2491.168	0.835	1322.528	73.966
Ti		60	11.453	17.388	0.373	90.163	1.518	41.690	2.147
Cr		60	1.797	1.383	0.025	3.542	0.769	3.380	0.075
Mn		60	4.099	2.840	0.226	11.042	0.693	9.589	0.601
Fe		60	232.934	238.458	20.873	1249.912	1.024	640.749	56.628
Co		60	2.074	1.836	0.003	3.914	0.886	3.734	0.005
Ni		60	1.150	1.428	0.025	3.965	1.242	3.773	0.025
Cu		60	5.775	3.928	0.277	16.804	0.680	12.279	0.879
Zn		60	41.886	40.886	2.012	195.966	0.976	120.943	6.554
As		60	3.510	2.290	0.201	12.577	0.652	10.615	1.449
Sc	ng/m³	60	3.629	0.033	3.619	3.808	0.009	3.640	3.621
V		60	1.467	0.707	0.466	3.170	0.482	2.473	0.494
Rb		60	0.753	1.212	0.008	4.654	1.610	4.652	0.066
Sb		60	1.516	0.494	0.395	2.843	0.326	2.352	0.861
Ba		60	2.767	2.126	0.402	12.550	0.768	6.510	1.657
Ce		60	1.391	1.116	0.015	2.512	0.802	2.398	0.045
Sm		60	2.359	2.431	0.000	5.104	1.030	4.869	0.002
W		60	1.509	1.813	0.003	3.993	1.202	3.802	0.008
Pb		60	8.347	5.584	0.679	21.984	0.669	20.528	2.182
Th		60	1.390	1.694	0.001	3.703	1.219	3.532	0.004
Cl		60	80.976	74.898	1.711	383.752	0.925	219.995	3.421
Se		60	2.554	1.376	0.025	3.835	0.539	3.665	0.221
Cd		60	3.981	0.701	2.790	7.949	0.176	4.951	3.796
EC		60	6749.37	3387.65	1358.00	13353.00	0.502	12243.65	1807.20
NH_4		60	901.82	691.88	54.50	3105.31	0.767	2004.10	108.08
SO_4		60	6090.39	9272.05	118.07	44220.47	1.522	22084.52	551.12
NO_3		60	1702.52	2144.83	18.17	9225.13	1.260	6292.32	25.43

Table. 20- a . Corelation matrix – GP Volkovo dataset

	PM2.5	Na	Mg	Al	Si	S	K	Ca	Ti	Cr	Mn	Fe	Co	Ni	Cu	Zn	As	Sc	V	Rb	Sb	Ba	Ce	Sm	W	Pb	Th	Cl	Se	Cd	EC	NH4	SO4	NO3
PM2.5	1.00																																	
Na	0.06	1.00																																
Mg	0.02	0.31	1.00																															
Al	0.05	0.29	0.97	1.00																														
Si	0.05	0.30	0.98	1.00	1.00																													
S	0.19	-0.14	0.08	0.15	0.13	1.00																												
K	0.54	-0.02	0.10	0.12	0.10	0.39	1.00																											
Ca	0.04	0.30	0.93	0.88	0.91	0.03	-0.01	1.00																										
Ti	0.04	0.28	0.96	1.00	0.99	0.15	0.13	0.88	1.00																									
Cr	-0.17	-0.19	-0.04	-0.02	-0.04	-0.02	0.00	-0.14	-0.04	1.00																								
Mn	0.03	0.09	0.60	0.48	0.50	-0.17	0.03	0.54	0.48	-0.13	1.00																							
Fe	0.15	0.29	0.97	0.98	0.98	0.17	0.24	0.90	0.98	-0.09	0.54	1.00																						
Co	0.20	-0.08	-0.49	-0.42	-0.46	0.30	0.51	-0.63	-0.41	0.09	-0.49	-0.41	1.00																					
Ni	-0.10	-0.24	-0.17	-0.16	-0.18	-0.25	0.01	-0.29	-0.18	0.34	-0.02	-0.22	0.24	1.00																				
Cu	0.20	0.01	0.16	0.01	0.05	-0.27	0.12	0.23	0.01	-0.15	0.50	0.11	-0.32	-0.08	1.00																			
Zn	0.17	-0.10	0.01	-0.12	-0.11	-0.02	0.24	-0.05	-0.13	-0.09	0.62	-0.03	0.02	0.09	0.53	1.00																		
As	0.26	0.11	-0.09	-0.06	-0.04	-0.30	-0.16	0.06	-0.07	-0.19	0.00	-0.06	-0.33	-0.07	0.25	-0.07	1.00																	
Sc	0.29	-0.09	-0.10	-0.07	-0.09	0.33	0.35	-0.18	-0.09	0.05	0.08	-0.05	0.16	0.08	0.06	0.25	-0.02	1.00																
V	0.10	0.10	0.49	0.52	0.52	0.07	-0.03	0.48	0.51	-0.19	0.28	0.51	-0.29	-0.27	-0.03	-0.01	-0.06	-0.12	1.00															
Rb	-0.11	0.09	-0.10	-0.10	-0.10	0.08	-0.23	-0.12	-0.12	0.32	-0.18	-0.17	0.01	0.23	0.00	-0.07	-0.06	-0.07	-0.23	1.00														
Sb	0.01	0.10	0.38	0.41	0.42	0.06	0.01	0.44	0.43	-0.19	0.06	0.39	-0.33	-0.23	-0.14	-0.29	-0.03	0.04	0.26	-0.12	1.00													
Ba	0.37	0.10	0.60	0.60	0.60	0.12	0.27	0.60	0.57	-0.07	0.33	0.64	-0.21	-0.15	0.11	-0.05	-0.06	-0.07	0.48	-0.13	0.20	1.00												
Ce	0.05	-0.22	-0.05	-0.03	-0.03	-0.02	-0.05	-0.08	-0.07	0.07	0.06	-0.06	-0.06	0.18	0.09	0.13	0.11	0.18	0.09	0.05	-0.23	0.18	1.00											
Sm	0.28	0.07	-0.16	-0.10	-0.14	0.42	0.57	-0.28	-0.09	0.19	-0.19	-0.04	0.67	0.11	-0.25	0.11	-0.21	0.20	-0.14	0.10	-0.20	-0.03	-0.11	1.00										
W	0.31	-0.03	-0.26	-0.25	-0.28	0.36	0.54	-0.31	-0.23	-0.06	-0.34	-0.16	0.63	-0.05	-0.17	0.10	-0.14	0.05	-0.11	-0.08	-0.23	-0.05	-0.17	0.60	1.00									
Pb	0.07	-0.05	0.12	-0.06	-0.03	-0.17	0.20	0.09	-0.05	-0.21	0.62	0.05	-0.20	-0.09	0.72	0.72	-0.03	0.05	0.01	-0.13	-0.12	0.02	-0.01	-0.09	-0.05	1.00								
Th	0.02	-0.24	-0.35	-0.29	-0.32	0.15	0.19	-0.44	-0.28	0.31	-0.34	-0.32	0.64	0.32	-0.29	0.01	-0.24	0.24	-0.21	0.15	-0.24	-0.29	-0.18	0.54	0.42	-0.25	1.00							
Cl	0.44	0.21	-0.12	-0.17	-0.17	0.11	0.73	-0.13	-0.17	-0.17	0.16	-0.05	0.32	-0.07	0.45	0.50	0.10	0.29	-0.19	-0.09	-0.11	0.01	-0.09	0.38	0.35	0.51	0.08	1.00						
Se	-0.10	0.11	0.12	0.19	0.16	0.23	0.10	0.05	0.19	-0.11	0.03	0.16	0.09	-0.05	-0.45	-0.14	-0.27	0.19	0.04	-0.16	0.22	0.01	-0.13	0.22	-0.03	-0.21	0.05	-0.05	1.00					
Cd	-0.17	-0.13	-0.14	-0.07	-0.08	0.21	-0.16	-0.12	-0.07	-0.26	-0.15	-0.10	-0.04	-0.17	-0.29	-0.17	-0.17	0.01	0.05	-0.03	0.20	-0.09	0.04	-0.18	-0.15	-0.15	-0.21	-0.20	0.27	1.00				
EC	0.34	-0.07	-0.26	-0.34	-0.34	0.10	0.64	-0.30	-0.32	-0.13	0.03	-0.19	0.47	0.02	0.36	0.50	-0.06	0.19	-0.24	-0.16	-0.36	-0.09	0.02	0.46	0.59	0.52	0.20	0.67	-0.17	-0.20	1.00			
NH4	0.28	-0.28	-0.33	-0.25	-0.29	0.75	0.56	-0.41	-0.25	0.01	-0.34	-0.20	0.55	-0.13	-0.33	0.06	-0.29	0.42	-0.18	-0.03	-0.03	-0.15	0.02	0.59	0.50	-0.04	0.30	0.34	0.27	0.20	0.36	1.00		
SO4	0.05	-0.11	-0.05	-0.08	-0.07	0.13	0.04	0.05	-0.09	0.11	-0.05	-0.03	-0.07	0.04	0.17	0.00	0.26	-0.03	-0.15	0.01	-0.22	-0.09	0.04	0.00	0.03	0.06	-0.10	0.12	-0.25	-0.10	0.17	0.10	1.00	
NO3	0.48	-0.15	-0.20	-0.16	-0.19	0.47	0.88	-0.28	-0.15	-0.02	-0.16	-0.05	0.60	-0.02	0.00	0.19	-0.15	0.34	-0.23	-0.15	-0.09	0.01	-0.09	0.63	0.60	0.19	0.26	0.70	0.15	-0.04	0.66	0.79	0.14	1.00

Table 21. Statistical analysis – Gazi baba dataset

	Units	N	Mean	SD	Minimum	Maximum	C.V.	95 th %	5 th %
PM2.5	µg/m³	56	46.62	34.20	8.40	153.04	0.73	133.80	10.26
Na		56	8.595	3.019	2.912	25.120	0.351	12.878	5.668
Mg		56	28.602	21.962	1.295	95.146	0.768	68.966	2.365
Al		56	73.413	70.783	2.887	411.714	0.964	153.147	12.493
Si		56	210.290	171.615	4.418	934.139	0.816	440.956	47.060
S		56	165.580	84.889	0.179	449.869	0.513	302.120	48.576
K		56	251.958	251.082	14.987	1100.182	0.997	713.964	35.231
Ca		56	681.435	523.854	31.029	2019.113	0.769	1552.094	109.818
Ti		56	10.541	8.301	1.653	41.013	0.788	23.608	2.390
Cr		56	0.801	0.775	0.050	4.175	0.967	2.301	0.125
Mn		56	4.602	2.684	0.297	14.691	0.583	9.204	1.415
Fe		56	301.624	236.445	21.339	947.605	0.784	716.579	64.996
Co		56	0.032	0.024	0.003	0.092	0.757	0.088	0.008
Ni		56	0.421	0.666	0.025	4.954	1.581	0.932	0.095
Cu		56	7.469	5.568	0.230	26.356	0.745	15.737	0.922
Zn		56	54.129	44.025	0.482	171.593	0.813	154.005	8.423
As		56	1.172	2.581	0.369	11.013	2.202	8.928	0.373
Sc	ng/m³	56	1.606	0.004	1.584	1.609	0.003	1.609	1.600
V		56	1.731	0.781	0.441	3.497	0.451	3.150	0.505
Rb		56	0.382	0.297	0.010	1.114	0.779	0.883	0.048
Sb		56	1.539	0.567	0.340	3.094	0.368	2.333	0.711
Ba		56	2.942	1.998	0.152	10.009	0.679	7.521	1.773
Ce		56	0.127	0.040	0.020	0.231	0.315	0.162	0.037
Sm		56	0.007	0.006	0.003	0.022	0.821	0.018	0.003
W		56	0.048	0.050	0.003	0.200	1.047	0.157	0.014
Pb		56	9.498	5.071	0.406	24.502	0.534	18.459	3.320
Th		56	0.032	0.040	0.000	0.128	1.227	0.115	0.004
Cl		56	103.098	107.570	0.206	504.459	1.043	269.953	0.240
Se		56	0.698	0.517	0.101	2.337	0.741	1.946	0.163
Cd		56	4.653	2.860	1.560	23.197	0.615	6.020	1.789
EC		56	11936.95	9469.74	1132.00	37116.00	0.79	29327.25	1848.25
NH_4		56	1253.30	969.80	54.44	3596.66	0.77	3505.14	99.33
SO_4		56	5989.32	9411.57	725.48	44254.22	1.57	22069.70	1345.33
NO_3		56	2739.71	3772.28	25.05	16163.60	1.38	9022.94	25.30

Table. 21- a . Corelation matrix – Gazi Baba dataset

	PM2.5	Na	Mg	Al	Si	S	K	Ca	Ti	Cr	Mn	Fe	Co	Ni	Cu	Zn	As	Sc	V	Rb	Sb	Ba	Ce	Sm	W	Pb	Th	Cl	Se	Cd	EC	NH4	SO4	NO3
PM2.5	1.00																																	
Na	-0.01	1.00																																
Mg	0.68	0.14	1.00																															
Al	0.61	0.04	0.90	1.00																														
Si	0.64	0.09	0.95	0.99	1.00																													
S	0.60	-0.10	0.53	0.47	0.51	1.00																												
K	0.78	0.11	0.64	0.47	0.54	0.73	1.00																											
Ca	0.64	0.10	0.84	0.62	0.73	0.62	0.75	1.00																										
Ti	0.69	0.03	0.93	0.95	0.97	0.53	0.59	0.76	1.00																									
Cr	0.68	0.14	0.63	0.50	0.55	0.45	0.70	0.67	0.57	1.00																								
Mn	0.34	0.41	0.43	0.27	0.32	0.36	0.53	0.33	0.29	0.33	1.00																							
Fe	0.80	0.13	0.87	0.75	0.81	0.68	0.86	0.82	0.83	0.76	0.50	1.00																						
Co	-0.45	0.57	-0.31	-0.35	-0.34	-0.58	-0.42	-0.37	-0.38	-0.21	0.12	-0.33	1.00																					
Ni	0.25	0.24	0.13	0.04	0.07	0.02	0.38	0.14	0.08	0.43	0.36	0.32	0.20	1.00																				
Cu	0.33	0.51	0.35	0.20	0.25	0.12	0.52	0.31	0.25	0.49	0.58	0.56	0.43	0.67	1.00																			
Zn	0.14	0.30	0.16	0.01	0.04	0.16	0.38	0.13	0.03	0.20	0.75	0.31	0.14	0.31	0.49	1.00																		
As	-0.27	0.29	-0.35	-0.24	-0.24	-0.30	-0.25	-0.25	-0.23	-0.18	-0.11	-0.23	0.45	0.09	0.14	-0.22	1.00																	
Sc	0.33	-0.02	0.25	0.19	0.22	0.43	0.35	0.35	0.22	0.19	0.06	0.25	-0.57	-0.16	-0.21	0.01	-0.28	1.00																
V	0.14	0.11	0.42	0.35	0.41	0.13	0.25	0.47	0.36	0.18	0.12	0.30	-0.15	-0.13	-0.01	0.00	-0.13	0.39	1.00															
Rb	0.24	0.61	0.22	0.04	0.10	0.02	0.43	0.23	0.11	0.40	0.48	0.41	0.57	0.56	0.88	0.40	0.23	-0.27	-0.03	1.00														
Sb	0.19	-0.17	0.33	0.20	0.26	0.25	0.24	0.50	0.29	0.17	-0.04	0.28	-0.32	-0.05	-0.06	0.01	-0.24	0.14	0.27	-0.13	1.00													
Ba	0.50	0.18	0.50	0.32	0.38	0.43	0.60	0.55	0.38	0.72	0.42	0.58	-0.06	0.40	0.46	0.19	-0.19	0.21	0.13	0.48	0.08	1.00												
Ce	-0.16	0.02	-0.06	-0.04	-0.05	-0.03	-0.06	-0.04	-0.07	-0.03	0.10	-0.01	0.01	0.06	0.03	0.02	0.17	0.12	0.16	-0.06	-0.01	0.14	1.00											
Sm	-0.54	0.41	-0.48	-0.47	-0.49	-0.56	-0.52	-0.56	-0.54	-0.32	0.00	-0.49	0.80	0.18	0.22	0.06	0.39	-0.47	-0.35	0.34	-0.45	-0.13	-0.01	1.00										
W	-0.46	0.42	-0.35	-0.36	-0.36	-0.58	-0.40	-0.40	-0.38	-0.22	0.07	-0.33	0.89	0.21	0.42	0.12	0.52	-0.44	-0.12	0.55	-0.28	-0.10	0.08	0.70	1.00									
Pb	0.39	0.43	0.38	0.13	0.20	0.30	0.65	0.36	0.19	0.40	0.76	0.55	0.19	0.45	0.79	0.73	-0.17	0.05	0.09	0.70	0.03	0.44	-0.04	0.03	0.16	1.00								
Th	-0.40	0.52	-0.30	-0.35	-0.33	-0.53	-0.28	-0.34	-0.37	-0.19	0.18	-0.24	0.92	0.33	0.55	0.19	0.53	-0.55	-0.18	0.68	-0.31	-0.05	0.02	0.75	0.93	0.30	1.00							
Cl	0.63	0.31	0.53	0.29	0.38	0.53	0.89	0.67	0.42	0.63	0.52	0.77	-0.09	0.52	0.74	0.42	-0.11	0.21	0.19	0.69	0.17	0.65	0.00	-0.25	-0.10	0.77	0.04	1.00						
Se	-0.16	0.35	-0.15	-0.22	-0.20	-0.39	-0.13	-0.16	-0.18	0.04	0.04	-0.07	0.70	0.21	0.49	0.19	0.27	-0.41	-0.08	0.64	-0.08	0.03	-0.07	0.45	0.76	0.30	0.75	0.15	1.00					
Cd	-0.02	-0.21	-0.18	-0.18	-0.20	-0.22	-0.10	-0.18	-0.17	-0.06	-0.11	-0.14	-0.01	-0.04	-0.10	-0.09	-0.04	-0.09	-0.11	-0.08	0.01	0.07	0.11	-0.06	-0.02	-0.15	-0.03	-0.09	-0.03	1.00				
EC	0.67	0.20	0.57	0.33	0.42	0.57	0.89	0.72	0.49	0.61	0.39	0.78	-0.21	0.33	0.56	0.26	-0.18	0.24	0.25	0.60	0.22	0.60	-0.06	-0.37	-0.21	0.62	-0.09	0.92	0.08	-0.07	1.00			
NH4	0.63	-0.16	0.31	0.23	0.27	0.83	0.76	0.45	0.33	0.46	0.24	0.56	-0.56	0.17	0.16	0.17	-0.30	0.43	0.06	0.09	0.15	0.43	-0.11	-0.55	-0.56	0.34	-0.48	0.61	-0.28	-0.07	0.64	1.00		
SO4	0.08	-0.14	0.22	0.36	0.30	0.15	-0.01	0.00	0.29	0.06	-0.09	0.11	-0.19	-0.15	-0.11	-0.22	-0.15	0.16	0.04	-0.23	0.15	-0.04	-0.16	-0.05	-0.14	-0.14	-0.24	-0.13	-0.16	-0.15	-0.09	0.06	1.00	
NO3	0.74	0.06	0.48	0.33	0.40	0.69	0.93	0.63	0.46	0.69	0.42	0.74	-0.38	0.40	0.46	0.32	-0.22	0.32	0.17	0.41	0.18	0.59	-0.11	-0.48	-0.38	0.58	-0.26	0.84	-0.06	-0.08	0.83	0.87	-0.05	1.00

4.3.2. Results and discussion

As shown above, daily average PM2.5 concentrations measured at all monitoring sites in Skopje urban area, exhibits significant seasonal and spatial variability, exceeding all of the European Union's limit, target, and threshold values for human health protection.

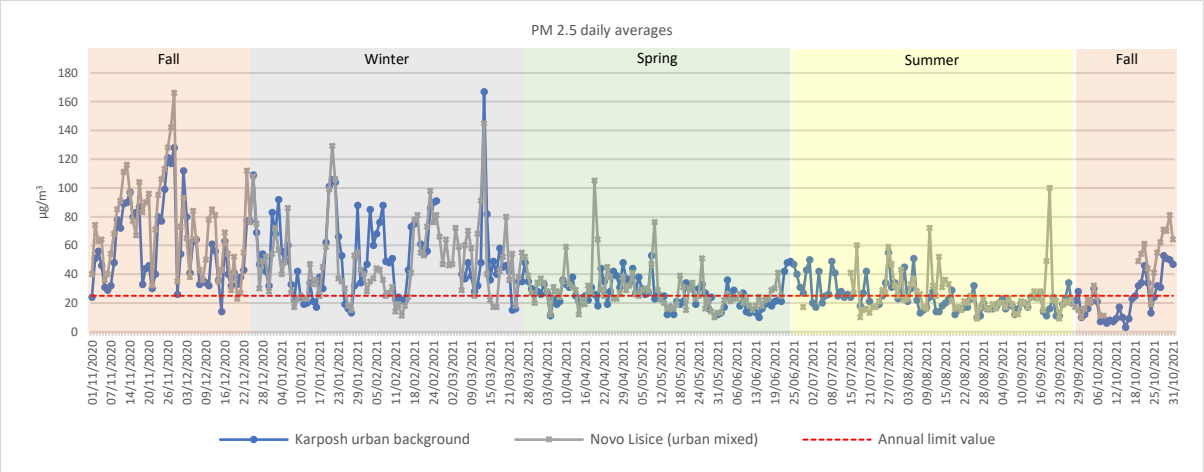

Figure 25. PM 2.5 Mass concentrations – permanent monitoring sites

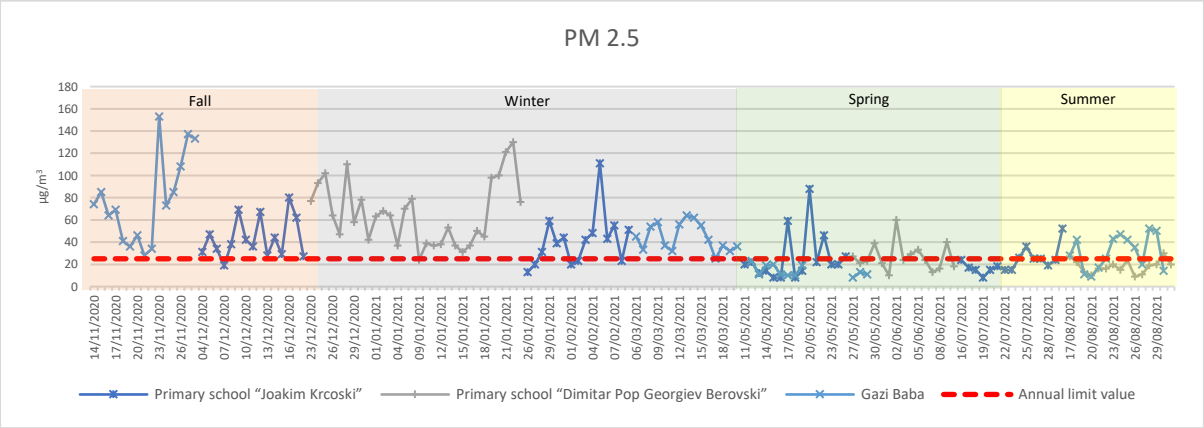

Figure 26. PM 2.5 Mass concentrations –indicative (short term) monitoring sites

The highest mass concentrations were measured in Gazi Baba (46.62 ± 34.20 µg/m³), followed by Novo Lisiche (45.68 ± 28.85 µg/m³), Gorce Petrov – Hrom (43.98 ± 30.26 µg/m³), Karposh (36.40 ± 24.18 µg/m³) and Gorce Petrov – Volkovo (35.75 ± 23.58 µg/m³). The particulate mass (PM 2.5) concentrations measured in Skopje, were among the highest reported in the Europe (PM2.5 annual average concentrations observed in Europe were found from 3 to 35 µg/m³) [26].

Percentage of days exceeding annual limit values for PM 2.5 (25 µg/m³) was 62.30 % for Novo Lisiche (195 out 313 valid daily values) and 58.97 % for Karposh site (194 out 329 valid daily values), with significantly higher concentrations recorded during the cold months.

Table 22. Statistical evaluation of PM 2.5 mass concentration in Skopje urban area

	Unit	Karposh	Novo Lisiche	GP - Hrom	GP- Volkovo	Gazi Baba
Mean	µg/m³	36.40	45.68	43.98	35.75	46.62
SD	µg/m³	24.18	28.85	30.26	23.58	34.20
Minimum	µg/m³	3.30	10.51	8.81	7.68	8.40
Maximum	µg/m³	167.35	165.61	129.87	111.32	153.04
N		331	255	60	60	56
C.V.		0.66	0.63	0.69	0.66	0.73
95 th %	µg/m³	87.818	104.84	102.29	85.95	133.80
5 th %	µg/m³	11.69	16.03	10.67	8.43	10.26

Average PM 2.5 concentrations recorded at Karposh urban background site during the cold season (November, December, January February and March) were 54.26 µg/m^3, and only 24.79 µg/m^3 during the warm season (May, June, July, August and September). Similar variations were found for all monitoring sites in Skopje urban area, as shown on the chart below.

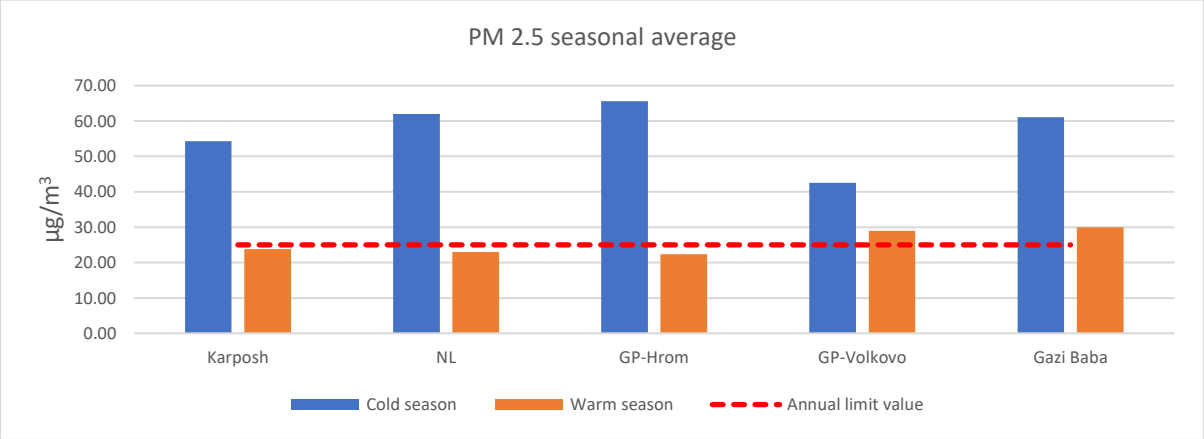

Figure 27. PM 2.5 seasonal variations in Skopje urban area

The chemical compositions of PM2.5 differ across Europe and on average, Central Europe has more carbonaceous matter in PM2.5, North-western Europe has more nitrate, and southern Europe has more mineral dust in all fractions [26].

Due to the fact that the majority of the pollutant concentrations in the Skopje valley originate from local emissions and are exacerbated by the local topography, along with poor atmospheric mixing conditions, this urban area typically displays an extremely homogeneous pollution field, both spatially and by component [27].

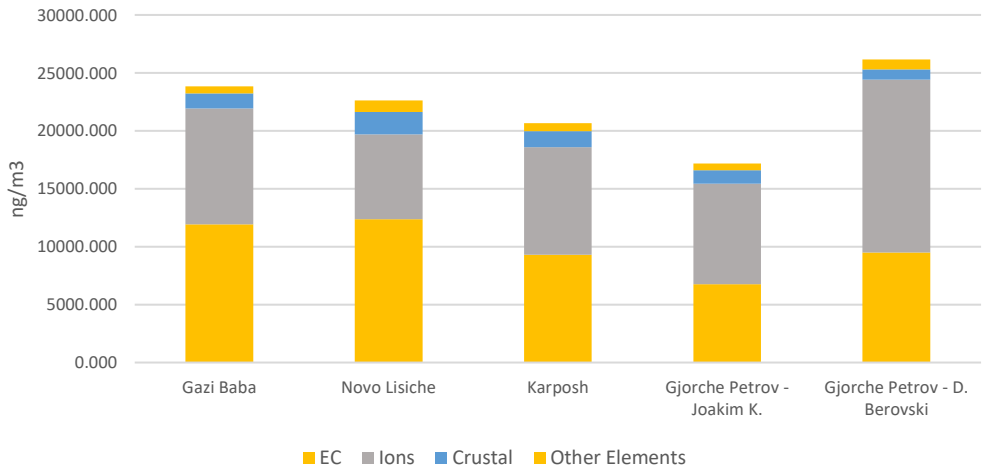

Figure 28. Major components and elemental groups in Skopje urban area

Similar composition of major components and elemental groups confirms that similar sources impact all receptors throughout the urban area.

Contribution of soil (mineral) dust observed in Skopje is similar to the values found in other parts of Europe [26], and starts from 4.9 % in Novo Lisiche, 4.8 % in Kapros, 4.46 % in GP- Volkovo, and slightly lower 3.2 % in GP-Hrom and 3.18% in Gazi Baba. Elements like Mg, Al, Si, Ca, Ti and Fe, usually used as tracers for soil dust, are well corelated, indicating common source for these elements and providing clear identification of this source in subsequent factor analysis.

Sea salt contributions are negligible, as would be expected for a typically continental location, and smaller amounts found could be attributed more to de-icing salt suspension, than to long range transport.

Sulphates and nitrates contributions are within the lower range of values recorded across Europe, and were found similar to the values recorded in Southern Europe [26]. Although this could be attributed to several factors, a relatively low average concentrations of their gaseous precursors like sulphuric and nitrous oxides must be noted. Average sulphate contribution to total particulate mass is 12.42 % in GP-Volkovo, 12.26 % in GP-Hrom, 11.51 % in Gazi Baba, 10.17 % in Karposh and 9.5 % in Novo Lisiche, while average nitrate contribution reach 4.85 % in GP-Hrom, 4.4% in Karposh, 4.29 % in Gazi Baba, 4.15 % in GP-Volkovo and 3.7% in Novo Lisiche.

However, elemental carbon (EC) contributions found in the urban area of Skopje are higher than European averages and fall within the range of those found in Central Europe, likely reflecting the mix of local sources, where wood combustion was identified as the most significant single source of particulate matter emission [8, 9] for all receptors, and traffic in particular for the Novo Lisiche site.

Table 23. Major contribution of PM2.5 in urban areas (%) [26]

%	N-Western Europe	Southern Europe	Central Europe	Skopje Urban area
Soil (mineral) dust	5	11	5	4.2
Road salt/Sea salt	4	6	1	0.2
SO_4	21	15	19	12
NO_3	16	7	13	4.3
EC	7	8	14	23.2

EC contributions to total particulate mass range from 33.7 % at Novo Lisiche (site exposed to traffic and residential heating emissions), 25.6 % at Gazi Baba, 21.6 % at GP-Hrom, 18.8 % at GP – Volkovo and 16.5 % at Karposh urban background site. Elemental carbon was shown to be correlated with K, Cl, Rb, ammonium, and nitrate ions, mostly associated with biomass burning emissions. All those elements corelate well with total particulate mass, indicating that biomass burning is a significant contributor to particulate mass.

According to the results of the assessment of regulated metals including lead, arsenic and nickel, it was determined that concentrations found were within the annual limit, upper assessment threshold, and lower assessment threshold values as specified in Directives 2008/51/EC and 2004/71/EC. However, the concentrations of As found at two sites (Volkovo and Gorce Petrov) were at or above the lower assessment target. Cadmium was excluded from the evaluation because more than 80 percent of the readings were close to or below the method limit detection.

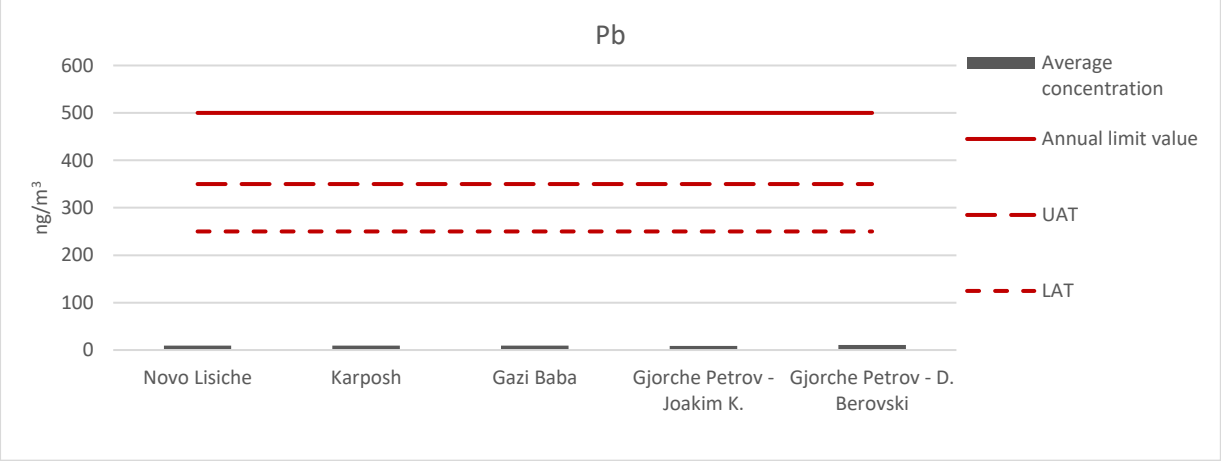

Figure 29. Annual concentration of lead (Pb) in particulate matter (PM2.5) in Skopje urban area

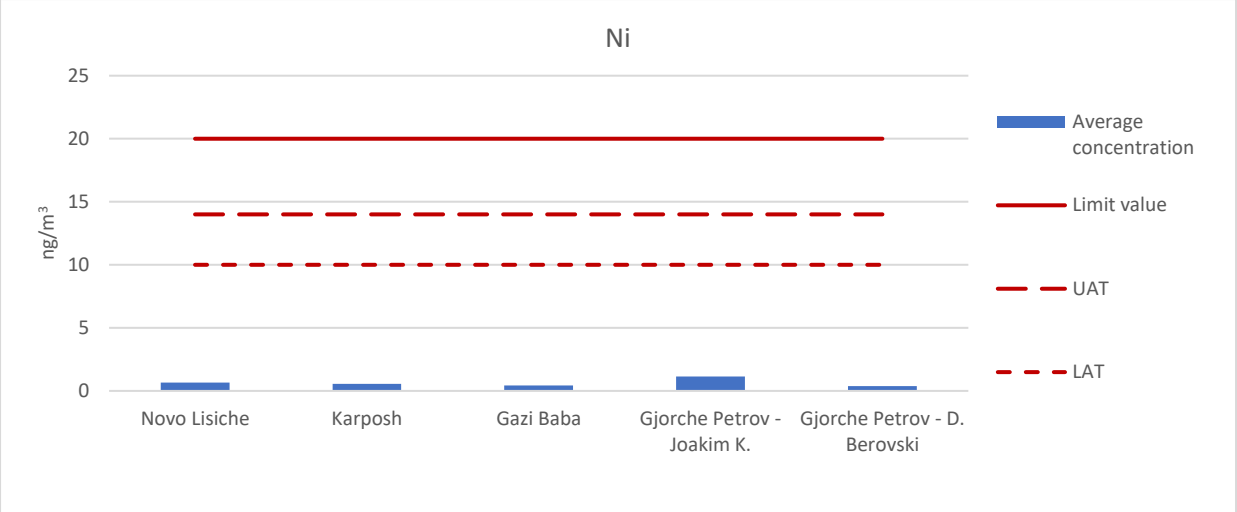

Figure 30. Annual concentration of nickel (Ni) in particulate matter (PM2.5) in Skopje urban area

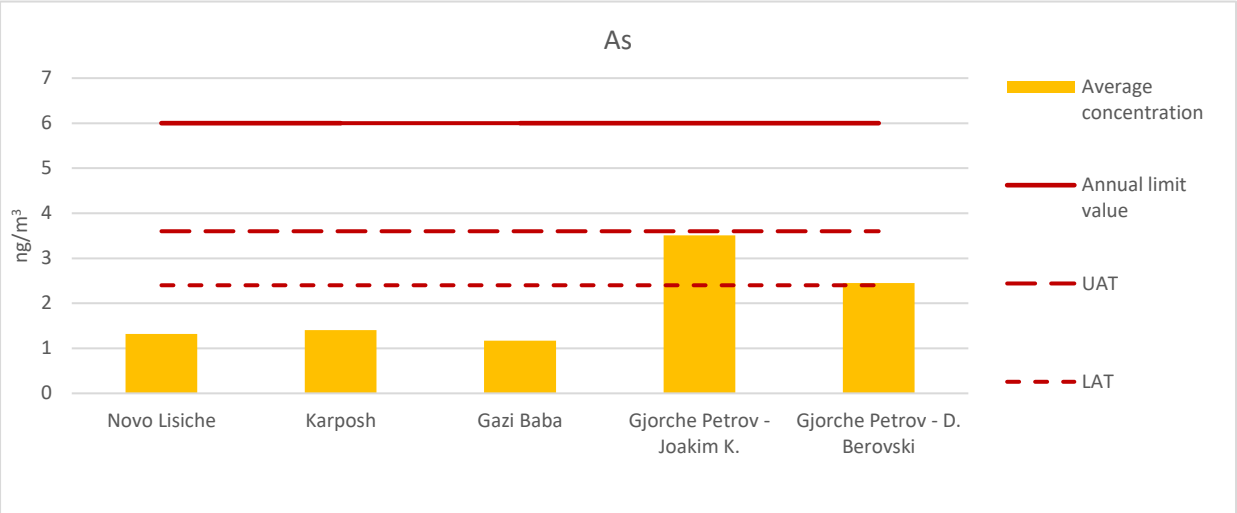

Figure 31. Annual concentration of nickel (Ni) in particulate matter (PM2.5) in Skopje urban area

According to additional analysis of the temporal distribution of arsenic concentrations for sites with sufficient data coverage (Karposh and Novo Lisiche), the sites' highest average arsenic concentrations appear to occur exclusively in the spring and early summer months, suggesting the impact of a single source with substantial contributions in both spring and early summer months.

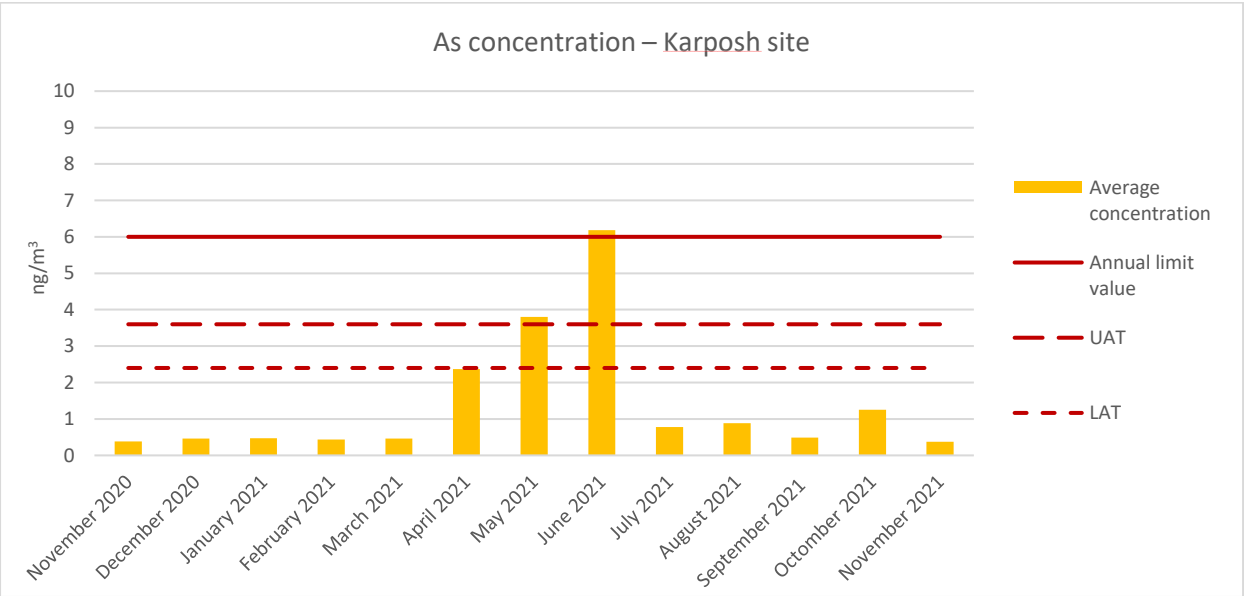

Figure 32. Arsenic average monthly concentrations at Karposh monitoring site

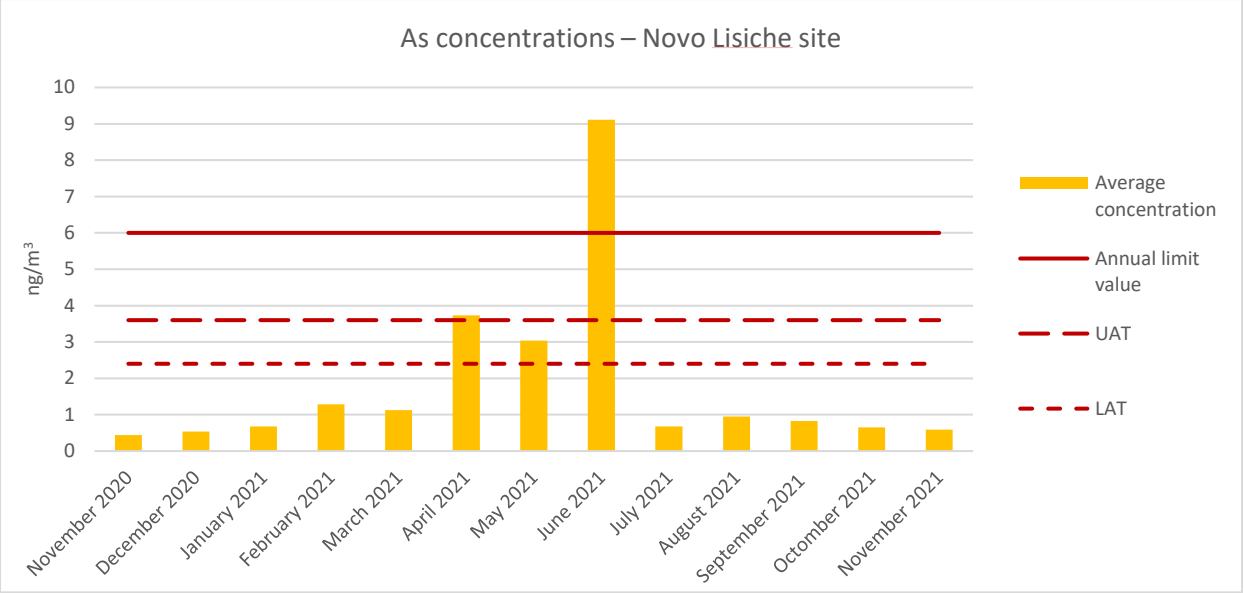

Figure 33. Arsenic average monthly concentrations at Novo Lisiche monitoring site

Further investigation into metal concentrations found higher levels of a specific set of metals (Cr, Co, Ni, As, Sc. Ce. Sm. W and Th) at the Volkovo site as compared to other locations, showing that this receptor is being influenced by a specific source. Increased metal concentrations are usually linked to anthropogenic sources, however further investigation is required to make a correct identification.

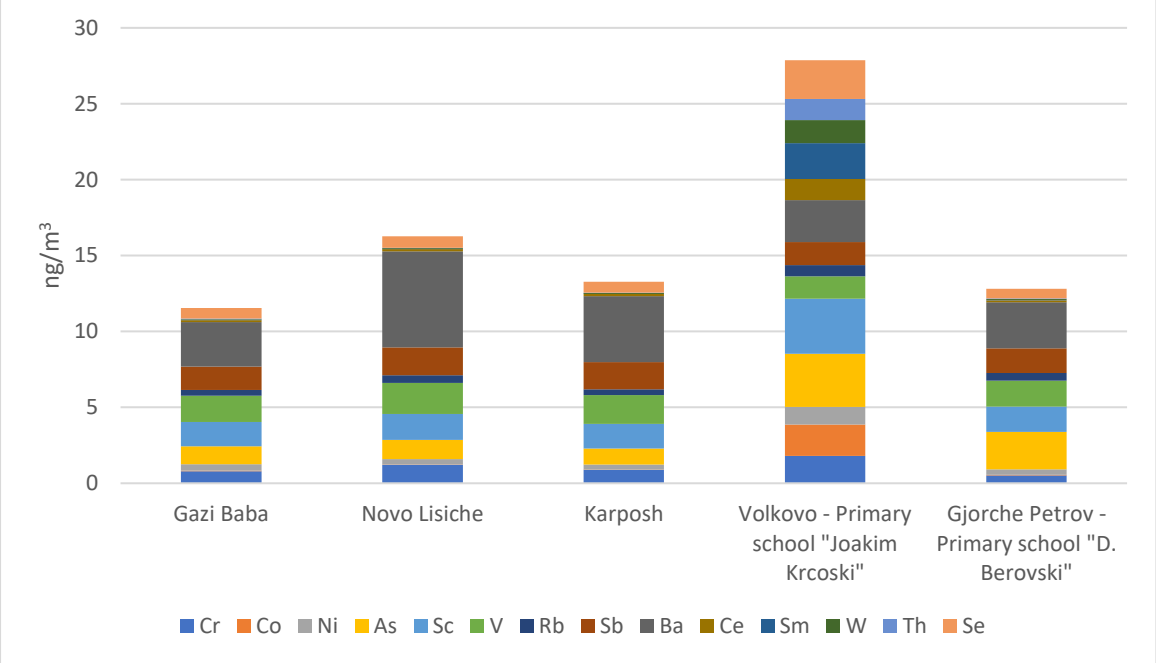

Figure 34. Average annual metals concentrations in Skopje urban area

5. Positive Matrix Factorisation

Environmental monitoring data are increasingly being handled in terms of mathematical models, which allow for the management of a variety of datasets with multiple observations to be performed. Different modeling techniques are available depending on the type of known information (input data) and the sort of results that would be obtained (output data) that are desired.

Source allocation (SA) is the practice of obtaining information about pollution sources and the amount of pollution that each source contributes to the level of ambient air pollution. Emission inventories, source-oriented models, and receptor-oriented models are three ways that can be used to do this task.

Recent years have seen the rise in importance of receptor-oriented models (also known as receptor models (RMs)) in environmental sciences, which are used to elicit information from datasets that contain a number of features (chemical or physical qualities) associated with the measured samples. For example, they can be used to assess the contribution of contamination and pollutant sources in various types of samples, starting with the information provided by the samples (which is recorded at the monitoring site) and progressing to the point of effect, or receptor.

Receptor models are also known as multivariate methods because they are used to analyze a data set containing a large number of numerical values as a whole. Receptor models, to be more precise, are mathematical methodologies for measuring the contribution of sources to samples based on their composition or fingerprints. To separate impacts, the composition or speciation is identified using media-specific analytical methods, and key species or combinations of species are required. A speciated data set can be considered of as a data matrix X with i by j dimensions, in which i samples and j chemical species were measured with u uncertainty.

The goal of receptor models is to solve the chemical mass balance (CMB) in Equation 1, between measured species concentrations and source profiles, where p is the number of factors, f is each source's element profile, g is each factor's mass in each sample, and e_{ij} is the "remaining" for each element/sample.

$$x_{ij} = \sum_{k=1}^{p} g_{ik} f_{kj} + e_{ij} \qquad (1)$$

A dataset containing a vast amount of data consisting of chemical elements (such as elemental concentrations) acquired from a large number of observations (samples) is required to find the answer. The larger the data matrix, the more likely the model is to uncover separate factors that can be used as sources. The number of samples required can vary depending on prior knowledge of the sources and the RMs methodology chosen (e.g., CMB vs. PMF).

If the number and nature (composition profiles/fingerprints) of the sources in the study area are known, then the only unknown term of equation (1) is the mass contribution of each source to each sample. To solve the chemical mass balance and to elicit information on sources type, number and contribution starting from observations (i.e. element concentrations data set) at receptor site, different factor analysis methods (multivariate methods) have been developed. Common factor analysis methods used include Principal Component Analysis (PCA), Unmix, Target Transformation Factor Analysis (TTFA), Positive Matrix Factorization (PMF) and Multilinear Engine (ME).

Dr. Pentti Paatero (Department of Physics, University of Helsinki) created Positive Matrix Factorization (PMF) in the mid-1990s to establish a new method for the analysis of multivariate data that addressed several drawbacks of the PCA.

PMF uses error estimates to weight data values and imposes non-negativity constraints in the factor computational process. The algorithm accomplishes weighted least squares fit with the objective of

minimizing Q, a function of the residuals weighted by the uncertainties of the species concentrations in the data matrix. The PMF factor model can be written as X = G·F + E, where X is the known n·m matrix of the m measured chemical species in n samples. G is an n·p matrix of factor (source) contribution in every sample (time series). F is a p·m matrix of factor compositions (factor profiles). G and F are factor matrices to be determined and E is defined as a residual matrix, i.e. the difference between the measured X and the modeled Y = G·F.

In this study, the free software US-EPA PMF 5.0 version 5.0.14 (Norris and Duvall, 2014), implementing the ME-2 algorithm developed by Paatero (1999), was used.

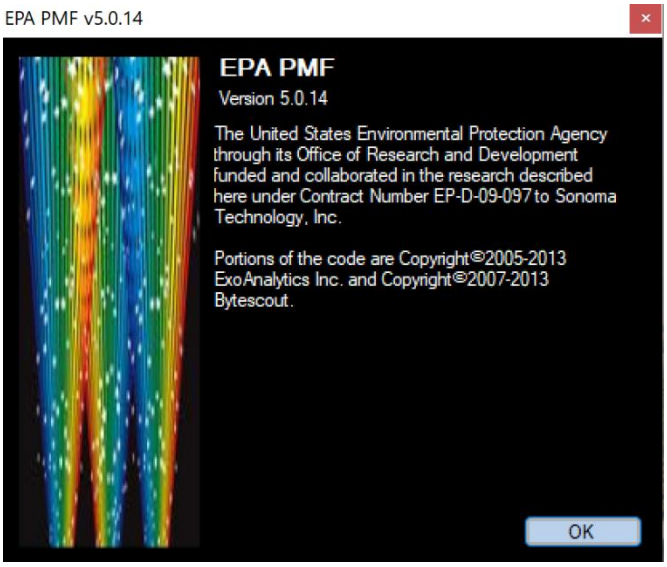

Figure 35. Free software US-EPA PMF 5.0 version 5.0.14 – splash screen

PMF was first employed in studies of air pollution and source apportionment [29, 35] as well as precipitation investigations [23]. Air quality and source apportionment applications [30, 37] have gain rapid popularity in recent years, but PMF has also been used on lake sediments [38], wastewater [39, 40], and soils [28]. This multivariate factor analysis tool has been used to analyze a variety of data, including 24-hour speciated PM2.5, size-resolved aerosol, deposition, air toxics, high time resolution measurements from aerosol mass spectrometers (AMS), and volatile organic compound (VOC) data.

The use of known experimental uncertainties as input data allows for individual handling of matrix members and can handle missing or below-detection-limit data, which is a prevalent feature of environmental monitoring. Because the PMF results are quantitative, it is feasible to determine the composition of the sources determined by the model.

Equation 2 was used to determine the uncertainty of the utilized method for each element separately, and Equation 3 was used to determine the uncertainty of the instrument for each element separately:

$$u = \sqrt{U_{instrument}{}^2 + U_{CRM}{}^2 + U_{sampling}{}^2} \quad (\%) \qquad (2)$$

$$U_{instrument} = \frac{STDEV}{average} * 100 \quad (\%) \qquad (3)$$

Where $U_{instrument}$ - uncertainty of the used instrument, U_{CRM} - uncertainty of the used certified referent material, $U_{sampling}$ - uncertainty of the sampling.

Before data processing, basic statistics tests including dispersion, distribution, correlation matrices, linear regression and time trends were performed in order to examine the relationships between the variables.

5.1. Input data and PMF model setting

Because the number of samples for indicative monitoring sites was limited, only data sets from Karpsoh and Novo Lisiche were subjected to comprehensive PMF analysis.

Species lists for both sites included water soluble ions NH_4, SO_4, NO_3, elemental carbon (EC), and following elements; Na, Mg, Al, Si, S, K, Ca, Ti, Cr, Mn, Fe, Co, Ni, Cu, Zn, As, Sc, V, Rb, Sb, Ba, Ce, Sm, W, Pb, Th, Cl, Se and Cd.

Following the EU protocol for receptor models [11], the data were first treated to remove values that potentially decrease the analysis quality. To validate the data and uncover values that were out of the usual when compared to the rest of the dataset, scatter plots and time series analysis were utilized. After data validation, original datasets included 34 species for both sites and 256 daily samples Novo Lisiche and 332 daily samples for Karposh.

As recommended in EU protocol for receptor models [11], data below the limit of detection (LOD) were substituted by half of the LOD and the uncertainties were set to 5/6 of the LOD. Missing data were substituted by the geometric mean of the measured concentrations and the corresponding uncertainties were set as 4 times these geometric mean [43].

Species with high noise were down-weighted based on their signal-to-noise (S/N) ratio to reduce the influence of poor variables on the PMF analysis. Species with S/N lower than 0.5 were considered as bad variables and excluded from the analysis, and species with S/N between 0.5 and 1 were defined as weak variables and down-weighted by increasing the uncertainty as recommended in the PMF users guideline. As the elemental concentration and uncertainties for both datasets are in the same order of magnitude, same spcies for both sites are set as weak (Na, Co and As), while five (Ce, Sm, W, Th and Se) were determined as bad and excluded from the modelling. Although with high signal to noise ratio, PM 2.5 was set as total (week) variable in order to reduce influence on profiles contribution.

After additional validation and outlier's filtration, 23 samples were excluded from the Karposh data set and 5 from Novo Lisiche data set, and percentage of modelled data ranged from 93.1 % for Karposh and 98.1 % Novo Lisiche.

Because each entry is weighted according to its uncertainty, uncertainty estimation is especially important in PMF analysis. Input uncertainty in PMF should account for all the uncertainty components that contribute to residuals. The analytical uncertainty indicated in the original dataset included expanded analytical uncertainty calculated according to SOPs following GUM approach and accounting all sources of uncertainties, and therefore only 10 % extra modelling uncertainty was added, using the methodology that is described from Ammato et. al [42].

Number of factors was determined through examination of Q-values and scaled residuals. A first estimate of the number of factors p was made by examining the Q values of several runs with increasing numbers of factors from 5 to 12 and final solution for both data sets included 10 factors. To identify plausible factors representing more than one source category or sources split across multiple factors, the quality of the fit (scaled residuals) and the interpretability of the results (in terms of chemical profile and temporal trend) were assessed.

Because permitting a modest negative value helps PMF accept real rotations even in the presence of a significant number of zero values in specific G factors, the lower limit of the normalised contributions is set to -0.2.

At least 100 base model runs in robust mode were performed for datasets from each site with start seed value set as random.

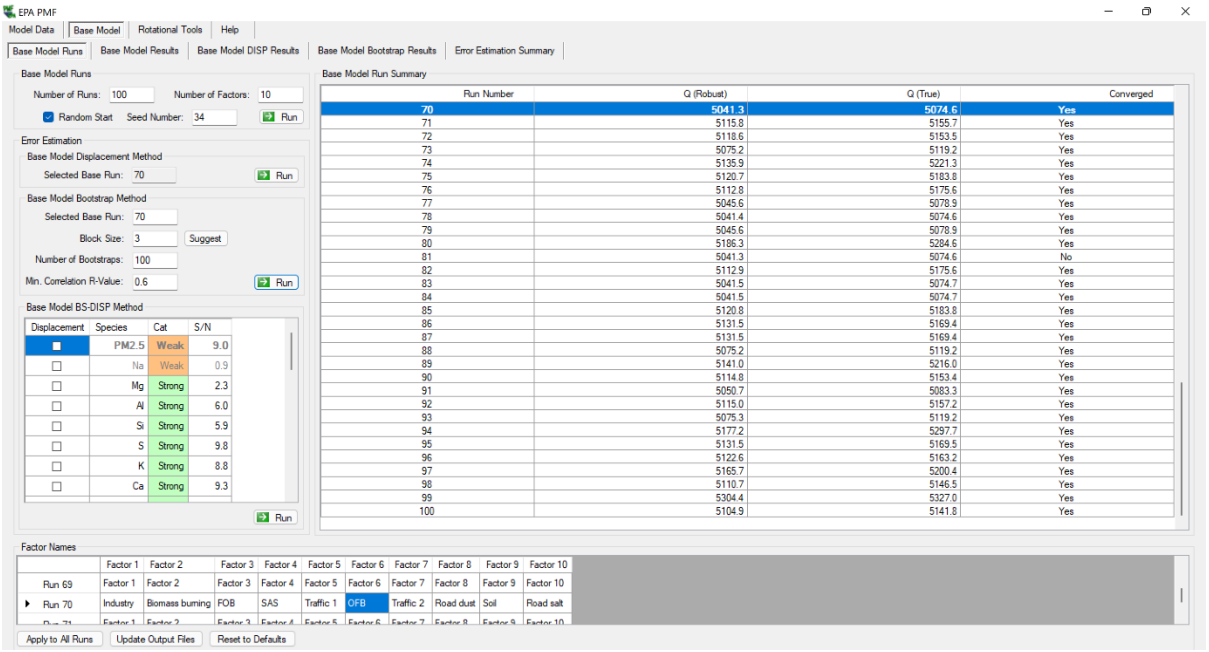

Figure 36. PMF screenshot - Base model run setting for Novo Lisiche site

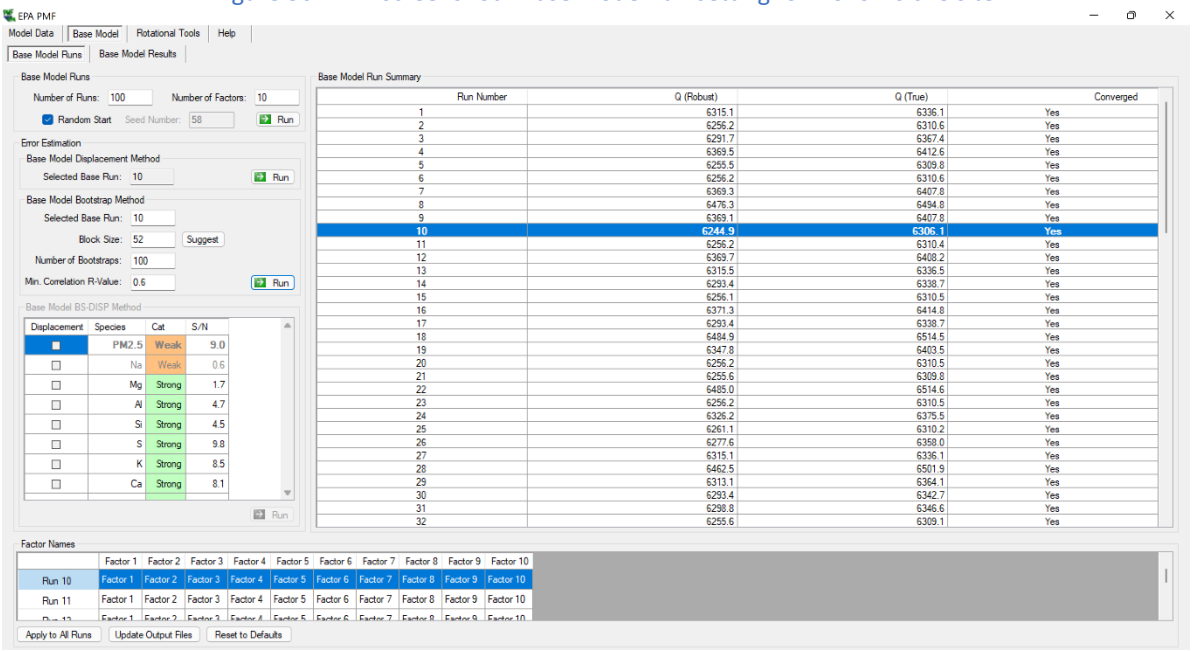

Figure 37. PMF screenshot - Base model run setting for Karposh site

Achieved Q robust/Q true was 0.67% for Novo Lisiche data set and 0.9% for Karposh data set (Figures 36 and 37).

A comparison between observed (input data) values and predicted (modeled) values was used to determine if the model fits the individual species well. Species that do not have a strong correlation (coefficient of determination r^2 is < 0.5) between observed and predicted values were evaluated and a decision was made whether they should be down-weighted as week or excluded from the model. For Karposh dataset, only Sc and Cd were down-weighted to weak, while Sc, Sb, Ba, and Cd were down-weighted to weak for Novo Lisiche data set. Coefficient of determination (r^2) values between observed and predicted values for total variable (PM 2.5) were 0.87 for Karposh and 0.83 for Novo Lisiche data set.

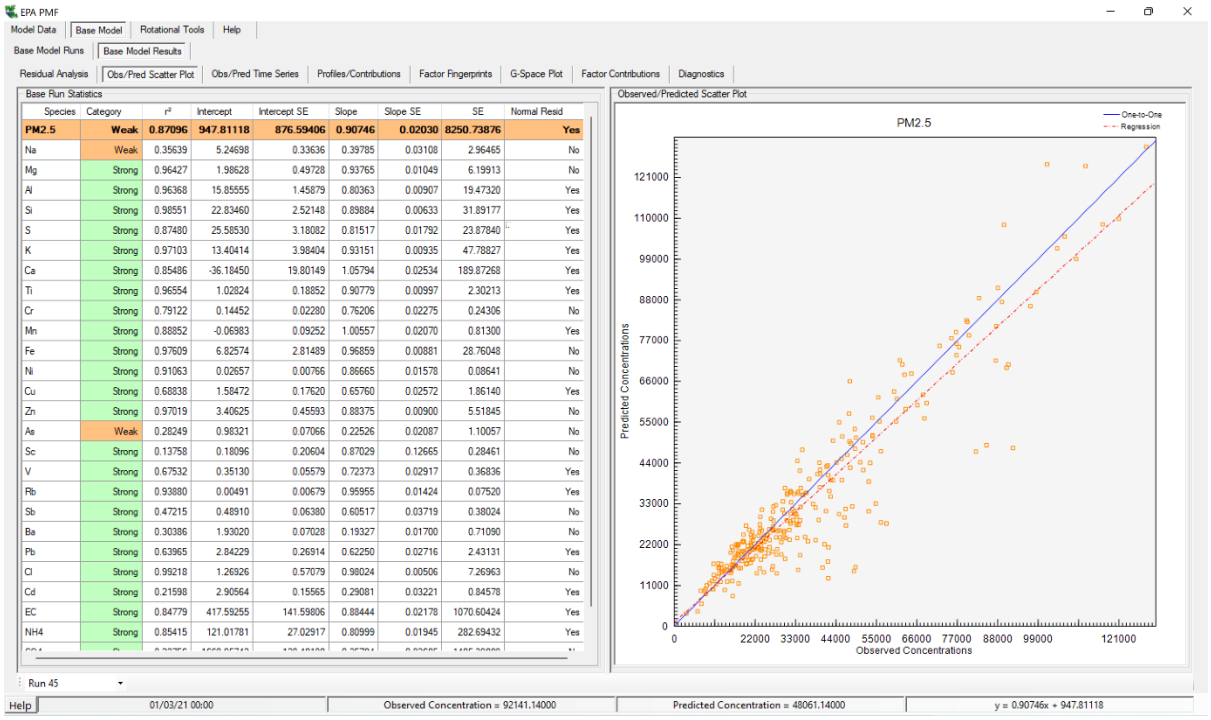

Figure 38. PM 2.5 observed vs. predicted concentration for Karposh site

In addition, the uncertainty-scaled residuals were evaluated in order to determine how well the model fits each species. The histograms for selected run display the percentage of all scaled residuals in a given bin (each bin is equal to 0.5). If a species has many large scaled residuals or displays a non-normal curve, it may be an indication of a poor fit. The species accounted as well-modeled if all residuals are between +3 and -3 and they are normally distributed. Large positive scaled residuals may indicate that PMF is not fitting the species, or the species is present in an infrequent source.

To improve the physical relevance of components in advanced PMF, existing source chemical profiles or contributions can be used to constrain a model run [44]. Because species determined, does not include unique tracers and no data from specific (local) sources were available, constrains were not applied.

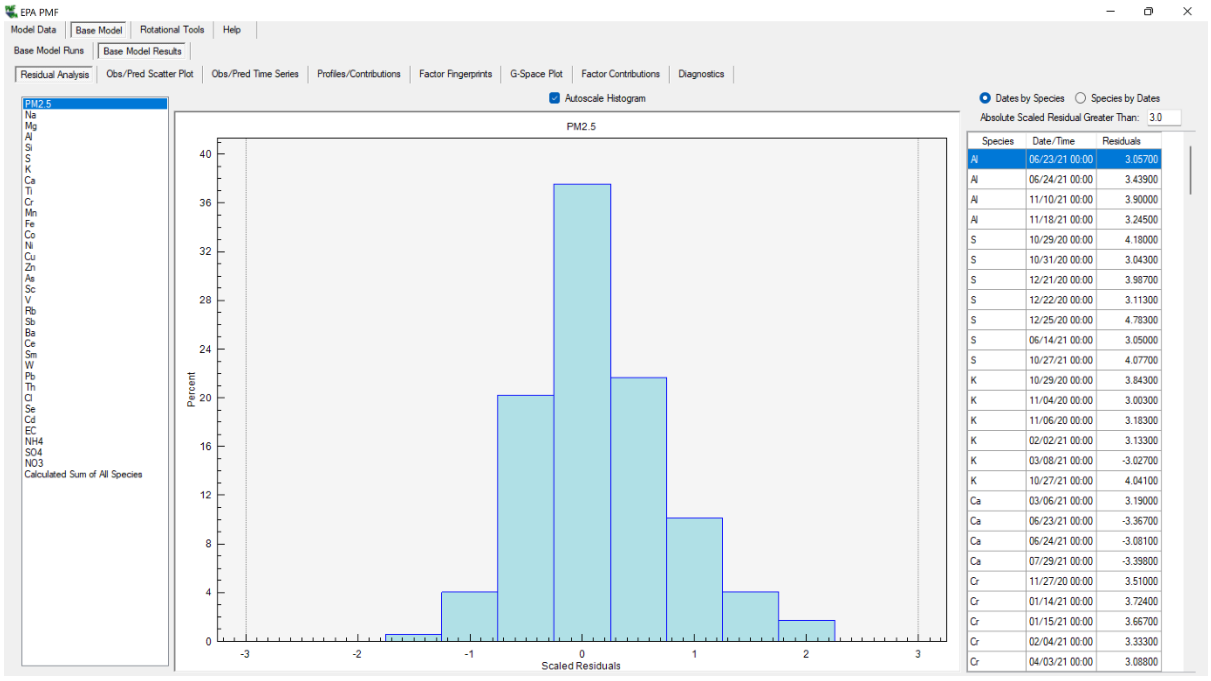

Figure 39. Uncertainty-scaled residuals for total variable PM 2.5

Even when a minimum is determined in the least squares fitting method, factor analysis solutions are not unique. There is a family of equally suitable solutions due to the free rotation of matrices; this is known as rotational ambiguity (PMF user guide, US EPA 2014). The rotational ambiguity of PMF solutions was investigated using the FPEAK tool for a variety of parameter values (ranging from 1 to +1). Small rotations had no significant effect on Q values, F and G matrices, and scaled residuals for both datasets.

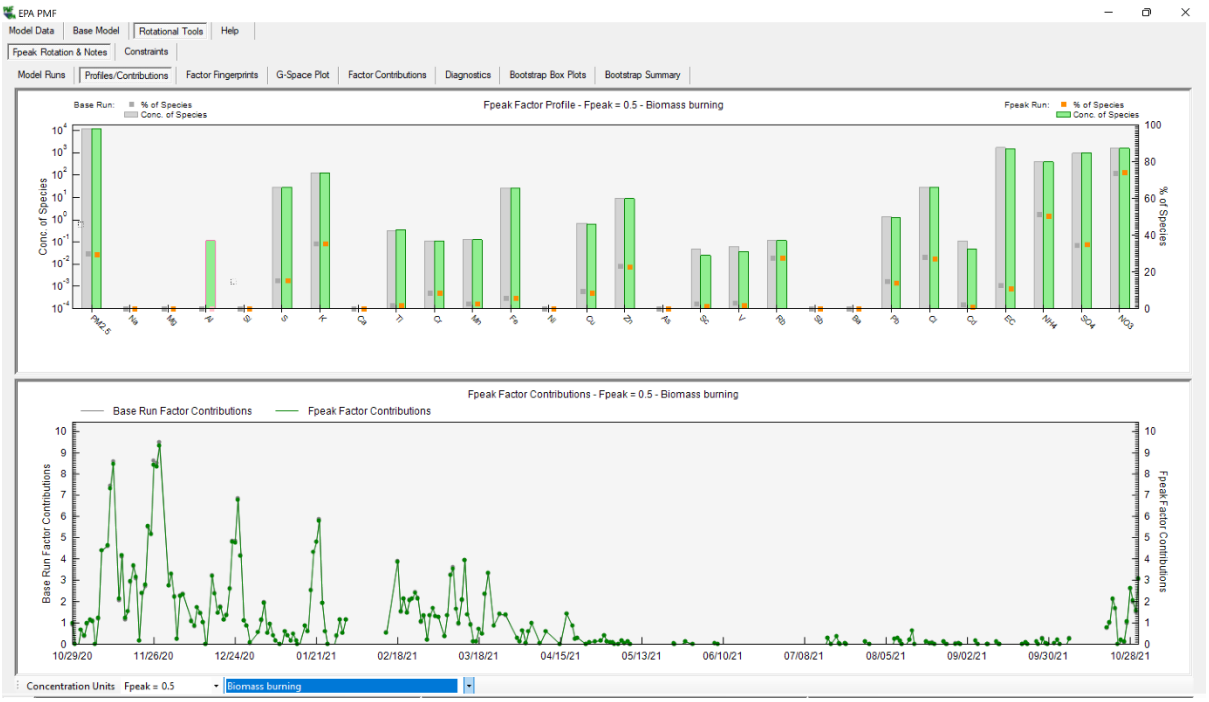

Figure 40. PMF screenshot – FPEAK rotation

The factor analytical solutions were analyzed using error estimation (EE) methods contained in the US-EPA PMF 5.0 software. The Bootstrap (BS) method was used for detecting and estimating probable random mistakes caused by disproportionate effects of a small number of data on the solution. To ensure the statistics' robustness, each dataset was subjected to 100 BS runs, with the 5th and 95th percentiles serving as the BS uncertainty range for each factor profile. The block size was to 3 and the minimum correlation value to 0.6 [5].

By examining the broadest range of source profile values without a notable rise in the Q-value, Displacement (DISP) was utilized to investigate the rotational ambiguity in the solutions more explicitly. In this strategy, each fitted element in a factor profile (only "strong" species) is "displaced" from its fitted value by a specified amount called dQmax from its fitted value. DISP is run for each dQmax, and the perturbed variable's upper and lower interval estimations produce an uncertainty estimate for each species in each factor profile. The focus of DISP is on how frequently components change sufficiently to swap identities, indicating a poorly defined solution (PMF user guide, US EPA 2014). If there are more than a few swaps for the least dQmax, there are either too many factors or substantial rotational uncertainty. On the other hand, if no or only a few swaps occur, the solution is statistically acceptable.

The Base Model Displacement Error Method was used to explore the rotational ambiguity in the PMF final solutions. With that methodology it is possible to estimate the effect of a small set of observations in the dataset has on the solution. The number of Bootstraps was set to 100, block size to 3 and the minimum correlation value to 0.6 [56].

5.2. Factor attribution to sources

As mentioned above, final PMF solution for both datasets included 10 factors. Factors were attributed to their sources though a quantitative and qualitative comparisons of the factor chemical profile with PM profiles reported EC-JRC SPECIEUROPE data base and profiles from previous source apportionment studies available in the literature. In addition, the standardised identity distance (SID) and the Pearson coefficient, expressed as Pearson distance (PD = 1 - r), were used to calculate the similarity between the factors and the reference source profiles available in the public datasets: EC-JRC SPECIEUROPE and US-EPA SPECIATE (Simon et al., 2010). The Delta SA tool (http://source-apportionment.jrc.ec.europa.eu/) was used to complete the work.

For Karposh- urban background site, 10 factors were attributed to; secondary aerosols, traffic 1, traffic 2, metal processing, industry 1, industry 2, fuel/residual oil, soil/road dust, open fire burning and biomass burning. Similarly, for Novo Lisiche – urban traffic site, factors were attributed to secondary aerosols, traffic 1, traffic 2, metal processing, industry, fuel/residual oil, soil dust, road dust, open fire burning, biomass burning and de-icing salt.

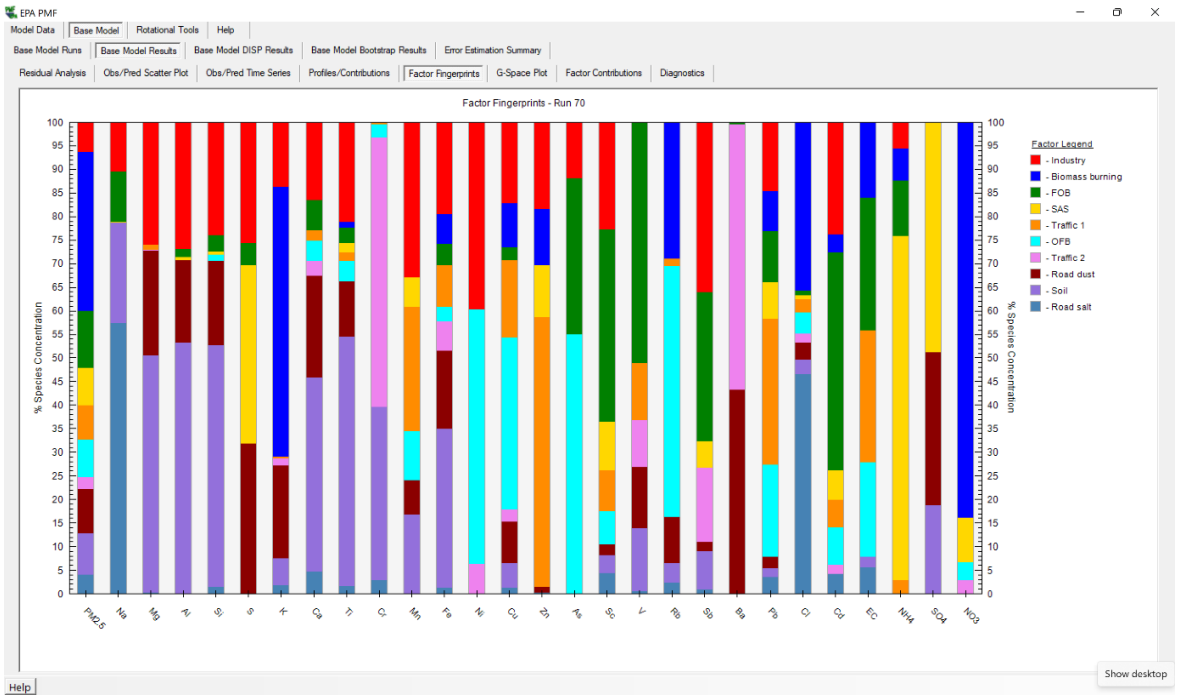

Figure 41. Factor fingerprint for Novo Lisiche dataset

Biomass burning incorporate emissions from different types of woodburning stoves and boilers used mostly in residential heating. Key species found is this factor include EC, K, Cl, NO_3^- and Rb. K is produced from the combustion of wood lignin [60,61]. Although this element can be emitted from other sources, such as soil dust [62], K has been used extensively as an inorganic tracer to apportion biomass burning contributions to ambient aerosol and was associated with biomass burning in PMF source profiles in Tirana, Skopje, Athens, Belgrade, Banja Luka, Debrecen, Chisnay, Zagreb and Krakow [5].

Cl can be emitted from biomass burning and also from coal combustion, especially during the cold period [63]. It is also associated with biomass burning in PMF source profiles in Belgrade and Banja Luka [5].

In addition, NO_3^-, and NH_4^+ also contributed significantly to the biomass burning factor. Biomass burning is an important natural source of NH_3 [65] which rapidly reacts with HNO_3 to form NH_4NO_3 aerosols. The presence of NH_4NO_3 aerosols in biomass burning plumes, has also been reported previously [65,66].

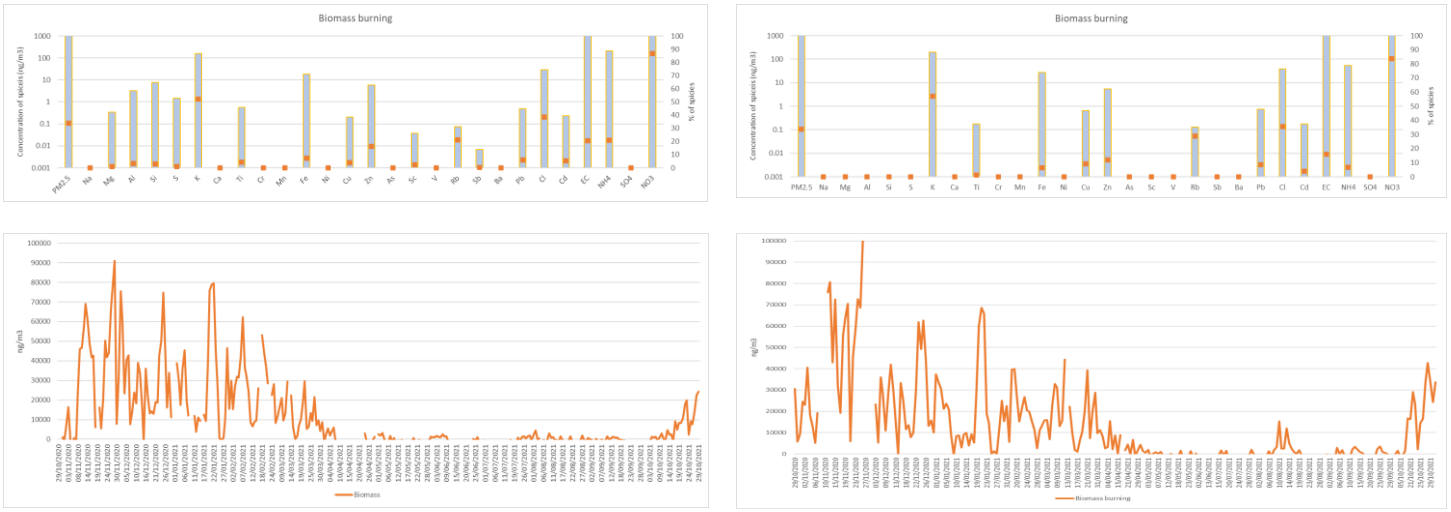

a. Karposh data set b. Novo Lisiche dataset

Figure 42. Biomass burning factor profiles

Evaluation of seasonal pattern of this factor at both sites clearly confirm attribution of this factors to biomass burning emissions that usually occur only during the cold months.

Traffic includes particles from several different sources including vehicles exhaust, mechanical abrasions of brakes and tires, road (resuspended) dust and road salting. All sources associated have their own specific fingerprints, and can be identified by EC, Ba, Cu, Mn, Pb and Zn, as well as crustal species like Mg, Al, Si, Ca, Fe, and Ti, or Na and Cl in the case of winter road salting.

The vehicle exhaust, including diesel and gasoline, consist high percentage of organic and elemental carbon, Fe, Pb, Zn, Al, Cu and sulphate. Similar species were also associated with traffic in PMF source profiles in most European and Central Asia urban areas [5].

Zn is a major additive to lubricant oil. Zn and Fe can also originate from tire abrasion, brake linings, lubricants and corrosion of vehicular parts and tailpipe emission [54-37]. As the use of Pb additives in gasoline has been banned, the observed Pb emissions may be associated with wear (tyre/brake) rather than fuel combustion [58].

Fe and Al is likely associated with vehicles part wear, such as tyre/brake wear and road abrasion, and are common species in case sampling sites are located close to major roads.

De-icing salt profile exhibit high percentage of Na and Cl (30 and 55%, respectively) and specific temporal pattern, associated with snowfalls occurrence during the cold season.

These results suggest the contribution of both exhaust and non-exhaust traffic emissions to several different factors that can be associated with traffic. Although elemental composition of particulate emissions associated with traffic can significantly vary due to differences in traffic volume and patterns, vehicle fleet characteristics, the climate and geology of the region [59]. Similar elements (Cu, Mn, Zn, Pb, Fe and EC) were identified as key species in PMF source profiles in most European and Central Asia urban areas [5].

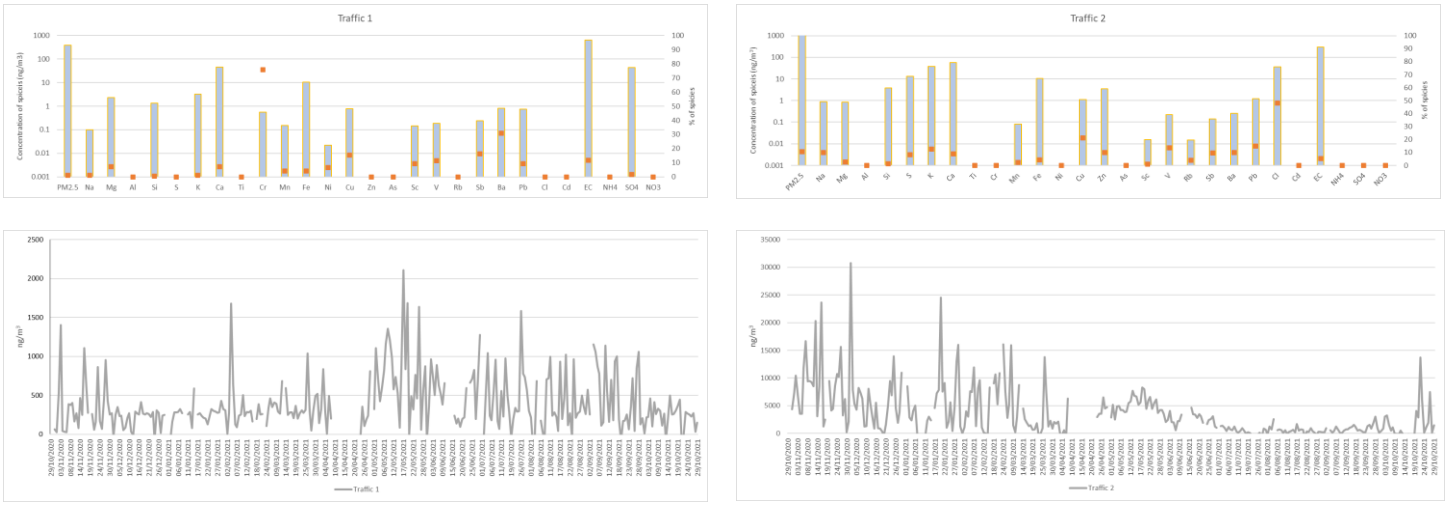

Figure 43. Traffic associated factors for Karposh dataset

Figure 44. Traffic associated factors for Novo Lisiche dataset

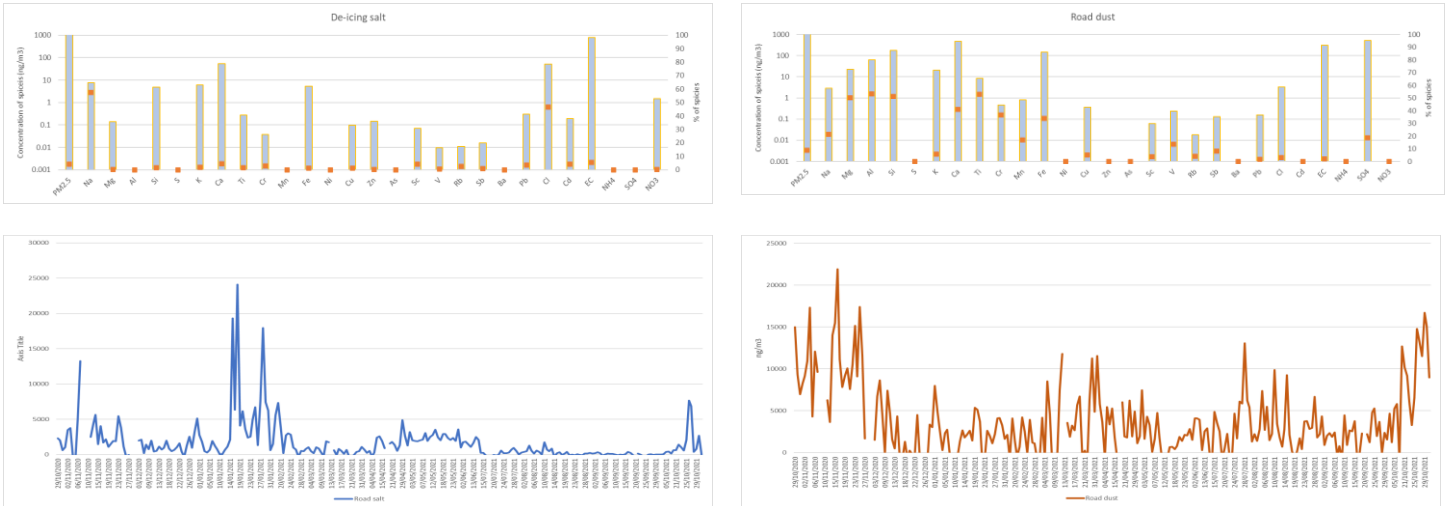

Figure 45. De -icing salt and Road Dust factors associated with traffic (Novo Lisiche dataset)

Fuel and residual oil combustion is a stand-alone factor that includes emissions from a wide range of sources, the majority of which are larger buildings heating systems (schools, hospitals, and other public institutions), industrial combustion emissions and to some extent older diesel-powered vehicles emissions, principally composed of EC, V, Cd and Ni [65, 66].

Organic carbon, sodium, and water-soluble ions including nitrates and sulphates are common key species for fuel oil emissions. The presence of V and Ni is also common marker. Water-soluble ions, V, Fe, and Ni are also important species for residual oil combustion, but increased quantities of elemental carbon, rather than organic carbon, are common for this source.

Vanadium, either alone or in conjunction with nickel, is a prevalent marker in PMF source profiles, in most European and Central Asian urban areas [5].

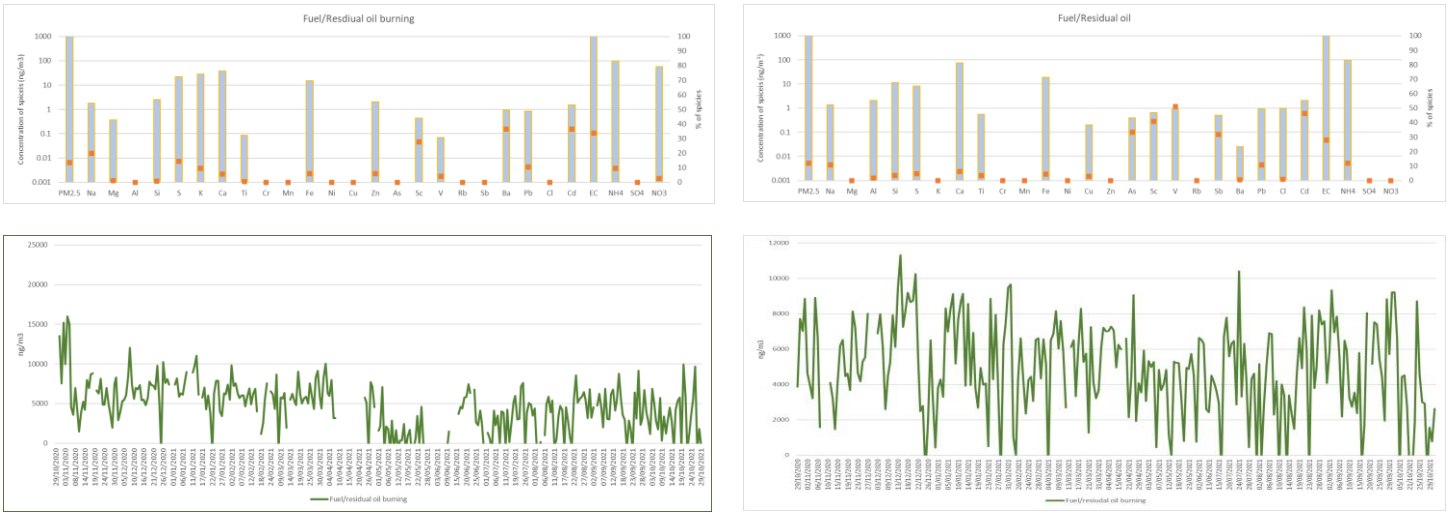

a. Karposh data set b. Novo Lisiche dataset

Figure 46. Fuel/residual oil factor profiles

Soil or mineral dust usually originates from construction/demolition activities, dust resuspension and wind erosion processes. This source is commonly identified with so called crustal elements like Mg, Al, Si, Ca, Fe and Ti [51]. Silicon and Ca are usually most abundant elements, followed by Fe, Al, Mg, and Ti with variations due to local geology.

Other research studies also reported significant contribution of soil dust to PM2.5 mass, suggesting that soil dust is an important contributor to PM2.5 mass especially in summertime [52,53]. Similar elements (Ca, Fe, Al, Si, Ba, Na and Ti) were identified as key species in PMF source profiles in most European and Central Asia urban areas [5].

Silicon and calcium are also prevalent species in the construction related source's chemical profile. Chemical profile of construction source also includes Si, Ca, Al and Fe, but also OC, EC and sulphates have significant contribution.

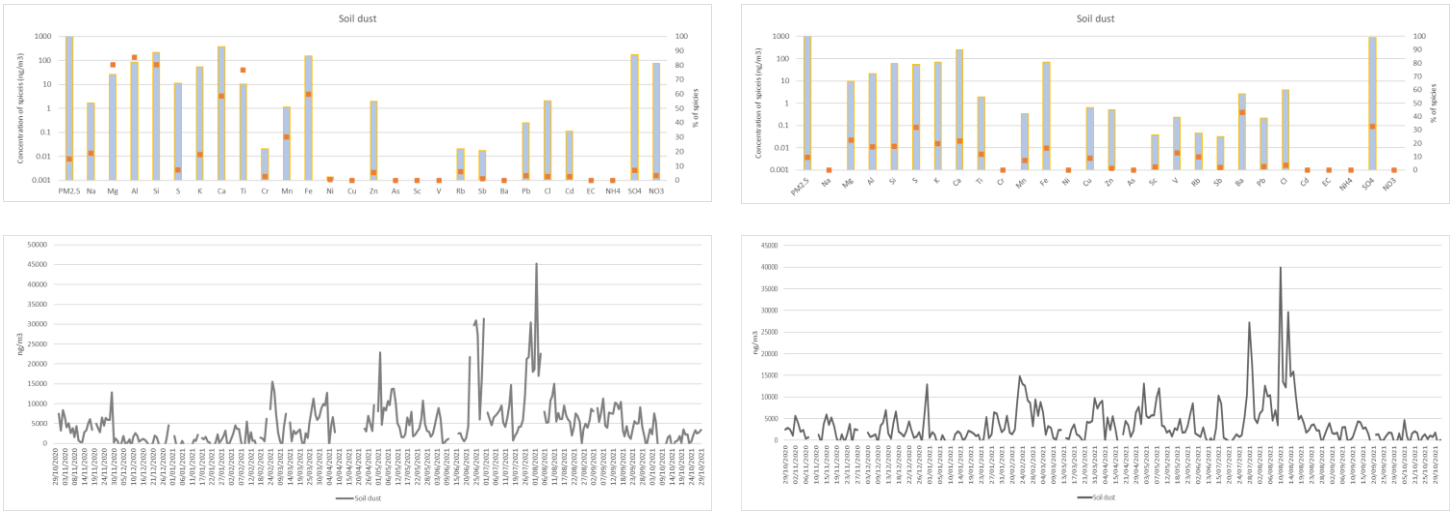

a. Karposh data set b. Novo Lisiche dataset

Figure 47. Soil/mineral dust factor profiles

All types of low efficiency burning of agricultural and garden waste, as well as other types of waste, are classified as open fire burning. This factor is identified by high contribution EC, As and Rb, but also includes some specific metals like Cu and Ni. Elemental carbon, Br, Co, V, Ti, and As were also found as important species in an analysis of agricultural waste open burning profiles, conducted in the Thessaloniki area in Northern Greece (SPECIEUROPE data base).

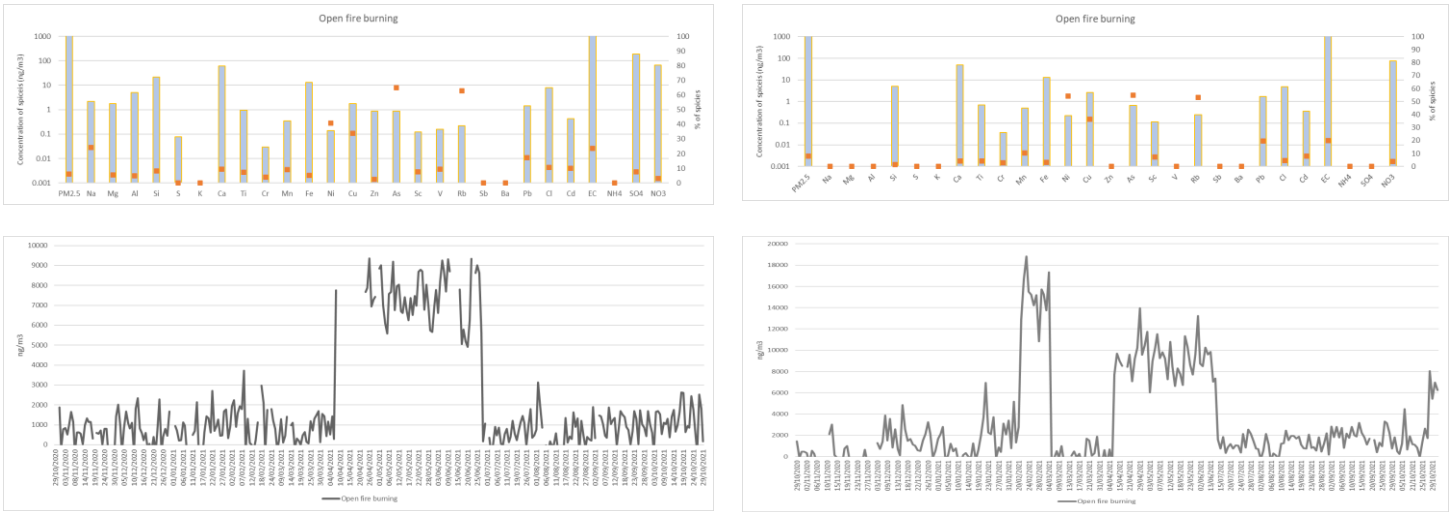

a. Karposh data set b. Novo Lisiche dataset

Figure 48. Open fire burning factor profile

Industrial emission includes complex mixture of stationary and diffuse emissions, associated with the various process and operations, mostly identified by a mixture of several metallic species Mn, Fe, Pb, Zn, Cu, and Cr, with consistent contribution over the year. Although those elements can be emitted from various sources, metals are commonly associated with anthropogenic sources and therefore used as tracers to apportion industrial sources.

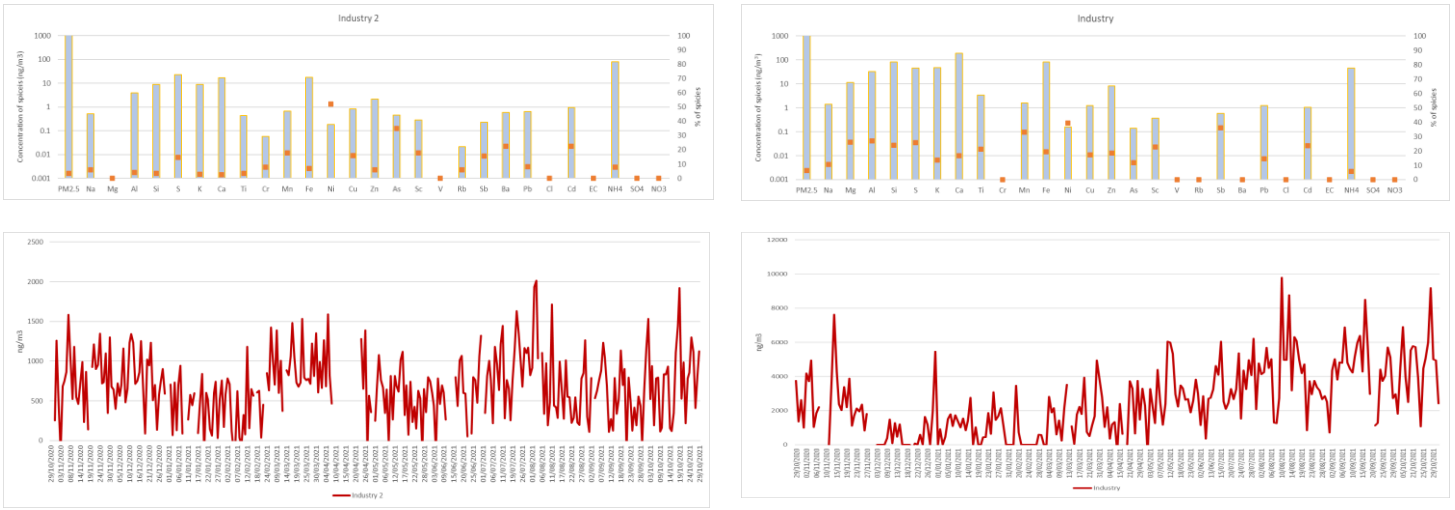

a. Karposh data set b. Novo Lisiche dataset

Figure 49. General industrial emissions factor profile

Rather than being discharged directly into the atmosphere by a single source, secondary aerosols are generated in the atmosphere as a result of complicated chemical and physical transformations of gaseous precursors to particulate matter. SA are mainly recognised by their high S and ion content (SO4 and NH4).

Secondary aerosols contribute the most during the coldest and warmest months, when there are high levels of gaseous percussors in the winter and high temperatures in the summer.

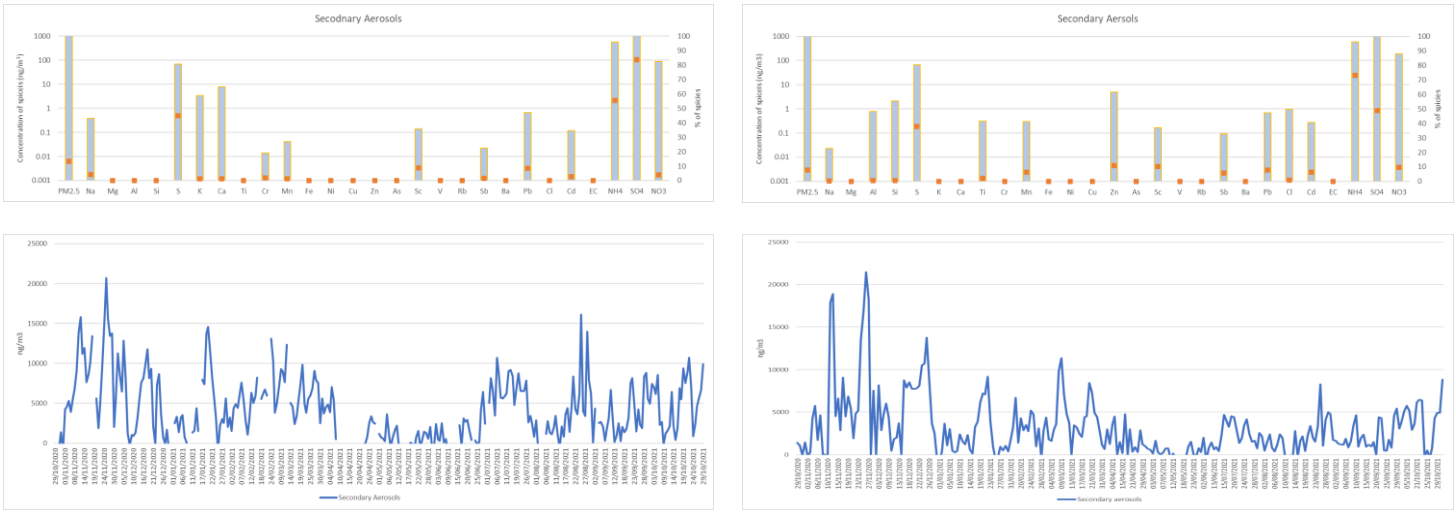

a. Karposh data set b. Novo Lisiche dataset

Figure 50. Secondary Aerosols factor profile

5.3. Sources Contribution

Using the data from measurements and modelling exercise, contribution of each source to total particulate mass (PM 2.5) was calculated. To provide most “real world” plausible solution, traffic and industry related factors were grouped in complex sources, thus producing 7 major sources for both sites. The major sources identified for Karposh urban background site include; biomass burning, open fire burning, secondary aerosols, soil/mineral dust and fuel/residual oil burning. Traffic contribution was calculated as a sum of 2 factors associated (traffic 1 and 2) and industry as a complex source with 3 factors associated (industry 1 and 2 + metal processing industry). The major sources identified for Novo Lisiche urban traffic exposed site include; biomass burning, open fire burning, secondary aerosols, industry, soil/mineral dust and fuel/residual oil burning, while traffic contribution was calculated as a sum of 4 factors associated, including traffic 1, traffic 2, road dust and road salt factors.

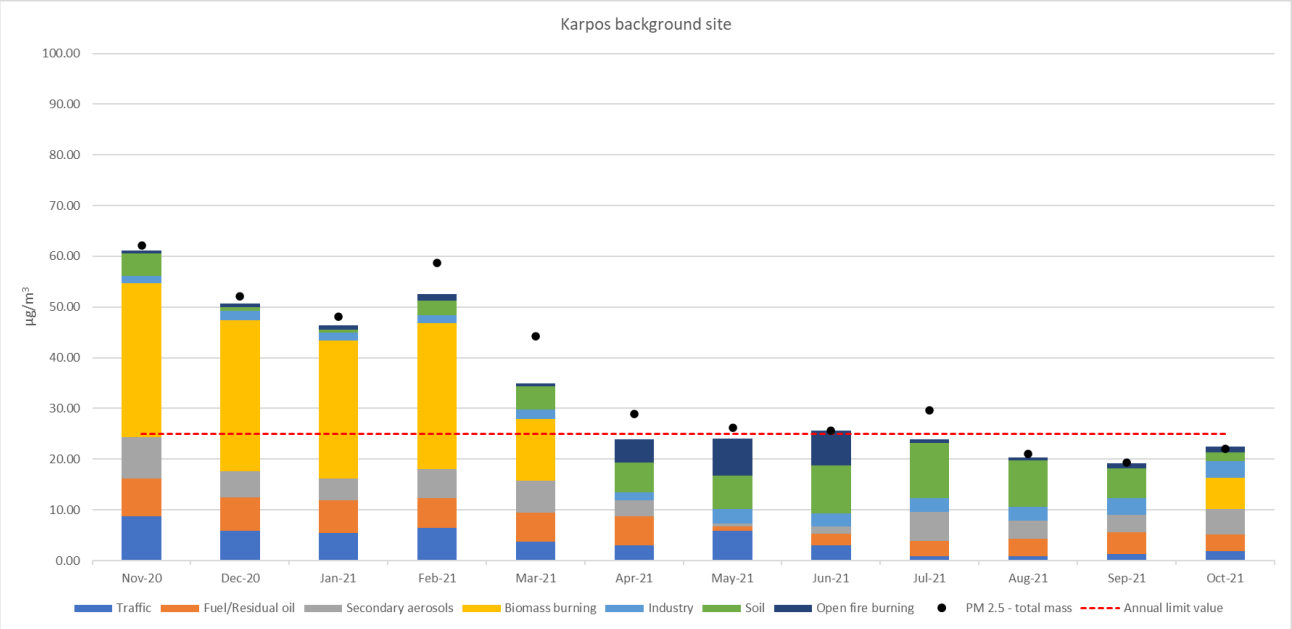

Figure 51. Average monthly contributions to total particulate mass (PM 2.5) – Karposh urban background site

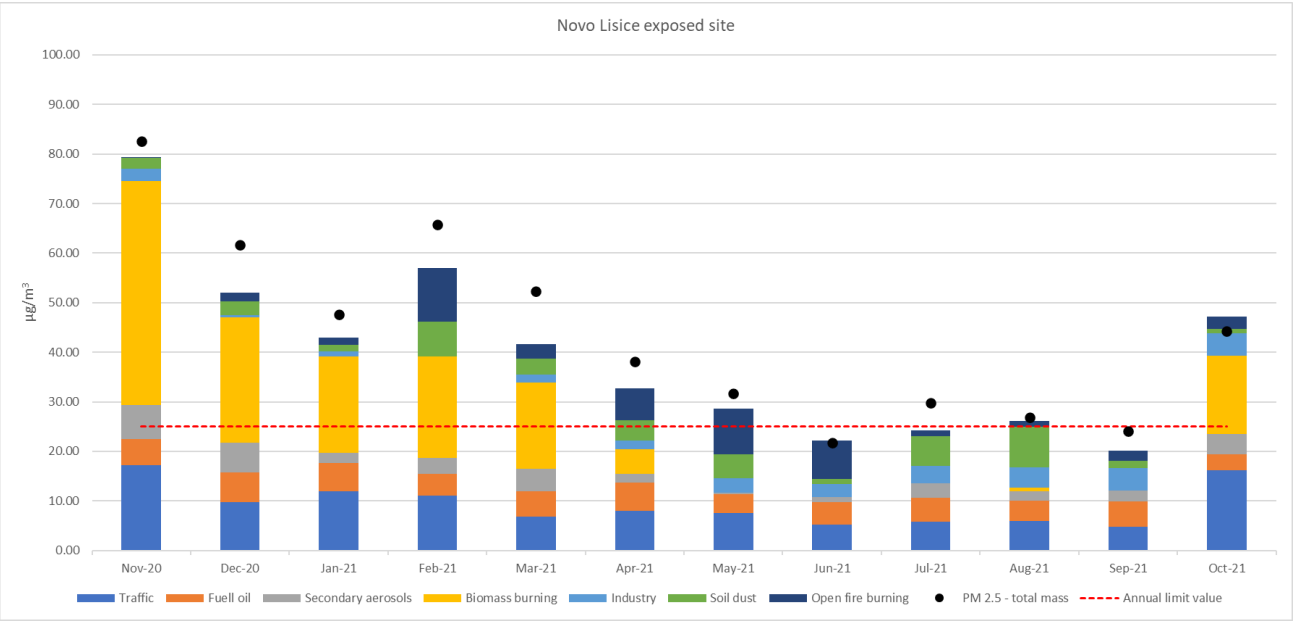

Figure 52. Monthly contributions to total particulate mass (PM 2.5) – Novo Lisiche urban traffic exposed site

As shown above, biomass burring was a major source at both sites with highest contribution to the total particulate mass over the cold season (Nov, Dec, Jan, Feb and March) no influence over the warm. At Novo Lisiche site, biomass burning average monthly contribution during the cold season was between 17.41 and 45.07 µg/m^3. For the same period, at the Karposh urban background site, biomass burning average monthly contribution was between 12.16 and 30.42 µg/m^3. This source alone, over the cold period, contribute above the annual limit values set for PM 2.5.

Traffic is the second most important source for the Novo Lisiche traffic exposed site, with a consistent contribution over the year, ranging between 4.82 and 17.21 µg/m^3, but a variable and substantially lower contribution at the Karposh urban background site ranging from 0.86 and 8.69 µg/m^3.

Fuel/residual oil contribute from 3.28 and 5.98 µg/m^3 to total particulate mass at Novo Lisiche and from 0.84 and 7.54 µg/m^3 at Karposh site, while industrial sources exhibit slightly lower contribution ranging between 0.33 and 4.59 µg/m^3 at Novo Lisiche and 1.33 and 3.35 µg/m^3 at Karposh site. Both are consistent over the year.

Soil dust has highest contribution over the summer months, ranging from 0.33 and 8.22 µg/m^3 at Novo Lisiche and 0.54 and 10.97 µg/m^3 at Karposh background site.

Open fire burning is detectable over the entire year, with largest contribution in spring and early summer months and range from 0.16 and 10.78 µg/m^3 at Novo Lisiche and 0.56 and 7.32 µg/m^3 at Karposh site.

Secondary aerosols exhibit highest contribution during the coldest and warmest months, probably associated with high levels of gaseous percussors during the winter months and photo-chemical reactions due to high temperatures over the summer months. Secondary aerosols range from 0.24 and 6.88 µg/m^3 at Novo Lisiche and 0.51 and 8.08 µg/m^3 at Karposh site.

Biomass burning relative contributions (%) in total particulate mass exhibit high seasonal variability and during the cold season (Nov, Dec, Jan, Feb and March), this is a major source at both sites, with contribution ranging from 15 to 57% at Novo Lisiche site, and from 27 to 59% at Karposh site. Despite being completely seasonal, biomass burning has the highest annual relative contribution, reaching 32% for Novo Lisiche and 33% for Karposh (Figures 55 and 56).

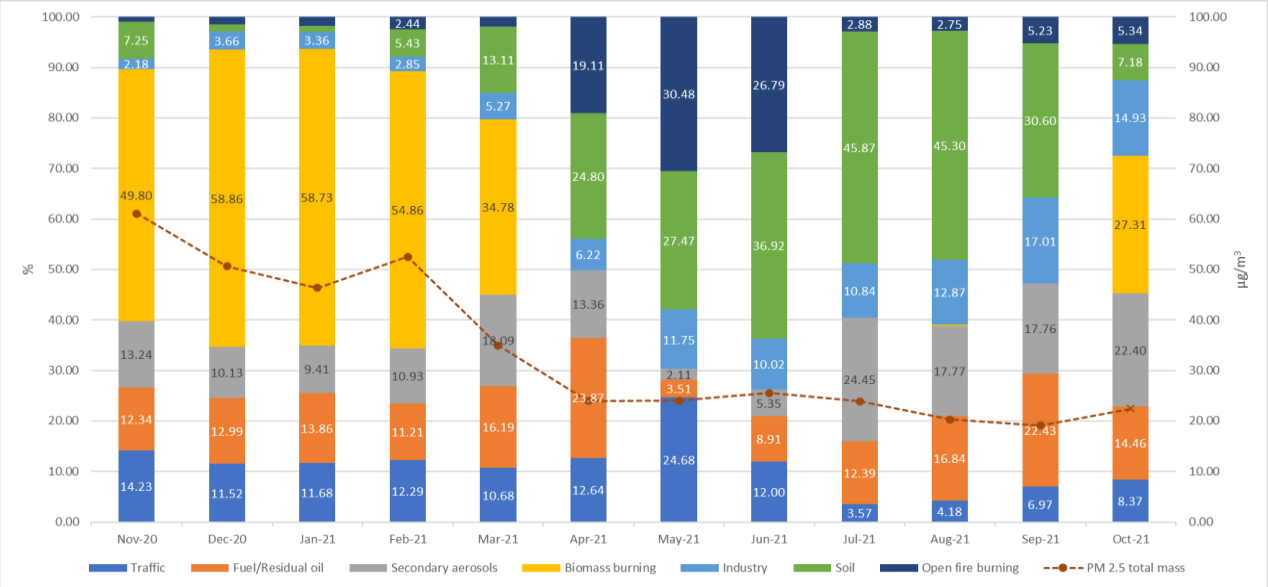

Figure 53. Relative monthly contribution – Karposh urban background site

Traffic annual relative contribution accounted for 18 % of the total particulate mass (PM 2.5) at Karposh site and 23% at Novo Lisiche (Figures 55 and 56), with monthly relative contribution ranging

from 4 to 25% at Karposh site and from 16 to 34 % at Novo Lisiche site (Figures 53 and 54). This source exhibit relatively consistent contribution over the year, especially at Novo Lisiche urban exposed site.

Annual relative contribution of fuel/residual oil combustion accounted for 5 % of the total particulate mass (PM 2.5) mass at Karposh site and 12 % at Novo Lisiche site (Figures 55 and 56). Relative monthly contribution at Karposh site ranged from 4 to 24 % and from 7 to 26 % at Novo Lisiche, exhibiting relatively consistent contribution over the year at both sites (Figures 53 and 54).

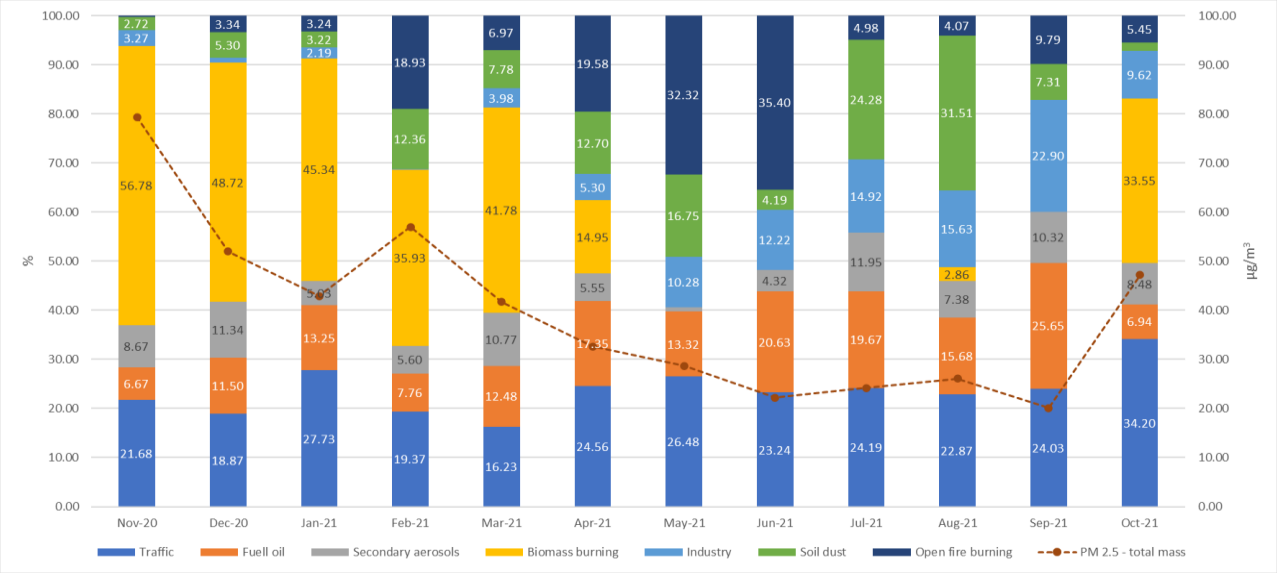

Figure 54. Relative monthly contribution – Novo Lisiche urban traffic exposed site

Industrial sources also exhibit consistent contribution over the year, reaching annual relative contribution of 9 % at Karposh site and 6 % at Novo Lisiche site (Figures 55 and 56). Monthly relative contribution ranges from 0.05 to 23% at Novo Lisiche site and from 2 to 17% at Karposh site (Figures 53 and 54).

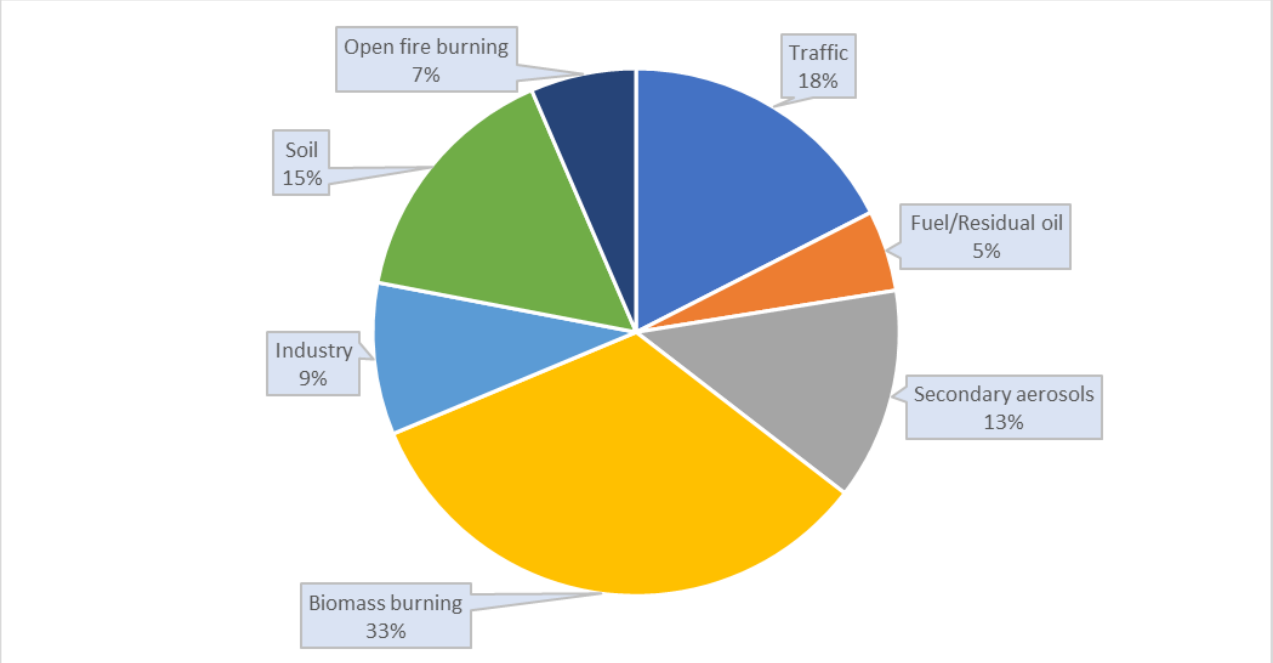

Figure 55. Relative annual contribution of PM 2.5 sources at Karposh urban background site

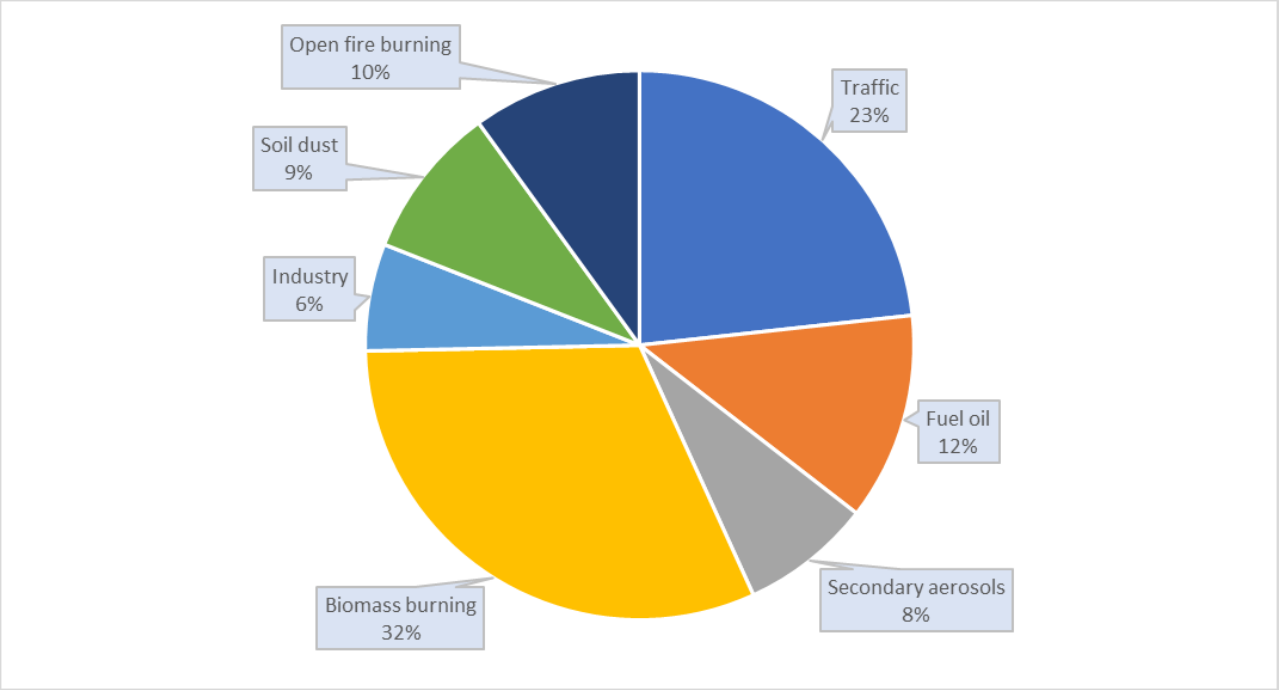

Figure 56. Relative annual contribution of PM 2.5 sources at Novo Lisiche urban traffic exposed site

Soil/mineral dust have also significant contribution to total particulate mass (PM2.5) especially during the warm season. Relative monthly contributions of this source vary from 1 % to significant 46 % at Karposh site and from 2 to 32 % at Novo Lisiche site, but for this traffic exposed site, road dust is identified as a separate factor attributed to traffic source also (Figures 53 and 54). Annual relative contribution reaches 15 % at Karposh site and 9 % at Novo Lisiche site (Figures 55 and 56).

All types of low efficiency open burning of agricultural and garden waste, as well as other types of waste, classified as open fire burning, exhibit strongest contribution during the spring and early summer months (April, May and June) with relative monthly contribution from 1 to 30 % at Karposh, and from 0.2 to 35 % at Novo Lisiche site (Figures 53 and 54). Relative annual contribution of this source was 7 % for Karposh site and 10 % for Novo Lisiche site (Figures 55 and 56).

As explained above, secondary aerosols exhibit specific seasonal pattern, with largest contributions during the coldest and warmest months, associated with high levels of gaseous percussors during the winter months and high temperatures over the summer months. Annual relative contribution of secondary aerosols was 13% of the total particulate mass (PM2.5) at Karposh and 8% at Novo Lisiche sites. Relative monthly contributions exhibit large variation and reach between 2 and 24 % at Karposh site and between 1 and 12 % at Novo Lisiche site.

6. Conclusions and recommendations

Biomass burning remain the largest single source of ambient air pollution, and due to specific temporal distribution, probably the main driver of extreme wintertime pollution episodes. During the winter months (Nov, Dec, Jan, Feb and March) biomass burning was a major source at both sites, with contribution ranging between 36 and 57 % at Novo Lisiche, and from 27 to 59% at Karposh background.

Most of the air quality improvement plans for similar situations, focus on exchanging heat sources and improving energy efficiency in single-family buildings [67]. In addition to this, so-called "anti-smog" regulations, typically involve huge informational and direct financial assistance efforts.

Air improvement plan for Krakow, a second largest city in Poland can be good example, having in mind similar size (780 000 residents), topography and key pollution sources (combustion of solid fuels in obsolete household boilers was responsible for 72% of PM10) [67].

The Małopolska Air Quality Plan was passed by Małopolska local parliament in September 2013, and updated in January 2017 and in September 2019. The first anti-smog resolution for Kraków was adopted in November 25, 2013. The second one in April 2017. As a result, from September 1, 2019, the use of solid fuels is completely prohibited.

Measures implemented include:

- inventory of stoves, boilers and fireplaces (2013 - 2015) (this constantly updated inventory include 24 000 heating units);
- implementation of local low-stack emission reduction programs – subsidies replacement of inefficient heating devices based on solid fuels. Subsidies were granted for:
    - connecting to the municipal heating networks,
    - installing gas heating,
    - installing electric heating,
    - installing efficient oil heating,
    - installing a heat pump.
- Subsidy amounts from:
    - 100% of eligible costs for applications submitted in the first years (2014 – 2016),
    - 80% of eligible costs for applications submitted in second phase (2017 and 2018),
    - 60% of eligible costs for applications submitted in the third phase 2019.
- expansion and modernization of municipal heating network and gas distribution networks to connect new users;
- thermo-modernization of buildings and support of energy efficient buildings in housing and public utilities;
- subsidies for bills for people who incur increased heating costs after replacement of stoves, based on their income levels;
- reduction of emissions from transport and industry;
- open observatory maps showing heating installations and the extend of pollution;
- daily operation of drone and thermal audits of buildings;
- cooperation with residents – reporting old furnace or pollution, and introducing fines for breaking the rules;

As a result of persistent program implementation over the 8 years (2012-2020), average annual particulate mass concentrations at Krakow City centre, for PM10 were reduced from 68 $\mu g/m^3$ in 2015 to 39 $\mu g/m^3$ in 2020, and for PM2.5 were reduced from 43 $\mu g/m^3$ in 2015 to 23 $\mu g/m^3$ in 2020, thus reaching EU annual limit values for both parameters. A total expenses for heating unit replacement in

Krakow in the same period, amount for 75 000 000 € and provided removal of approximately 25 000 old heating units.

However, there are other significant sources, especially fuel/residual oil burning, soil dust and open fire burning, that can and must be tackled in much shorter time frame.

Fuel and residual oils burning includes emissions from a wide range of sources, the majority of which are larger buildings heating systems (schools, hospitals, and other public institutions), industrial combustion emissions and to some extent older diesel-powered vehicles emissions.

Rapid plan for reducing this fuels usage could be easily justified with their clear economic and environmental benefits.

Soil dust usually originates from construction/demolition activities, dust resuspension and wind erosion, thus exhibiting high seasonal variation. Relative monthly contribution over the summer months reaches up to 32% at Novo Lisiche and up to 46% at Karposh.

Specific policies for reduction of fugitive dust during construction and simple street cleaning/washing in combination with long term measures like increased urban vegetation could significantly reduce soil/road dust emissions.

Open fire burning is among the sources that exhibit strongest contribution during the spring and early summer months with average relative monthly contribution up to 35 % for Novo Lisiche site and 30 % for Karposh site. Zero tolerance to agricultural/garden waste burning and improved waste management practices could virtually eliminate this source.

For the future improvement of air quality in Skopje's urban and suburban areas, it is necessary to draft targeted and well-detailed air quality management plans based on existing scientific data, and to commit strongly to their execution.

Supplementary material

A - 1 Determination of mass concentration of ambient particulate matter

A - 2 Particulate matter chemical speciation

References

1. Crippa, P., Castruccio, S., Archer-Nicholls, S. et al (2016). Population exposure to hazardous air https://doi.org/10.1038/srep37074
2. World health statistics 2021: monitoring health for the SDGs, sustainable development goals. Geneva: World Health Organization; 2021. Licence: CC BY-NC-SA 3.0 IGO.
3. Pierre Sicard, Evgenios Agathokleous, Alessandra De Marco, Elena Paoletti and Vicent Calatayud (2021). Urban population exposure to air pollution in Europe over the last decades, Environmental Sciences Europe, 33:28, https://doi.org/10.1186/s12302-020-00450-2
4. Mirakovski et al (2019) Wintertime urban air pollution in Macedonia – composition and source contribution of air particulate matter, Proceedings of the 18th World Clean Air Congress 2019, pp 492-500.
5. Almeida et al. (2020) Ambient particulate matter source apportionment using receptor modelling in European and Central Asia urban areas, Environmental Pollution, Volume 266, Part 3, https://doi.org/10. 1016/j.envpol.2020.115199

6. Belis et al. (2019), Urban pollution in the Danube and Western Balkans regions: The impact of major PM2.5 sources. Environment International, 133, 105-158, doi:10.1016/j.envint.2019.105158
7. MAKStat Database https://makstat.stat.gov.mk/, State Statical Office, assessed on 21.04.2022
8. Air quality improvement plan for Skopje agglomeration, Finish Meteorological Institute and Ministry of Environment and Physical Planning, Skopje, 2016.
9. Integrated Polluters Inventory for Skopje, Tehnolab, Skopje, 2019.
10. Pernigotti, D., Belis, C.A., Spanó, L., 2016. SPECIEUROPE: The European data base for PM source profiles. Atmospheric Pollution Research, 7 (2), pp. 307-314. DOI: 10.1016/j.apr.2015.10.007
11. Belis C.A., Favez O., Mircea M., Diapouli E., Manousakas M-I., Vratolis S., Gilardoni S., Paglione M., Decesari S., Mocnik G., Mooibroek D., Salvador P., Takahama S., Vecchi R., Paatero P., European guide on air pollution source apportionment with receptor models - Revised version 2019, EUR 29816 EN, Publications Office of the European Union, Luxembourg, 2019, ISBN 978-92-76-09001-4, doi:10.2760/439106, JRC117306.
12. Thomas M. Peters, Eric J. Sawve, Robert Willis, Roger R. West, and Gary S. Casuccio, Performance of Passive Samplers Analyzed by Computer-Controlled Scanning Electron Microscopy to Measure PM10–2.5, Environ. Sci. Technol. 2016, 50, 14, 7581–7589
13. Andrew P. Ault, Thomas M. Peters, Eric J. Sawve, Gary S. Casuccio, Robert D. Willis, Gary A. Norris, and Vicki H. Grassian, Single-Particle SEM-EDX Analysis of Iron-Containing Coarse Particulate Matter in an Urban Environment: Sources and Distribution of Iron within Cleveland, Ohio, Environ. Sci. Technol. 2012, 46, 8, 4331–4339
14. Anna Turek-Fijak, Joanna Brania, Katarzyna Styszko, Damian Zięba, Zdzisław Stęgowski, Lucyna Samek, Chemical characterization of PM10 in two small towns located in South Poland, NUKLEONIKA, 2021, 66(1), 29-34, doi: 10.2478/nuka-2021-0004
15. Diapouli, E., Manousakas, M., Vratolis, S., Vasilatou, V., Maggos, T., Saraga, D., Grigoratos, T., Argyropoulos, G., Voutsa, D., Samara, C., Eleftheriadis, K., Evolution of air pollution source contributions over one decade, derived by PM10 and PM2.5 source apportionment in two metropolitan urban areas in Greece, Atmospheric Environment (2017), doi: 10.1016/j.atmosenv.2017.06.016
16. M.G. Perrone, S. Vratolis, E. Georgieva, S. Török, K. Šega, B. Veleva, J. Osán, I. Bešlić, Z. Kertész, D. Pernigotti, K. Eleftheriadis, C.A. Belis, Sources and geographic origin of particulate matter in urban areas of the Danube macro-region: The cases of Zagreb (Croatia), Budapest (Hungary) and Sofia (Bulgaria), Science of the Total Environment 619–620 (2018) 1515–1529, doi.org/10.1016/j.scitotenv.2017.11.092
17. Tomohiro Kyotani, Masaaki Iwatsuki, Determination of water and acid soluble components in atmospheric dust by inductively coupled plasma atomic emission spectrometry, ion chromatography and ion-selective electrode method, Analytical sciences, 1998, vol.14
18. Tony Byrd, Mary Stack, Ambrose Furey, An Analytical Application for the Determination of Metals in PM10, Advanced Air Pollution, InTech, 2011, 473-494
19. Eiji Fujimori, Tatsuya Kobayashi, Masanori Aoki, Masahiro Sakaguchi, Tsuyoshi Saito, Taku Fukai, Hiroki Haraguchi, Annual Variations of the Elemental Concentrations of PM10 in Ambient Air of Nagoya City as Determined by ICP-AES and ICP-MS, Analytical Sciences, 2007, 23, 12, 1359-1366 doi.org/10.2116/analsci.23.1359
20. M. Manousakas, H. Papaefthymiou, E. Diapouli, A. Migliori, A.G. Karydas, I. Bogdanovic-Radovic and K. Eleftheriadis, Assessment of PM2.5 sources and their corresponding level of uncertainty in a coastal urban area using EPA PMF 5.0 enhanced diagnostics, Science of The Total Environment, 2017, DOI: 10.1016/j.scitotenv.2016.09.047
21. Fabien Mercier, Philippe Glorennec, Olivier Blanchard, Barbara Le Bot, Analysis of semi-volatile organic compounds in indoor suspended particulate matter by thermal desorption coupled with

gas chromatography/mass spectrometry, Journal of Chromatography A, Volume 1254, 7 September 2012, Pages 107-114, doi.org/10.1016/j.chroma.2012.07.025
22. Ewa Dabek, Meghan Kelly, Heidi Chen, Chuni L Chakrabarti, Application of capillary electrophoresis combined with a modified BCR sequential extraction for estimating of distribution of selected trace metals in PM2.5 fractions of urban airborne particulate matter, Chemosphere, 2004, 58(10):1365-76 DOI: 10.1016/j.chemosphere.2004.09.082
23. Sukon Aimanant & Paul J. Ziemann (2013) Development of Spectrophotometric Methods for the Analysis of Functional Groups in Oxidized Organic Aerosol, Aerosol Science and Technology, 47:6, 581-591, DOI: 10.1080/02786826.2013.773579
24. Rigaku NEX CG, website: https://www.rigaku.com/products/edxrf/nexcg
25. Standard Operating Procedure for PM2.5 Cation Analysis, revision 7, August 2009, Environmental and Industrial Sciences Division RTI Intemational, Research Triangle Park, North Carolina
26. Putaud, J.P., Van Dingenen, R., Alaustey, A., Bauer, H., Birmili,W., et al., 2010. A European aerosol phenomenology – 3: physical and chemical characteristics of particulate matter from 60 rural, urban, and kerbside sites across Europe. Atmos. Environ. 44, 1308–1320.
27. Anttila P, Stefanovska A, Nestorovska-Krsteska A, et al (2016) Characterisation of extreme air pollution episodes in an urban valley in the Balkan Peninsula. Air Qual Atmos Health 9:129–141. https://doi.org/10.1007/s11869-015-0326-7
28. Hopke P.K., (2003). Recent developments in receptor modeling. Journal of chemometrics, 17, 255–265.
29. Lee E, Chan C.K., Paatero P., (1999). Application of positive matrix factorization in source apportionment of particulate pollutants in Hong Kong. Atmospheric Environment, 33, 3201–3212.
30. Xie Y., Berkowitz C.M., (2006). The use of positive matrix factorization with conditional probability functions in air quality studies: an application to hydrocarbon emissions in Houston, Texas. Atmospheric Environment, 40, 3070–3091.
31. DelValls T.A., Forja J.M., González-Mazo E., Gómez-Parra A., (1998). Determining contamination sources in marine sediments using multivariate analysis. Trends in analytical chemistry,17, 181–192.
32. Reimann C., Filzmoser P., Garrett R.G., (2002). Factor anlysis applied to regional geochemical data: problems and possibilities. Applied Geochemistry, 17, 185–206.
33. Paatero P., Tapper U., (1994). Positive Matrix Factorization: a non-negative factor model with optimal utilization of error estimates of data values. Environmetrics, 5, 111–126.
34. Anttila P., Paatero P., Tapper U., Järvinen O., (1995). Source identification of bulk wet deposition in Finland by positive Matrix Factorization. Atmospheric Environment, 14, 1705–1718.
35. Polissar A.V., Hopke P.K., Paatero P., Kaufmann Y.J., Hall D.K., Bodhaine B.A., Dutton E.G., Harris J.M., (1999). The aerosol at Barrow, Alaska: long-term trends and source locations. Atmospheric Environment, 33, 2441–2458.
36. Juntto S, Paatero P., (1994). Analysis of daily precipitation data by positive matrix factorization. Environmetrics, 5, 127–144.
37. Begum B.A., Kim E., Biswas S.K., Hopke P.K., (2004). Investigation of sources of atmospheric aerosol at urban and semi-urban areas in Bangladesh. Atmospheric Environment, 38, 3025-3038.
38. Bzdusek P.A., Christensen E.R., Lee C.M., Pakadeesusuk U., Freedman D.C., (2006). PCB congeners and dechlorination in sediments of Lake Hartwell, South Carolina, determined from cores collected in 1987 and 1988. Environmental Science and Technology, 40, 109–119.
39. Singh K.P., Malik A., Singh V.K., Sinha S., (2006). Multi-way data analysis of soils irrigated with wastewater. A case study. Chemometrics and Intelligent Laboratory Systems, 83, 1-12.

40. Soonthornnonda P., Christensen E.R., (2008). Source apportionment of pollutants and flows of combined sewer wastewater. Water Research, 42, 1989–1998.
41. Vaccaro S., Sobiecka E., Contini S., Locoro G., Free G., Gawlik B.M., (2007). The application of positive matrix factorization in the analysis, characterization and detection of contaminated soils. Chemosphere, 69, 1055-1063.
42. Amato F, Pandolfi M, Escrig A, et al (2009) Quantifying road dust resuspension in urban environment by Multilinear Engine: A comparison with PMF2. Atmos Environ 43:2770–2780. https://doi.org/10.1016/j.atmosenv.2009.02.039
43. Polissar, A. V., Hopke, P. K., & Poirot, R. L. (2001). Atmospheric aerosol over Vermont: chemical composition and sources. Environmental science & technology, 35(23), 4604–4621. https://doi.org/10.1021/es0105865
44. Amato, F., Hopke, P.K., (2012). Source apportionment of the ambient PM2.5 across St. Louis using constrained positive matrix factorization. Atmos. Environ. 46, 329–337.
45. Denise Pernigotti, Claudio A. Belis, Luca Spanò, (2016). SPECIEUROPE: The European data base for PM source profiles, Atmospheric Pollution Research, 7/2, 307-314, https://doi.org/10.1016/j.apr.2015.10.007.
46. D. Pernigotti, C.A. Belis, (2018). Delta SA tool for source apportionment benchmarking, description and sensitivity analysis, Atmospheric Environment, 180, 138-148, https://doi.org/10.1016/j.atmosenv.2018.02.046.
47. Viana, M., Kuhlbusch, T. A. J., Querol, X., Alastuey, A., Harrison, R. M., Hopke, P. K., Winiwarter, W., Vallius, M., Szidat, S., Prévôt, A. S. H., Hueglin, C., Bloemen, H., Wåhlin, P., Vecchi, R., Miranda, A. I., Kasper-Giebl, A., Maenhaut, W., and Hitzenberger, R. (2008): Source apportionment of particulate matter in Europe: A review of methods and results, J. Aerosol Sci., 39, 827-849, http://dx.doi.org/10.1016/j.jaerosci.2008.05.007,
48. Mazzei, F., D'Alessandro, A., Lucarelli, F., Nava, S., Prati, P., Valli, G., and Vecchi, R. (2008): Characterization of particulate matter sources in an urban environment, Sci. Tot. Environ., 401, 81-89, https://doi.org/10.1016/j.scitotenv.2008.03.008.
49. Pant, P., Shukla, A., Kohl, S. D., Chow, J. C., Watson, J. G., and Harrison, R. M. (2015): Characterization of ambient PM2.5 at a pollution hotspot in New Delhi, India and inference of sources, Atmos. Environ., 109, 178-189, http://dx.doi.org/10.1016/j.atmosenv.2015.02.074.
50. Huang, X., Tang, G., Zhang, J., Liu, B., Liu, C., Zhang, J., Cong, 898 L., Cheng, M., Yan, G., Gao, W., Wang, Y., and Wang, Y. (2021): Characteristics of PM2.5 pollution in Beijing after the improvement of air quality, J. Environ. Sci., 100, 1-10, https://doi.org/10.1016/j.jes.2020.06.004.
51. Liao, H.T., Chou, C.C.K., Chow, J.C., Watson, J.G., Hopke, P.K., Wu, C.F., (2015). Source and risk apportionment of selectes VOCs and PM2.5 species using partially constrained receptor models with multiple time resolution data. Environ. Pollut. 205, 121-130.
52. Yu, L., Wang, G., Zhang, R., Zhang, L., Song, Y., Wu, B., Li, X., An, K., and Chu, J.(2013): Characterization and source apportionment of PM2.5 in an urban environment in Beijing, Aerosol Air Qual. Res., 13, 574-583, 10.4209/aaqr.2012.07.0192.
53. Zhang, Y., Sun, J., Zhang, X., Shen, X., Wang, T., and Qin, M.(2013): Seasonal characterization of components and size distributions for submicron aerosols in Beijing, Sci. China Earth Sci., 56, 890- 900, 10.1007/s11430-012-4515-z.
54. Pant, P., and Harrison, R. M.(2013): Estimation of the contribution of road traffic emissions to particulate matter concentrations from field measurements: A review, Atmos. Environ., 77, 78-97, https://doi.org/10.1016/j.atmosenv.2013.04.028.
55. Pant, P., and Harrison, R. M.(2012): Critical review of receptor modelling for particulate matter: a case study of India, Atmos. Environ., 49, 1-12.
56. Grigoratos, T., and Martini, G (2019): Brake wear particle emissions: a review, Environ. Sci. Pollut. Res., 22, 2491-2504, 10.1007/s11356-014-3696-8, 2015.

57. Piscitello, A., Bianco, C., Casasso, A., and Sethi, R.: Non-exhaust traffic emissions: Sources, characterization, and mitigation measures, Sci. Total Environ., 766, 144440, https://doi.org/10.1016/j.scitotenv.2020.144440, 2021.
58. Smichowski, P., Gómez, D., Frazzoli, C., and Caroli, S.: Traffic-Related Elements in Airborne Particulate Matter, Applied Spectroscopy Reviews, 43, 23-49, 10.1080/05704920701645886, 2007.
59. Duong, T. T. T., and Lee, B.-K.: Determining contamination level of heavy metals in road dust from busy traffic areas with different characteristics, J. Environ. Manage., 92, 554-562, https://doi.org/10.1016/j.jenvman.2010.09.010, 2011.
60. Zhang, X., Hecobian, A., Zheng, M., Frank, N. H., and Weber, R. J.: Biomass burning impact on PM2.5 over the southeastern US during 2007: integrating chemically speciated FRM filter measurements, MODIS fire counts and PMF analysis, Atmos. Chem. Phys., 10, 6839-6853, 10.5194/acp-10-6839-2010, 2010.
61. Lee, S., Liu, W., Wang, Y., Russell, A. G., and Edgerton, 948 E. S.: Source apportionment of PM 2.5: Comparing PMF and CMB results for four ambient monitoring sites in the southeastern United States, Atmos. Environ., 42, 4126-4137, 2008.
62. Duvall, R. M., Majestic, B. J., Shafer, M. M., Chuang, P. Y., Simoneit, 846 B. R. T., and Schauer, J. J.: The water-soluble fraction of carbon, sulfur, and crustal elements in Asian aerosols and Asian soils, Atmos. Environ., 42, 5872-5884, https://doi.org/10.1016/j.atmosenv.2008.03.028, 2008.
63. Sun, Y., Zhuang, G., Tang, A., Wang, Y., and An, Z.: Chemical Characteristics of PM2.5 and PM10 in Haze−Fog Episodes in Beijing, Environ. Sci. Technol., 40, 3148-3155, 10.1021/es051533g, 2006.
64. Wang, H., Zhuang, Y., Wang, Y., Sun, Y., Yuan, H., Zhuang, G., and Hao, Z.: Long-term monitoring and source apportionment of PM2.5/PM10 in Beijing, China, J. Environ. Sci., 20, 1323-1327, https://doi.org/10.1016/S1001-0742(08)62228-7, 2008.
65. Zhou, Y., Zheng, N., Luo, L., Zhao, J., Qu, L., Guan, H., Xiao, H., Zhang, Z., Tian, J., and Xiao, H.: Biomass burning related ammonia emissions promoted a self-amplifying loop in the urban environment in Kunming (SW China), Atmos. Environ., 118138, https://doi.org/10.1016/j.atmosenv.2020.118138, 2020.
66. Paulot, F., Paynter, D., Ginoux, P., Naik, V., Whitburn, S., Van Damme, M., Clarisse, L., Coheur, P. F., and Horowitz, L. W.: Gas-aerosol partitioning of ammonia in biomass burning plumes: Implications for the interpretation of spaceborne observations of ammonia and the radiative forcing of ammonium nitrate, 44, 8084-8093, https://doi.org/10.1002/2017GL074215, 2017.
67. Dariusz Kobus (2021), What measures are needed to effectively improve air quality- Case study of Kraków, ppt presentation for Millennium Foundation Kosovo, February 24, 2021